LIGHT EMITTING CHARACTERISTICS AND DIELECTRIC PROPERTIES OF POLYELECTROLYTE MULTILAYER THIN FILMS

by

Michael Frederick Durstock

B.S. Materials Science and Engineering
University of Cincinnati (1994)

Submitted to the Department of Materials Science and Engineering
in partial fulfillment of the requirements for the degree of

DOCTOR OF PHILOSOPHY
in Electronic Materials

at the

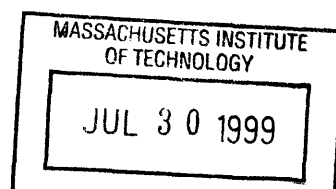MASSACHUSETTS INSTITUTE OF TECHNOLOGY

JUNE 1999

Signature of Author:_____
Department of Materials Science and Engineering
April 30, 1999

Certified by:_____
Michael F. Rubner
TDK Professor of Materials Science and Engineering
Thesis Supervisor

Accepted by:_____
Linn W. Hobbs
John F. Elliott Professor of Materials
Chairman, Departmental Committee for Graduate Students

LIGHT EMITTING CHARACTERISTICS AND DIELECTRIC PROPERTIES OF POLYELECTROLYTE MULTILAYER THIN FILMS

by

Michael F. Durstock

ABSTRACT

This thesis focuses on the use of a new sequential adsorption technique to deposit thin polyelectrolyte multilayer films. This involves alternately dipping a substrate into dilute aqueous solutions of a positively charged polyelectrolyte followed by a negatively charged polyelectrolyte, with a rinsing step in between. By repeating this process an arbitrary number of times, a thin film can be built up due to the electrostatic interaction between the two oppositely charged polyelectrolytes.

This technique was used to create thin film electroluminescent devices based on poly(p-phenylene vinylene) (PPV) using a water soluble precursor to PPV and poly(acrylic acid) (PAA). The structure of such films has been shown to be highly dependent on the conditions of the dipping solutions. The pH of the solutions controls the degree of ionization of the PAA which influences the deposition process by affecting both the conformation of the PAA in solution as well as the charge density of the PAA on the surface. These films exhibited a light output of greater than 1000 cd/m^2 (about 10 times the brightness of a computer monitor), significantly higher than that typically reported for films of pure PPV. A time dependent charging process together with a reduction in the turn-on voltage with charging, and a non-rectifying device behavior, suggest an electrochemical mode of operation. In such a case, ions present in the film play an active role by modifying the electrical injection characteristics.

More fundamental studies on the impedance and dielectric characteristics of sequentially adsorbed films were performed on layers of poly(allylamine hydrochloride) (PAH) with PAA as well as PAH with sulfonated polystyrene (SPS). This provided some insight into the level of ionic conductivity present in these films. Typically ionic conductivites were observed that ranged from about 10^{-12} S/cm at room temperature up to about 10^{-8} to 10^{-9} S/cm at 110°C. The apparent dielectric constant also increased to relatively large values at low frequencies implying the buildup of ions at the interface. The PAH/SPS system required much higher temperatures than the PAH/PAA system before any significant change in the electrical characteristics were observed suggesting that ionic motion is much more hindered in PAH/SPS films.

TABLE OF CONTENTS

LIST OF FIGURES AND TABLES

ACKNOWLEDGEMENTS

To Rhonda, with love

1. INTRODUCTION AND BACKGROUND

1.1 General Introduction

The field of conducting polymers has grown significantly since its birth in the 1970's with the work of MacDiarmid, Shirakawa, and others on polyacetylene. Other conducting polymers were quickly realized and this soon led to the discovery of electroluminescence in some of these conjugated systems. The goal of making cheap flat panel displays has spurred intense research on many of these materials, but perhaps the most thoroughly studied has been poly(p-phenylene vinylene), or PPV, which luminesces green. It was quickly realized that a thin film of this material, spin coated between two electrodes (one of which is transparent), results in low light levels and a poor electroluminescence efficiency. Ways to improve this performance have been sought through the creation of heterostructures, changing the electrode material, and modifying the chemical structure. Although significant improvements have been made, there is still a lot of work to be done before an actual flat panel display comes into production.

PPV itself is completely insoluble in common organic solvents and so soluble derivatives and precursors had to be devised in order to process the material into thin films. The processing method of choice has usually been spin coating whereby a solution of the material is dropped onto a rapidly rotating substrate and once the solvent evaporates, a thin polymer film remains. However a relatively new technique of thin film fabrication has been developed by Decher[1-11], Rubner[12-23], and others which involves the alternate deposition of oppositely charged polyelectrolytes from dilute solution (this will be discussed in more detail later). This sequential adsorption technique affords control of the film structure and composition at the molecular level and so provides a unique opportunity to fine tune the architecture of thin polymer films.

It is the subject of this thesis to study the light emitting and electrical characteristics of thin polymer films made using this sequential adsorption technique. Initially the deposition characteristics of a PPV precursor material are looked at, followed by an examination of the performance of light emitting devices made from this material. This then leads into a more fundamental study of the impedance and dielectric

characteristics of sequentially adsorbed layers of several more well known polyelectrolytes.

1.2 Polyelectrolytes

1.2.1 General information and solution behavior

It is the point of this section to describe polyelectrolytes in general, but also to examine, phenomenologically, their solution characteristics. Simply put, polyelectrolytes are polymers that contain functional groups that are either charged or are capable of becoming charged. That is to say when a polyelectrolyte is dissolved in a solvent, most commonly water, some of the groups can become ionized leading to charges distributed along the polymer chain. It is the presence of these charges, and their associated counter-ions, which give rise to the unusual and interesting properties of polyelectrolytes as compared to uncharged polymers. Some of the functional groups most commonly encountered in this context are carboxylates $(-COO^-)$ and sulfonates $(-SO_3^-)$ as anions as well as protonated amines $(-NH_3^+$ or other secondary or tertiary amines) and quaternary ammonium ions $(-NR_3^+)$ as cations. Several well studied polyelectrolytes with these particular functional groups are shown in Figure 1-1.

Polyanions
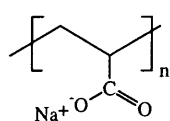
Sodium salt of
Poly(acrylic acid) (PAA)
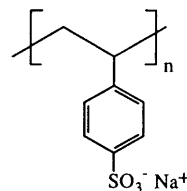
Sodium salt of
Sulfonated Poly(styrene) (SPS)

Polycations
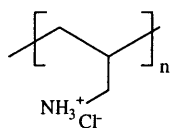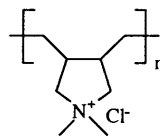
Poly(allylamine hydrochloride) (PAH)   Poly(diallyl-dimethylammonium chloride) (PDAC)

Figure 1-1 - Some typical polyelectrolytes

Polyelectrolytes in solution can be understood on the basis of a simple two-phase model put forth by Oosawa[24, 25]. When a polyelectrolyte molecule is in dilute solution, each molecule occupies its own apparent volume and so the two phases of interest are the apparent volume of the molecules themselves and that where only solvent is present. Furthermore, the molecule has a finite charge density along the chain and the associated counter-ions have an equilibrium distribution between the two phases. Those outside the apparent volume of the molecule are said to be free while those within it are bound. Ions move out of the region of the molecule and into the surrounding solvent causing the molecule to acquire a net charge which tends to repel other chains and prevent overlapping.. Equilibrium is established when the attractive force due to the potential difference developed between the two phases balances the difference in concentration (chemical potential). In other words, when a balance between entropy and enthalpy is established. Using mean-field theory, this condition is approximately given by a Boltzman distribution of the form shown in equation (1) which can be recast as equation (2).

$$n_1 = n_2 \exp\left[-\frac{e\delta\phi}{kT} \right]$$

(1)

$$\ln\left(\frac{1-\beta}{\beta} \right) = \ln\left(\frac{\varphi}{1-\varphi} \right) - \frac{e\delta\phi}{kT}$$

(2)

Here, n_1 is the concentration of counter-ions inside the apparent volume of the molecule, n_2 is the concentration of those outside, e is the electronic charge, $\delta\phi$ is the potential difference between the two phases, k is Boltzman's constant, T is the temperature, β is the apparent degree of dissociation of the molecule (i.e. the number of counter-ions outside the volume of the molecule), and φ is the volume fraction of the polymer. In addition to being dependent on the counter-ion distribution, the potential difference furthermore depends on the geometry of the polymer and has been calculated for spherical and cylindrical geometries[24]. From these analyses, the Manning parameter (ξ_M) is defined as $\xi_M = L_B/b$ where b is the distance between charges along the chain and L_B is

the Bjerrum length which is defined as the distance between two unscreened charges at which the Coulombic interaction energy equals the thermal energy ($L_B=e^2/[4\pi\varepsilon_o\varepsilon kT]$). In water at 293K, L_B has a value of about 7Å. It is found that as the volume fraction of polymer goes to zero ($\varphi\rightarrow0$), the degree of dissociation (β) of the molecule tends to one of two values. It goes to 1 (i.e. counter-ions completely dissociated from the molecule) for low charge densities ($\xi_M<1$), and to a value of $1/\xi_M$ for high charge densities ($\xi_M>1$). So it is seen that as the charge density of the molecule increases from zero, initially the potential difference, as well as the number of free and bound counter-ions, increase (all counter-ions are free at infinite dilution). At a certain charge density, however, $b=L_B$ and so any further increase in the charge density results in the associated counter-ions being bound to the molecule while the number of free ions remains constant. This situation is called counter-ion condensation due to its resemblance of condensation of a gas to a liquid. The pressure of a gas increases until it reaches a critical pressure at which any increase in the number of gas molecules results in liquid being condensed. Similarly, the number of free ions increases until the critical point above which any increase in the number of counter-ions results in condensation of these ions onto the molecule. In effect, this results in a maximum degree of dissociation of the molecule (i.e. apparent charge density) which is less than the expected one when $b>L_B$. A more exact treatment is made using a Poisson-Boltzman treatment and is given in the references[24, 25].

The above analysis assumed that the bound and free counter-ions were uniformly distributed within each of the two phases. In fact, however, the electrical potential of the molecule is such that the bound counter-ions are not uniformly distributed even within this region. In the absence of counter-ions, each charged group on the molecule creates a potential well at its position, the chain itself creates a potential valley along its length, and the molecule as a whole creates a potential trough in its apparent volume. The bound counter-ions can then further be classified as mobile (delocalized) or immobile (localized) depending upon whether they are localized next to the chain, by the potential well or valley, or are free to move about the apparent volume still contained, however, by the overall potential trough of the molecule. The relationship between mobile and immobile bound charges is likened to free ions and ion pairs in simple electrolyte

solutions. For strong electrolytes, it is dominated by the existence of a Coulombic attraction between ions.

As stated above, when these polyelectrolytes are in aqueous solution, some of the functional groups can become ionized (charged) and this degree of ionization is dependent upon the pH of the solution. For simple low molecular weight electrolytes, this relationship is given by the Henderson-Hasselbalch equation as shown in equation (3) where K_a is the acid dissociation constant and α is the degree of ionization of the electrolyte.

$$pH = pK_a - \log \frac{(1-\alpha)}{(\alpha)}$$

(3)

Modifications to this equation must be made for polyelectrolytes since their behavior is more complex. As discussed above, polyelectrolytes can be simply described by a two phase model where everything is not homogeneous. In general, the concentration of free H^+ ions (those not within the apparent volume of the molecule) gives the experimentally measured pH. On the other hand, the equilibrium between the localized and delocalized (immobile and mobile) bound counter-ions determines the pK_a value. The equilibrium between these two phases has already been discussed above in equations (1) and (2) and from this, a modified version of the Henderson-Hasselbalch equation can be given as equation (4)[24, 25].

$$pH = pK_a^o - \log \frac{(1-\alpha)}{(\alpha)} + 0.43 \frac{\Delta G_{el}}{kT}$$

(4)

Here ΔG_{el} is the change in free energy of the molecule due to the dissociation of a functional group and is related to the potential difference described in equations (1) and (2) by $\Delta G_{el} = e\delta\phi$. The result of this extra energy term is to decrease the amount of ionization due to the repulsive interaction between the other charged groups on the molecule. Equations (3) and (4) are often combined to give an apparent pK_a value which depends upon the degree of ionization. In general then, for a given pH, polyelectrolytes tend to have a lower degree of ionization than would be expected for a small molecule with the same functional group.

In the above analysis, the geometry of the polymer in solution has not really been discussed. As with uncharged polymers, the geometry of the polymer depends upon the quality of the solvent and the structure of the polymer, however now a further complication results from the interaction of charged groups along the backbone. The electrostatic repulsion between like charges along the chain tends to cause the polymer to adopt a more extended chain conformation. This, however, decreases the entropy of the system which favors a more contracted and coiled conformation. The balance between these enthalpic and entropic contributions determines the equilibrium conformation in solution and so by controlling them, the conformation can also be controlled. One way to control these parameters is by adding salt into the solution. These excess salt ions tend to shield the charges attached to the polymer chain from each other thereby reducing the amount of electrostatic repulsion and causing the chain to adopt a more coiled conformation. Another very interesting possibility is to vary the actual charge density along the chain. A higher charge density results in a larger degree of electrostatic repulsion between groups and consequently a more extended chain conformation. This is easily done for weak polyelectrolytes whose charge density depends upon the pH of the solution as described above. For polyacids such as poly(acrylic acid) (PAA), a higher pH corresponds to a larger degree of ionization and charge density. So an increase in the pH of the PAA solution results in a more extended chain conformation in solution.

1.2.2 Sequential multilayer adsorption

The new sequential adsorption technique that was mentioned above, which was initially disclosed by Decher *et al.* and further advanced by Rubner *et al.*, allows molecular level control over the deposition of thin polymer films. The underlying principle behind the technique is that of electrostatic attraction between oppositely charged species in solution. It was initially investigated for polyelectrolytes, but since its inception it has been applied to a wide variety of other systems including colloidal particles, proteins, and nanoparticles, among others.
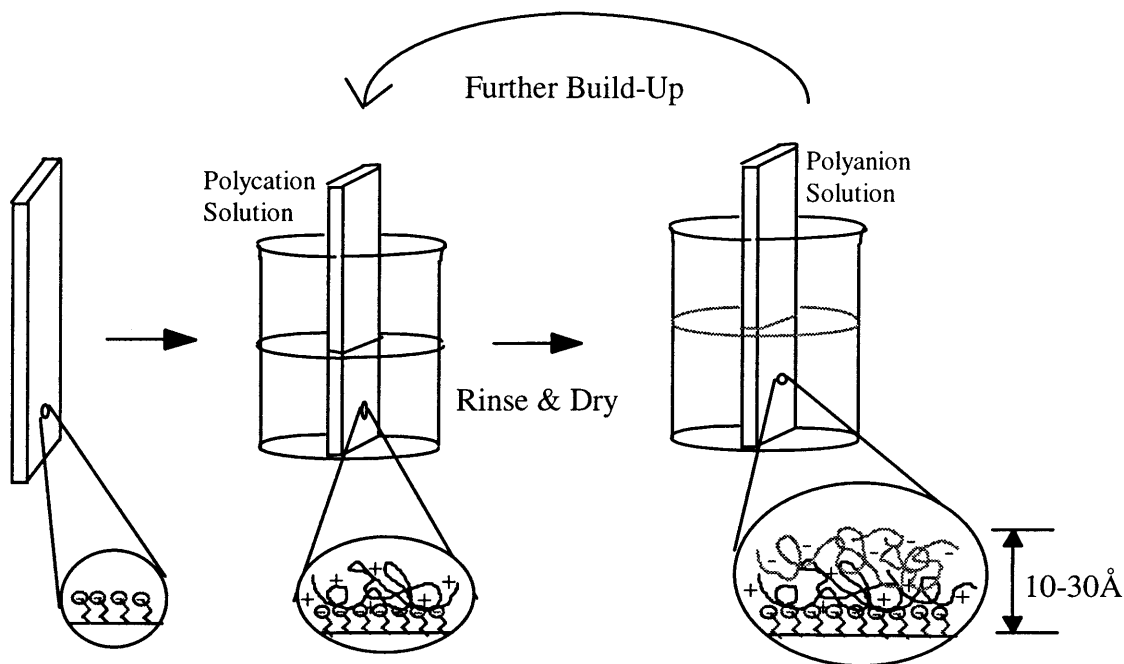
Figure 1-2 - Schematic of the electrostatic sequential adsorption technique[18]

The process, shown schematically in Figure 1-2, consists of two dilute solutions of oppositely charged polyelectrolytes. By dipping a substrate into one of the solutions, say the polycation, a very thin layer of this polyelectrolyte spontaneously adsorbs onto the surface. Some of the charges on the adsorbing material are bound to the surface, while others are left dangling and impart a net charge to the surface. The substrate is then rinsed with deionized water to remove any loosely bound material on the surface, but a thin layer of the polymer remains adsorbed onto the surface giving it a net positive charge. The substrate is then dipped into the second solution, the polyanion, in which a thin layer of this polymer is electrostatically attracted and adsorbed onto the surface, thereby reversing its charge. Once again the sample is thoroughly rinsed with water, but a thin adsorbed layer of this oppositely charged polyelectrolyte remains intact. This combination of a polycation plus a polyanion layer constitutes one bilayer. Simply by alternate dipping between the polycation and polyanion solutions, with a rinsing step in between, a film can be built up whose thickness is accurately controlled simply by changing the total number of bilayers deposited.

In theory any two oppositely charged polyelectrolytes can be used to build up a thin film using this technique. Indeed, the polycation or polyanion need not be kept the same throughout the adsorption process, but rather they can be changed to build up a heterostructure film of arbitrary complexity with an arbitrary number of components. Those polyelectrolytes already shown in Figure 1-1 are some of the more common ones used in this process. Figure 1-3, however, shows a polycation which is a precursor to an electroactive polymer, poly (p-phenylene vinylene) (PPV), and will be of major interest in this thesis.

Tetrahydrothiophene (THT)
Precursor to PPV

Poly(p-phenylene vinylene)
(PPV)

Δ

HCl↑
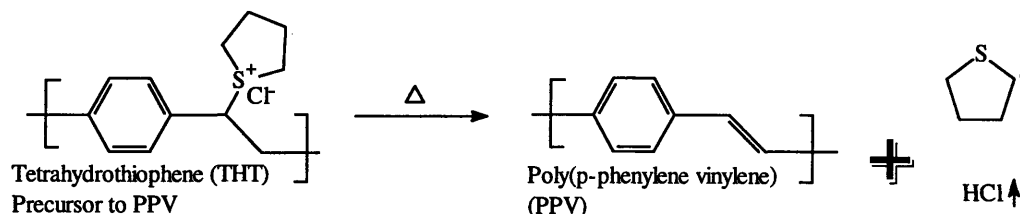
Figure 1-3 - Polyelectrolyte precursor to PPV used to fabricate light emitting devices

1.3 Organic Materials as Light Emitters

1.3.1 General information and materials of interest

Most of the polymers that are encountered on a daily basis (commodity plastics and rubbers being just a couple of examples) are in general non-electroactive. They are considered insulators because they effectively do not have any intrinsic conductivity. In relatively recent years, however, a new class of polymers has been developed that can be made electrically conductive and there has been a significant amount of effort devoted towards developing and understanding these materials. Some of the ones that have been studied the most are shown in Figure 1-4. Polyacetylene, in particular, which is structurally the simplest of these conductive polymers, has received a lot of attention and can be made such that its conductivity approaches that of copper ($\sim10^6$ S/cm).

What distinguishes these polymers from the majority of others is the fact that they are conjugated. To a first approximation, this can be thought of as alternating single and

Polyacetylene (trans)

Poly(p-phenylene vinylene) (PPV)

Poly(p-phenylene) (PPP)

Polythiophene

Polypyrrole
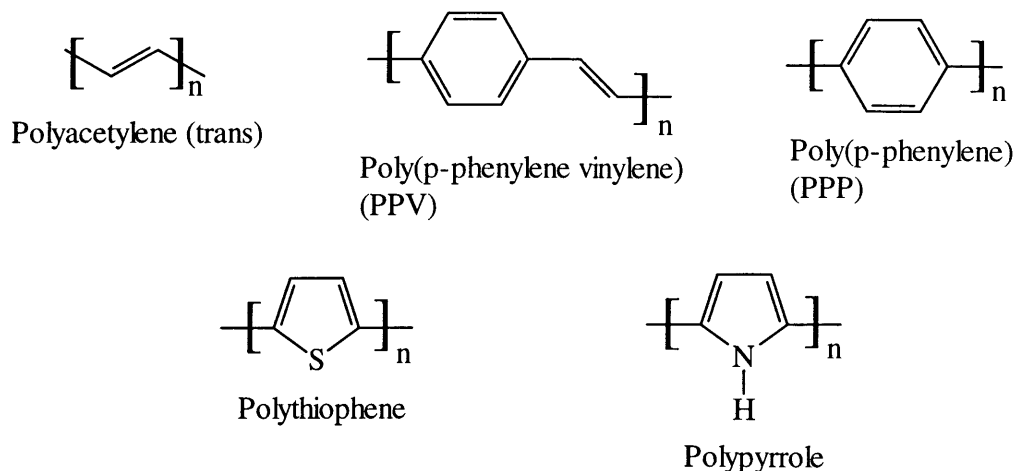
Figure 1-4 - Chemical structures of some representative conducting polymers

double bonds, where the double bond comes about because of overlapping p orbitals on neighboring atoms. Unlike polymers with isolated double bonds, however, in conjugated materials every atom has an unhybridized p orbital capable of overlapping with its neighbors and this creates an extended system of π orbitals. The electrons in this system are not isolated between two atoms, as might be expected from the simple single-double bond alternation representation, but rather they are delocalized over a number of repeat units of the polymer. This delocalization does not extend completely over the length of the chain for a number of reasons. If complete delocalization were to happen, then all of the bonds would be of the same length (somewhere in between that for a single and double bond) and a true "one-dimensional metal" would be formed. That is to say, the Fermi energy (E_F) would be located in the middle of the highest occupied band and metallic like behavior would be observed. Instead, however, a lower energy configuration results when some degree of bond length alternation occurs. In polyacetylene, for example, the π electron density is slightly higher between alternating carbon atoms[26, 27]. The reality, then, lies somewhere in between the case when all the bonds are identical and the case when strict alternation between single and double bonds occurs. This "relaxation" of bond lengths is termed the Peierls instability and results in the formation of a gap at the Fermi level which in turn makes these materials semiconductors instead of metals. Furthermore, in order to maintain this system of

overlapping π orbitals, the carbon atoms must remain coplanar with each other. If this planarity is broken by the chain adopting a different conformation, then the p orbitals can no longer overlap and the conjugation is broken. There is a trade off between the entropy and enthalpy of the conformation of the polymer which results in an average number of adjacent carbon atoms being coplanar with a subsequent break in the conjugation. This average length is called the conjugation length and is likened to the width of the particle in a box problem in quantum mechanics. The larger the conjugation length, the smaller the energy difference between ground and excited states (i.e. the bandgap) of the material.

Because these materials are semiconductors, in pure form there are few free charge carriers and hence the conductivity is low. In analogy with traditional semiconductors like silicon, however, they can be chemically "doped" by other materials to create mobile species, similar to "electrons" and "holes", and hence become conducting. There are, however, a few important differences between doping in traditional semiconductors and in these organic semiconductors. In inorganic semiconductors, doping takes place by introducing impurities onto the crystalline lattice which donate or accept an electron to the conduction or valence band of the host material, respectively. The electronic states within the gap near the band edges are states of the impurity atom. That is, when these states are ionized, the charge is localized around the impurity atom. In addition, because individual dopant atoms donate (or accept) a single electron to (or from) the bands, doping, and hence high conductivity, is associated with unpaired charges of spin ½. In contrast, one of the main differences of organic semiconductors is that upon doping, high conductivities are observed but the charge carriers apparently have no net spin[26]. In conducting polymers, "doping" means chemical oxidation (p-type) or reduction (n-type) of a particular polymer chain. Electronic states within the gap are still introduced, but they are of a different nature than in inorganic materials, as will be discussed.

For the majority of these conducting polymers, such as PPV and PPP, the energy of the electrons on the chain depends on the configuration of the double bonds. Resonance structures can be drawn showing different possible configurations for the same material, as shown in Figure 1-5(a) and (b) for PPP. The lower energy

configuration is the aromatic-type structure while the higher energy configuration is the quinoid-type structure. An electron in the conduction band, or a hole in the valence band, can obtain a lower overall energy by causing a geometric distortion (or relaxation) of the polymer chain and becoming localized over several repeat units of the polymer in the quinoid-type structure. The combination of the electron (or hole) and its associated chain distortion is called a polaron. The increase in energy caused by the geometric distortion is overcome by the electronic energy gained by localization. Taking this one step further, two polarons migrating along a single polymer chain can interact with each other to form a bipolaron, or they can remain separated as individual species. Which of the two cases is more stable depends on the lattice interaction energy and the Coulomb repulsion energy of like charges and can vary from one polymer to the next. However, because the lattice distortion energy is similar for both cases and the ionization energy for the bipolaron is smaller, the bipolaron is usually the more stable species[26]. Having said all of this, however, it should be understood that it is still very common to refer to the charge carriers in conducting polymers as holes and electrons, instead of positive and negative polarons, with the implication being understood.

(a) Aromatic-type structure of PPP

(b) Quinoid-type structure of PPP

(c) (+) Polaron on PPP

(d) (+) Bipolaron on PPP
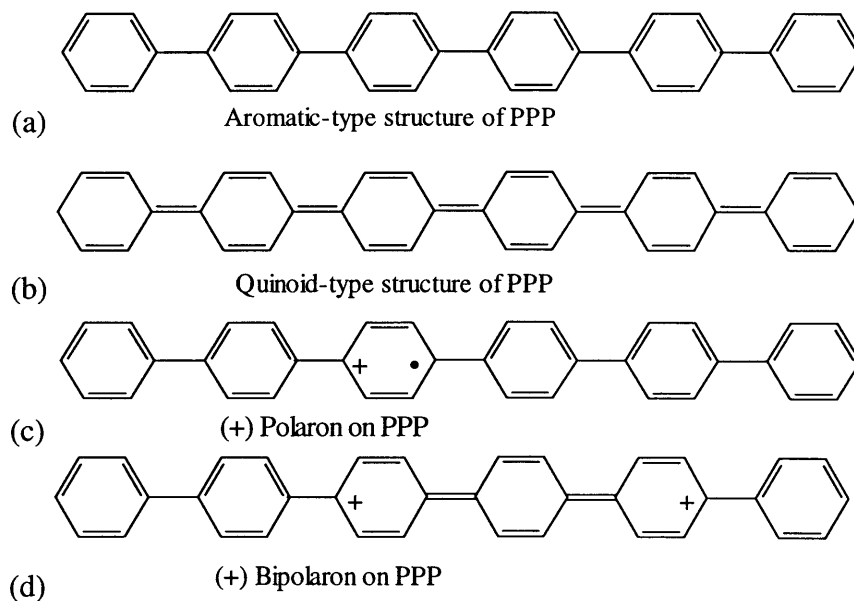
Figure 1-5 - Structures of Polarons, Bipolarons, and Excitons in a conjugated polymer[28]

The effect of introducing these charge carriers onto the polymer can also be examined from the point of view of its band diagram, as shown in Figure 1-6. When the charge carrier becomes localized, the resultant geometric distortion changes the relative energies of the states that were previously part of the conduction and valence bands so that they now lie within the gap. These discrete states, having come initially from the bands, represent electronic states of the polymer and not of the dopant material as in inorganic materials. As such, it should be noted that the conduction and valence bands of
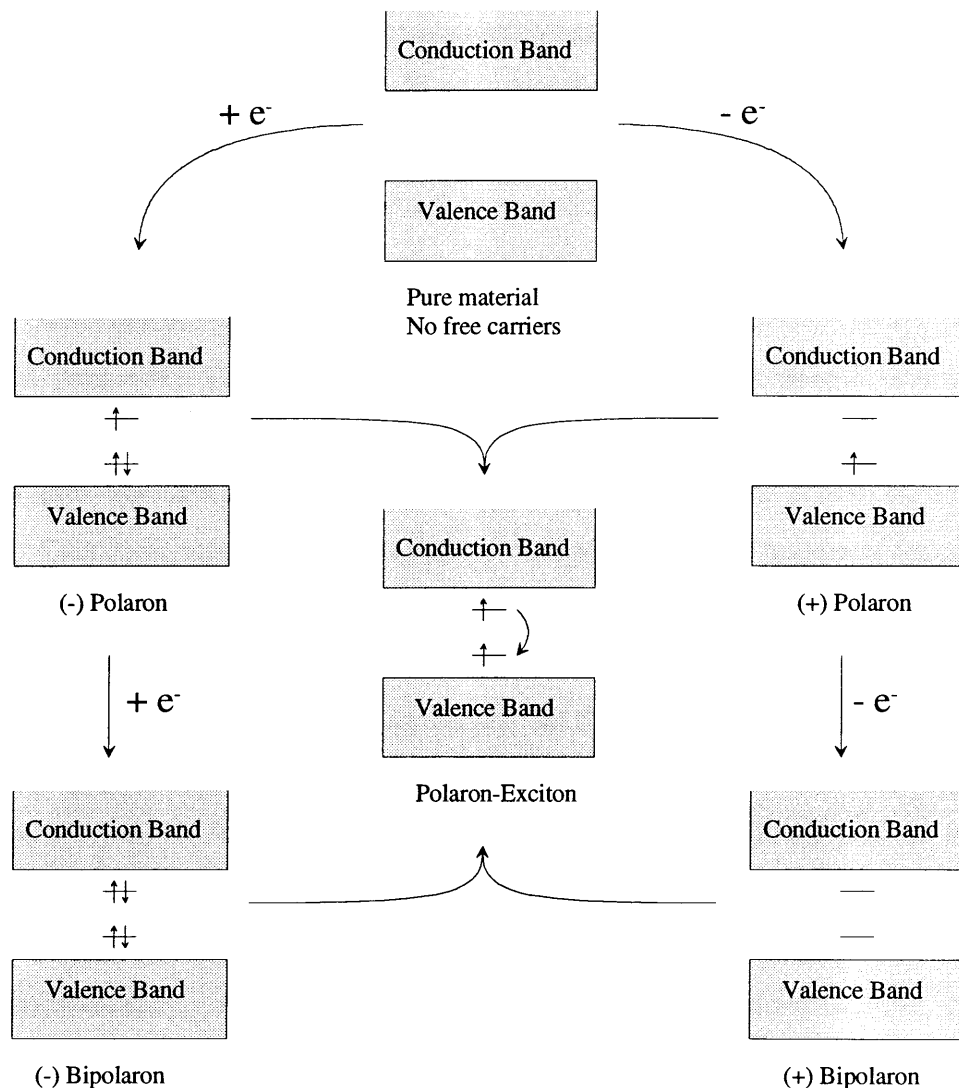
Figure 1-6 - Band diagrams of Polarons, Bipolarons, and Excitons in a conjugated polymer

these polymers are completely empty and full, respectively, and in general do not contribute to the conductivity. Taking this one step further, the bipolaron states are either completely filled or completely empty, as shown in the same figure, and therefore account for the observation of conduction via spinless charge carriers. In addition, these charge carriers are free to migrate along the polymer chain, however conduction between chains is usually described by some kind of interchain hopping model (i.e. thermally assisted tunneling between states)[27]. Increasing the amount of doping translates into a closer spatial proximity of one polaron to another and hence increases both the probability of tunneling and the conductivity. Furthermore, transitions between these states within the gap and the bands can be observed as a broad peak in the UV-visible absorption spectrum. The degree of doping, which is typically much higher than in inorganic semiconductors (i.e. on the order of a few percent), can then be directly related to the absorption intensity of this so called "doping peak".

These charges can also be introduced onto the polymer chain in ways other than chemical doping[29]. These include photogeneration, whereby a photon is absorbed to create an electron-hole pair, and charge carrier injection, in which electrons and holes are injected into the device through separate electrodes under the action of an applied voltage. This is of importance because many of these conjugated polymers are capable of luminescence. Electrons and holes (i.e. negative and positive polarons) moving around in the material can become bound to each other due to their electrostatic interaction to form an exciton (i.e. polaron-exciton), as shown in Figure 1-6. This species can then recombine radiatively to emit a photon resulting in the observed luminescence. When the electron-hole pair is created by the absorption of light, the resulting process is termed photoluminescence. Alternatively, when electrons and holes are injected into the material at opposite electrodes by applying an electrical potential, the resulting emission is termed electroluminescence. Alternatively, cathodoluminescence could result from excitation via an electron beam, but this has not been as widely studied as the first two.

Organic electroluminescent devices based on these conjugated polymers have received a lot of attention recently. This is due, in large part, to the possibilities of making cheap flat panel displays. Applications in other niche markets include a host of

back-lighting applications, such as for watches, and in places where a large area, flexible light emitting panel might be desired. One major problem, however, is the poor stability of these devices, especially in air. Oxygen and moisture can permeate and react with the polymer, causing film degradation and device failure. To that end, poly (p-phenylene vinylene) (PPV), or PPV derivatives, has been the most widely studied electroluminescent polymers due, at least in part, to its relatively high stability[30, 31].

The structures of the polymers shown in Figure 1-4 are mostly rigid rod type structures and are generally insoluble in water and common organic solvents. Therefore the development and synthesis of derivatives and precursors which are soluble in such solvents has allowed for these polymers to be processed into useful devices using fairly conventional techniques. Derivatives of PPV are materials that have the same basic structure as PPV shown above but with side groups, such as alkoxy substituents, attached to the main chain, rendering it soluble in common organic solvents. Precursors of PPV are not conjugated, but rather have structures which are readily soluble in water or other solvents which can then be converted into the conjugated form (usually by heating) after processing into thin films. The PPV precursor based on a tetrahydrothiophenium (THT) leaving group is probably the most widely used. Its structure has already been shown in Figure 1-3 and this material will be of major interest in this thesis.

1.3.2 Light emitting devices - LEDs and LECs

A typical device architecture for a light emitting diode (LED) is a simple sandwich structure as shown in Figure 1-7 together with a simplified band structure diagram. It consists first of a transparent electrode material on a glass substrate. This is most frequently Indium Tin Oxide (ITO) which acts as the anode (hole injecting electrode). A thin film of the light emitting polymer is then put on top of this anode by spin coating. This involves dissolving the polymer in a suitable solvent and then placing several drops of the solution onto a rapidly rotating substrate. The solution spreads out onto the substrate and as the solvent evaporates, the substrate is coated with a thin film of the polymer. The solvent, in addition to being able to dissolve the polymer, must be
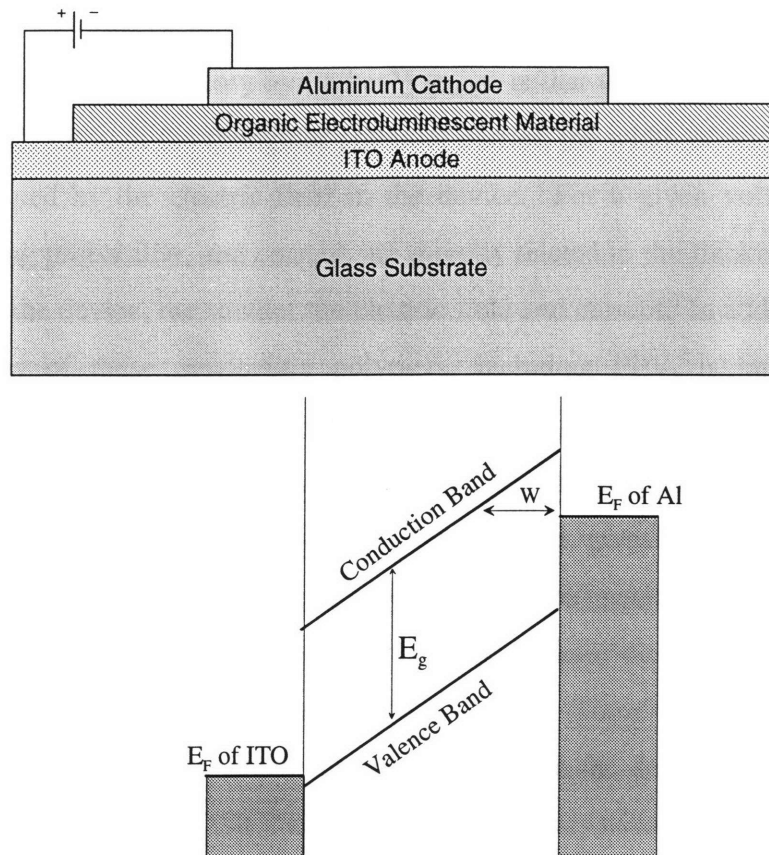
Figure 1-7 - A schematic and band diagram representation for a PPV light emitting device under forward bias

sufficiently volatile so that it quickly evaporates as the substrate is being coated. The substrate rotation speed, volume of solution deposited, solution concentration, plus many other factors, all play an important role in determining the quality and other characteristics of the film. The cathode (electron injecting electrode) is then vapor deposited on top of the polymer to complete the structure.

The mechanism of charge injection and transport are still under investigation even for relatively simple architectures consisting of a single layer of PPV sandwiched between the two electrodes. Several working theories of operation have been proposed, however, which can be used to understand fundamental ideas. As shown in Figure 1-7, the energy difference between E_F of the ITO and the valence band is less than that between E_F of the aluminum and the conduction band, and it is these energy differences that determine the barriers to hole and electron injection, respectively. Charge carriers

could potentially be injected into the polymer via thermionic emission over the barrier, however a separate theory by Parker[32] suggests that tunneling of carriers into the device can occur through the triangular potential barrier, the width of which (W in the figure) is determined by the electric field in the device. For a given voltage, the electric field, tunneling probability, and current, are directly related to the thickness of the device. The thicker the device, the smaller the electric field and current. In addition, the hole mobility in many of these conducting polymers, including PPV, is larger than the electron mobility. The result of both of these observations is that a larger number of holes are injected at the ITO anode than electrons at the aluminum cathode, and they drift across the device faster than the electrons. This, in turn, gives a recombination region that is close to the aluminum/PPV interface which is detrimental to device performance for a number of reasons. Holes can reach the aluminum electrode before encountering an electron, and this gives rise to a leakage current. Those holes that do combine with an electron form excitons which can move around in the device. Since these excitons are located near the metal interface where surface states usually exist, the luminescence can be quenched thus resulting in a lower quantum efficiency[33-37]. If the device is operated in reverse bias with the ITO acting as the electron injecting electrode and the aluminum acting as the hole injecting one, not much happens. Now the barriers to electron and hole injection are both quite high and so few carriers are injected into the device, little current flows, and no light is created. The device, therefore, acts as a rectifier by passing current and producing light in forward bias but not in reverse bias, hence the term light emitting diode (LED).

There have been quite a few techniques employed to increase device efficiency. If the cathode is changed from aluminum to a lower work function metal, such as calcium or magnesium , the barrier to electron injection decreases[38]. In Figure 1-7, this would correspond to raising the Fermi level of the cathode. When the rates of injection of both electrons and holes are equal, the device will be most efficient (neglecting differences in mobilities). Indeed, the device efficiency does increase significantly when these lower work function metals are used as the cathode in place of aluminum. The problem with this solution, however, is that the very nature of these metals having a low work function

also causes them to be highly reactive in an ambient atmosphere with moisture and oxygen. Extreme care must be taken to avoid electrode degradation which makes handling and processing difficult.

Another common solution is to make heterostructure devices in which the location of the recombination zone can be independently varied. An electron transport layer can be placed between the aluminum electrode and the emitting polymer to increase the number of electrons being injected and hence increase its efficiency[39, 40]. Alternatively, both an electron and a hole transport layer can be used, near the cathode and anode respectively, with the emitting layer in between.

A new type of device, called a light emitting electrochemical cell or LEC, has recently been introduced by Heeger *et al.*[41-46]. In such a device, the single layer of PPV described above for LEDs is replaced by a blend of PPV (or another electroluminescent polymer), a salt, and an ion transporting polymer such as PEO sandwiched between the two electrodes. These devices typically have a much larger light output and quantum efficiency than their LED counterparts. Several explanations have been put forth to explain the mechanism of device operation and the debate is still ongoing[41, 43, 47-51]. In general, the dissociated salt ions can move under the application of an applied bias, and this results in the buildup of cations on one side of the device and anions on the other. The presence of these ions modifies the band energies such that the barrier to both electron and hole injection becomes very small resulting in a balance of injected carriers and consequently an increase in the light output and quantum efficiency. The mechanism of device operation will be discussed more fully in Chapter 3.

1.4 Impedance Spectroscopy (IS)

1.4.1 General information and theoretical background

When a DC voltage (V) is applied to a conducting material, a current (I) flows through the material, the value of which is determined by the resistance (R). In the simplest case, such as in metals, the resistance is a constant and is described by Ohm's law (R=V/I). A plot of the measured current versus the applied voltage yields a straight line. For a nonlinear material, the resistance is not constant but rather depends upon the

voltage and so the differential resistance is defined at a particular voltage by R=dV/dI. If a DC voltage is applied to an insulating material, instead of a conducting material, a charge (Q) proportional to the applied voltage becomes stored on the electrodes. The proportionality factor is the capacitance (C) and the relationship is given as Q=CV. All real materials are never perfectly conducting or insulating, however, and consequently have both a finite resistance and capacitance as can be probed by AC techniques.

When a sinusoidal AC field is applied to the material, the voltage and resulting current now oscillate between maximum and minimum values and are, in general, out of phase by an angle θ. The response is now characterized by a complex quantity, called the impedance (Z), having two parts. The first part gives the magnitude of the impedance ($|Z| = V_{max}/I_{max}$) and characterizes the opposition to current flow, while the second part is the phase angle θ that the current makes with respect to the applied voltage. Since the impedance is a vector quantity, it can equivalently be represented in the complex plane by its real and imaginary components $(Z = Z' + jZ'')$ instead of its magnitude and phase $\left(Z = |Z|e^{j\theta}\right)$. Here Z' and Z'' are the real and imaginary parts, respectively, of the impedance and $j = \sqrt{-1}$. The relationships between these quantities are shown in equations (5) and (6).

$$\text{Re}(Z) = Z' = |Z|\cos(\theta) \quad \text{and} \quad \text{Im}(Z) = Z'' = |Z|\sin(\theta) \tag{5}$$

$$|Z| = \left[(Z')^2 + (Z'')^2\right]^{1/2} \quad \text{and} \quad \theta = \tan^{-1}\left(Z''\!\!\big/Z'\right) \tag{6}$$

In addition to the impedance (Z), there are three other fundamental quantities that are frequently of use in the AC behavior of materials. These are the admittance $\left(Y = Y' + jY''\right)$, the dielectric permittivity $\left(\varepsilon = \varepsilon' - j\varepsilon''\right)$, and the modulus $\left(M = M' + jM''\right)$. These four immittances, as they are called, are related by equations (7) and they are all completely equivalent. That is to say that if one quantity is known or measured, then the others are determined. Each one, however, emphasizes a different aspect of the data. In general, the interpretation of the data depends upon whether the material is considered to be predominantly a 'conducting' or an 'insulating' material.

When one is looking at a 'conducting' system, it is typically Z and/or Y that are shown while for 'insulating' systems, it is generally ε and/or M which are of primary interest. It must be reemphasized, though, that while all are completely equivalent and contain the same data, looking at it in one representation sometimes brings out certain characteristics that are difficult, if not impossible, to observe in another.

$$Z = \frac{1}{Y} \qquad \varepsilon = \frac{1}{M} \qquad \varepsilon = \frac{1}{j\omega C_o Z} \qquad (7)$$

Here ω is the angular frequency, which is related to the frequency of the AC oscillation (v) by $\omega = 2\pi v$, and C_o is the capacitance of the empty cell. For a parallel plate geometry with plate area A and distance between the plates d, $C_o = \varepsilon_o A/d$ where ε_o is the permittivity of free space. There are a number of other derived quantities that are frequently considered and reference is made to the literature for a thorough discussion[52-57].

Once the AC characteristics have been determined and are qualitatively understood, a model is generally fit to the data in the form of an electrical circuit (resistors, capacitors, etc.). This is done in an attempt to separate out and describe each of the different physical responses occurring in the materials. Actual materials characteristics (relaxation times, conductivities, etc.) can then be calculated. It is therefore helpful to understand the basic frequency response of resistors and capacitors. An ideal resistor has an impedance which is real, independent of frequency, and given by $Z_{res} = R$. An ideal capacitor, on the other hand, has an impedance which varies with frequency as $Z_{cap} = -j/\omega C$. That is, it increases without bound as the frequency decreases and becomes infinite at zero frequency. There is also an inductive impedance but these are not nearly as common and so will not be discussed.

It is customary to plot the impedance data in the complex plane ($-Z''$ versus Z') to create what is known as a Cole-Cole, or a complex plane, plot where the frequency is an implicit variable. In this domain, the impedance of a resistor is represented as a single point on the real axis at a position equal to its value of resistance, while the impedance of a capacitor is a vertical line coincident with the imaginary axis. Individual impedances

can be added together in a manner which depends upon if they are connected in series or in parallel. For those connected in series, the individual impedances are simply added to get the total $\left(Z_T = Z_1 + Z_2 + \cdots\right)$, while for those in parallel, the inverse of the individual impedances are added $\left(1/Z_T = 1/Z_1 + 1/Z_2 + \cdots\right)$. It should be remembered, however, that these are complex quantities and should be treated accordingly. A resistor and capacitor in parallel and in series are shown, together with their respective complex plane plots, in Figure 1-8. The series combination is a superposition of the individual responses for a resistor and a capacitor. It is a vertical line located at a position along the real axis that is equal to the value of the resistor. The parallel combination gives a semicircle centered on the real axis and whose diameter is equal to the value of the resistor. The frequency at the peak of the semicircle, ω_{max}, corresponds to the point at which the impedance of the resistor and capacitor are equal and hence $\omega_{max}\tau = 1$ where τ, which is equal to RC, is called the time constant. More complicated circuits are generally necessary to accurately model the system under investigation, as will be discussed, but frequently they can be understood as combinations of the above two important cases.
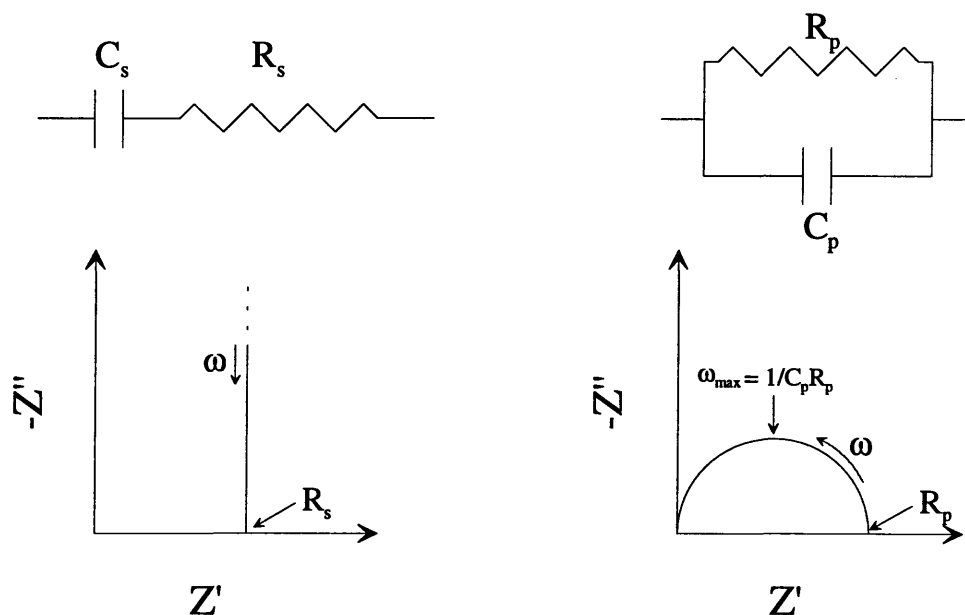
Figure 1-8 - Ideal impedance response of a resistor and capacitor in series and in parallel

The presence of semicircular arcs in impedance data is quite common, as just shown for the parallel RC circuit, however they are usually not perfect. One common perturbation is the displacement of the arc so that its center lies below the real axis. This is generally associated with a distribution of relaxation times $\langle \tau \rangle$, rather than one that is single-valued. Other deviations from ideality can include incomplete, overlapping, skewed, or misshapen arcs. The analysis of impedance arcs has been thoroughly treated by Macdonald[52] and specific cases will be given in this thesis when required.

Complex plane plots can be created for any of the four fundamental immittances described above (Z, Y, ε, M) by plotting the imaginary versus the real component of the quantity of interest. The occurrence of semicircles is frequent in all of them, however they have different meanings. It should be emphasized that the presence of a semicircle in one domain (i.e. Z) does not correlate to another (i.e. ε). This is demonstrated by the fact that when a semicircle is present in the Z complex plane, corresponding to a parallel combination of R and C (as shown above), the same data represented in the ε complex plane yields a vertical spike. Thus understanding the data can be facilitated by examining it in more than one domain.

As mentioned above, in complex plane plots the frequency is an implicit variable. In order to gain a more explicit understanding of the frequency response, it is common to plot the real and imaginary components against the frequency (in any domain). When the complex plane plot displays a semicircle, the real component shows a step in its frequency response while the imaginary component shows a peak, and both of these are centered at ω_{max} from the complex plane. This is shown for ε in Figure 1-9.
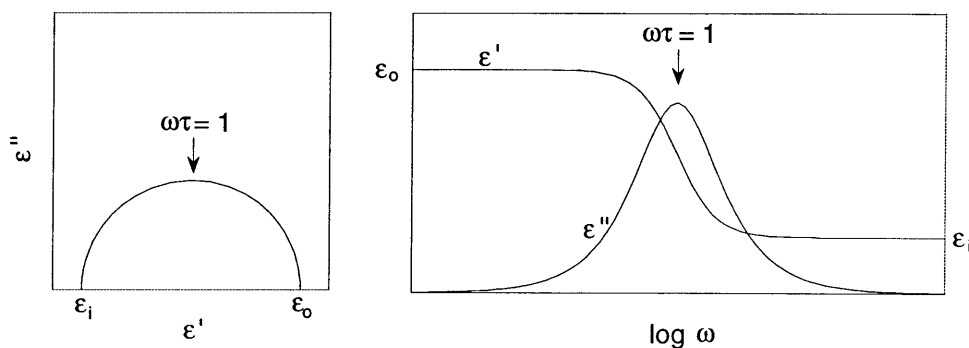
Figure 1-9 - Ideal dielectric response for a single relaxation process

1.4.2 Theory of Dielectrics

The analysis of intrinsically insulating materials has traditionally been carried out in the dielectric domain. Charges within these dielectric materials can respond to an alternating electric field by becoming polarized if the field is alternating slow enough. If the field is oscillating too fast, however, the charges are not capable of keeping up with the field. This results in various resonances, or relaxations, that occur at different frequencies corresponding to electronic, atomic, dipole, or space charge polarization processes. The first two are active in a frequency range (> 10^{11} Hz) that is higher than what is accessible in normal impedance spectroscopy (10^{-3} to 10^8 Hz). Permanent dipoles in the material, however, can respond in this lower frequency range. Space charge polarization, which results from free ions present in the material that can move under the influence of an electric field and accumulate at interfaces, can also occur at these lower frequencies.

The basic theory of dipolar relaxation was examined by Debye and is based upon the concept that when an electric field is applied to a material, the equilibrium orientation of the dipoles is approached exponentially. An outline of the derivation is given by Blythe[53] but only the results are given here. For a process with a single-valued relaxation time, the Debye dispersion equation gives the relation between ε and frequency as shown in equation (8).

$$\varepsilon = \varepsilon_i + \frac{\varepsilon_0 - \varepsilon_i}{(1 + j\omega\tau)} \qquad (8)$$

This can be separated out into real (ε′) and imaginary (ε″) components as shown in equations (9) and (10), the graphical form of which has already been shown in Figure 1-9.

$$\varepsilon' = \varepsilon_i + \frac{\varepsilon_0 - \varepsilon_i}{(1 + \omega^2\tau^2)} \qquad (9)$$

$$\varepsilon'' = (\varepsilon_0 - \varepsilon_i)\frac{\omega\tau}{1 + \omega^2\tau^2} \qquad (10)$$

The real part (ε′) corresponds to the charge storage capabilities of the material while the imaginary part (ε″) is associated with energy losses in the material. Above the resonance frequency, the dipoles cannot respond because the field is oscillating too rapidly and so

they do not contribute anything to ε. At the frequency which corresponds to the resonance between the oscillating field and the dipoles (that frequency at which the dipoles can just keep up with the field), ε'' (the loss) exhibits a maximum and ε' is at its maximum rate of change. At lower frequencies, the dipoles can easily follow the field and so ε' levels off at its maximum value. The response is slow enough, however, so that no energy loss occurs and ε'' again decreases to zero.

As stated above, the presence of depressed semicircular arcs, where the center of the circle lies below the real axis in complex plane plots, is quite common. In frequency plots, this translates into broader dispersion curves and lower loss maxima as compared to that described by the Debye dispersion relation in equations (8), (9), and (10). This is generally interpreted as being due to the presence of Debye-like elements with a distribution of relaxation times rather than a single one. This was initially suggested by Cole and Cole[58] by modifying the Debye dispersion relation with an α parameter as shown in equation (11) (let $\beta = 1$). This α parameter gives a relative measure of the breadth of the relaxation and can be related to the depression of the complex plane semicircular arc below the real axis. Davidson and Cole[59] introduced the β parameter (letting $\alpha = 1$) to account for a skewed complex plane arc corresponding to a skewed distribution of relaxation times. Havriliak and Negami[60, 61] combined the two parameters to give what is know as the Havriliak-Negami equation as shown in equation (11).

$$\varepsilon = \varepsilon_i + \frac{\varepsilon_0 - \varepsilon_i}{\left(1 + \left(j\omega\tau\right)^\alpha\right)^\beta} \qquad (11)$$

The temperature dependence of the dielectric properties is, in general, due to a temperature dependence of the relaxation times, τ. Many dielectric transitions in polymers have been successfully explained by a thermally activated model. Dipole orientation, for instance, can be modeled as consisting of a number of minimum energy orientations separated by an energy barrier. Then, the rate of thermal activation over the barrier, and hence the relaxation time, can be described by a simple Arrhenius law of the form shown in equation (12) where U_a is the activation energy barrier[53].

$$\ln \tau = \frac{U_a}{kT} + \text{constant}$$

(12)

Frequently, however, a simple Arrhenius behavior is not observed and a plot of $\ln(\tau)$ versus $1/T$ shows curved rather than linear behavior. In such situations, more empirical equations, such as in the Williams-Landel-Ferry (WLF) model, are used to describe the response.

2. SEQUENTIAL ADSORPTION CHARACTERISTICS OF PPV/PAA POLYELECTROLYTE MULTILAYERS

2.1 Introductory remarks

The majority of research done on light emitting devices (LEDs) based on electroactive polymers has been performed on films that are spin coated onto an electrode with the subsequent evaporation of the opposite electrode. An alternative way of depositing this polymer film, however, is by the electrostatic sequential adsorption of polyelectrolytes, as described in detail in Chapter 1. This process allows for the continuous buildup of a film whose thickness can be accurately controlled by the number of bilayers that are deposited. By dipping a substrate first into a polycation solution and then into a polyanion solution, with a rinsing step in between, a so-called bilayer, essentially the repeat unit of the structure, is formed. It is by repeating this process an arbitrary number of times that a thin film is built up. Therefore a characterization of the bilayer structure is, in effect, a characterization of the film. It is the characterization of this bilayer building block, for the system based on PPV and PAA, and how the system responds to changes in processing parameters, that is of major interest in this chapter.

2.2 Experimental

The PPV precursor that was used in this study was purchased from Lark Enterprises in Webster, Massachusetts and it was polymerized using standard conditions. According to the vendor, it has quite a high molecular weight of around a million. It was received as approximately a 1% aqueous solution and it was stored in this form in a refrigerator and in the absence of any light in order to minimize any degradation or premature elimination that can occur. The UV-Visible absorption spectra was taken for each batch of PPV precursor solution received. Two peaks in the UV region of the spectra, one at about 200nm and another of lower intensity at about 230 nm, were observed and attributed to the aromatic ring. The solution to be used for sequential adsorption was made by diluting this stock solution with pure water until an absorbance value of 2, for the peak at 230 nm, was obtained. For the studies in which the PPV precursor concentration is varied, this extent of dilution will then change. The solution is

then filtered through a 20-50 micron glass frit filter. The pH is measured using an Orion model 230A pH meter and it is adjusted by the slow addition of either dilute NaOH or HCl. The poly(acrylic acid) (PAA) was purchased from Polysciences and it had a molecular weight of about 90,000. It was received in the form of a 25% aqueous solution and it was diluted with pure water to obtain the desired concentration for sequential adsorption. The solution was then filtered through 2.5 micron filter paper and its pH was adjusted as described above. All of the solutions used in the sequential adsorption process, as well as the rinse baths and anything else requiring the use of water, used water that was filtered through a Milli-Q® filtration system. This removed, among other contaminants, any residual ions and the water had a resistivity of at least 18 Mohm•cm at the output.

All of the substrates used here were cleaned prior to sequential adsorption. Glass microscope slides were cleaned by immersing them into a 5:1:1 mixture of $H_2O:H_2SO_4:H_2O_2$ for one hour followed by a water rinse and then immersion into a 7:3 mixture of $H_2O:NH_4OH$ also for one hour. The slides were then thoroughly rinsed with water and dried. This treatment makes the slides very hydrophilic as evidenced by the fact that a drop of water placed on the slide completely wets the surface. Cut pieces of silicon wafers that were used for the ellipsometric measurements were cleaned by immersing them in a Chromerge® solution (Chromic-Sulfuric Acid mixture) for at least 1 hour. They were then thoroughly rinsed with water before use.

The sequential adsorption process was performed automatically in a Carl Zeiss HMS Series microscope slide stainer, or 'dipper'. These 'dippers' are made up of a sequence of troughs together with a moveable arm which holds the substrates and which can be programmed to move from one trough to another and held in each one for a certain amount of time. The substrates are typically held in the polycation solution for 15 minutes followed by three separate water rinse baths for 2 minutes, 1 minute, and 1 minute. This same procedure is then repeated for the polyanion solution which completes the bilayer. The whole process is then repeated to build up an arbitrary number of bilayers. The water rinse baths are replaced periodically with fresh ones to minimize any cross contamination. After the process is complete, the samples are removed and blown

dry with filtered compressed air. The PPV precursor is then converted into its conjugated form by heating the samples in a vacuum oven for 11 hours at the prescribed temperature. Thickness measurements were performed on a Gaertner ellipsometer at 633 nm and/or a Tencor surface profiler with a 5 mg stylus force. Absorption spectra were taken on a Cary 5E Spectrophotometer.

2.3 Film thickness

The absorbance of the PPV chromophore can be used to monitor the growth of sequentially adsorbed layers based on PPV precursor and PAA. The PAA is not conjugated and so does not contribute to the absorption spectra in this regime. Figure 2-1 shows the absorption spectra of PPV/PAA films as the number of bilayers that are deposited increases. The PPV precursor was converted into its conjugated form by heating the completed films in vacuum at 230°C for 11 hours. It can be seen that as more bilayers are deposited, the film continues to grow as indicated by an increase in the peak absorbance. If this peak absorbance is plotted as a function of the number of bilayers, as shown in the inset, it can be seen that the growth is, in general, a linear process. That is
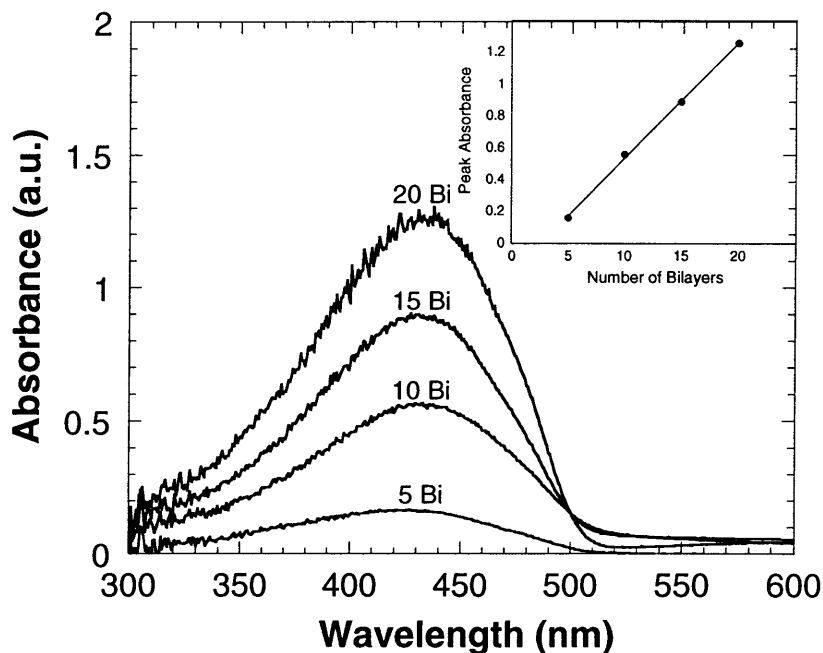
Figure 2-1 - Absorbance spectra of PPV/PAA films as a function of the number of bilayers deposited - PPV precursor solution pH=4.5 and concentration=10⁻⁴ M, PAA solution pH=2.5 and concentration=10⁻² M

to say that roughly the same amount of material is deposited for every bilayer created. It can be seen, however, that a line fit to the data passes through a point below the origin which tends to indicate that the first few layers deposited have a smaller average thickness than the rest. These first few layers are in close proximity to the surface and this can affect the deposition. In general, a number of these layers are required to be deposited to eliminate any substrate effects. This sequential adsorption process is inherently different than the conventional spin coating process. There are a number of issues that are simply not present in pure spin coated PPV films, which are used to make light emitting devices, that must be addressed in sequentially adsorbed films. One of the most important is the presence of the polyanion that was used to build up the film as well as the resulting structure of the film created by this alternate dipping between polycation and polyanion. As a means of getting at this structure, we used ellipsometry to measure the increment in film thickness that occurred upon depositing each layer. Figure 2-2 shows the total film thickness, as measured by ellipsometry, as a function of the number of bilayers of a PPV precursor/PAA film. Here, the total film thickness is measured after every layer and the figure indicates the incremental thickness that occurs due to either the
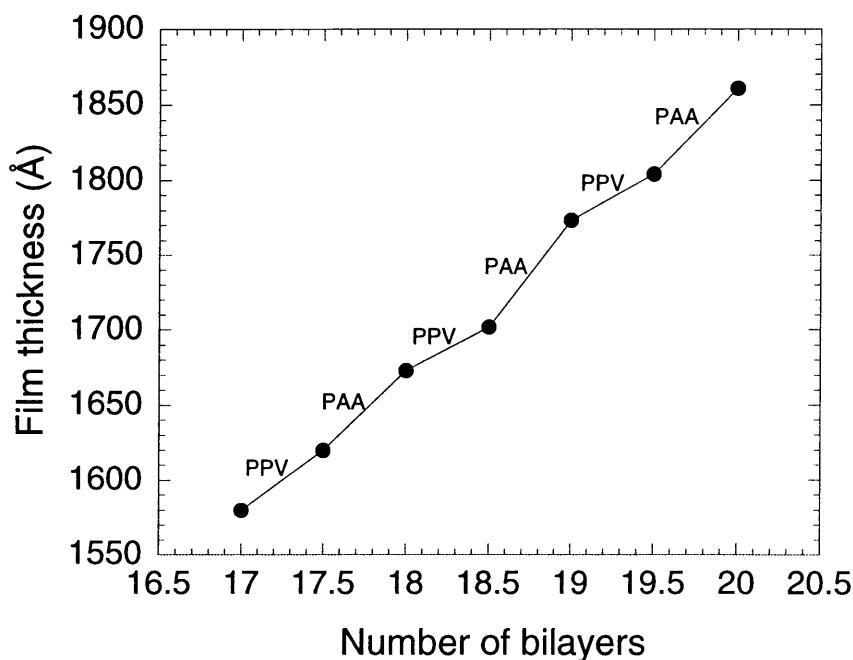
Figure 2-2 - Ellipsometric film thickness - same deposition conditions as in previous figure

PAA or the PPV precursor. The average of these incremental thicknesses for both the PAA and the PPV precursor is then taken. In the figure, the data corresponding to a half integer number of bilayers is when the PPV precursor is the topmost layer, while PAA is topmost for an integer number of bilayers. It can be seen that for this case, the thickness increment due to the PAA is larger than that due to the PPV precursor. The incremental thickness of the PAA is approximately 58Å, while that of the PPV precursor is about 37Å, and these give a total bilayer thickness of about 95Å. So in this case, the PPV precursor composes only about 40% of the total film thickness. As will be discussed in the following sections, the concentration of the polymers in solution and the pH of the individual solutions both significantly affect these values. It must be emphasized, however, that these measurements do not imply that the structure of the film is such that one discrete lamellae is layered on top of another, as might initially be thought. Rather, it simply gives the film thickness increment that occurs upon adsorption. It does not give information on the level of interpenetration between the polymer chains. Indeed, the bilayer is likely made up of chains which form interpenetrating, diffuse interfaces whereby gradual changes occur from one layer to the next, and this level of interpenetration can vary from one system to the next.

2.4 Solution concentration effects

Typical concentrations of polymers used in this sequential adsorption process are in the range of 10^{-3} M to 10^{-2} M based on the repeat unit molecular weight. For a typical hydrocarbon polymer such as poly(acrylic acid), this translates into approximately 0.1 to 1 kg/m^3 which is generally within the dilute region of polymer concentration. This regime is sufficiently dilute so that individual polymer chains do not overlap, but rather are isolated from each other in solution. Since the polyelectrolytes are adsorbed from these dilute aqueous solutions, it might be expected that the concentration of polymer in the solution may affect the deposition process and, as will be seen , this is indeed the case under certain circumstances.

Films of PAA and PPV precursor were sequentially adsorbed onto cleaned silicon wafers using conditions under which the polyelectrolyte concentrations were independently varied. Using the same technique based on ellipsometry that was

described above, the incremental thicknesses of both the PAA and the PPV precursor were measured simultaneously. Figure 2-3 shows the effect that changing the PAA concentration has on the relative thickness values (the PPV precursor concentration is held constant at 10^{-4} M). Within experimental error, little or no change was observed for either the total bilayer thickness or for the individual thickness contributions when the PAA was reduced in concentration by an order of magnitude from 10^{-2} M to 10^{-3} M.

On the other hand, the concentrations used for the PPV precursor were necessarily much more dilute. This material is quite temperamental for a number of reasons. In addition to the fact that the viscosity of even dilute solutions is quite high, it also tends to form a gel upon storage making it even more viscous. Furthermore, partial elimination of the precursor material can occur in solution. This results in a slight yellowing of the solution and can further increase the viscosity. For these reasons, the PPV precursor solution had to be used at or below a concentration of around 10^{-4} M. Above this limit, the viscosity became too high for the solution to be used effectively in sequential adsorption. Figure 2-4 shows the effect that changing the PPV precursor concentration, below this limit, has on the relative thickness values (the PAA concentration is held constant at 10^{-2} M). As the PPV precursor concentration decreases, both the total bilayer thickness as well as the individual contributions decrease. The adsorption of a monolayer of polymer onto a solid substrate from a dilute solution has been the source of study for quite a while[62]. Typically these systems show an adsorption isotherm (a plot of the amount adsorbed versus solution concentration) consisting of an initial sharp increase in the amount adsorbed followed by a plateau region as the concentration is increased. This is shown schematically in Figure 2-5. This monolayer adsorption is very similar to the sequential adsorption process used here and they differ only in the nature of the substrate. The surface is now composed of a previously adsorbed layer of polymer, instead of a solid substrate, and so the same qualitative aspects should be observed. As shown in Figure 2-3, the PAA concentration in the range
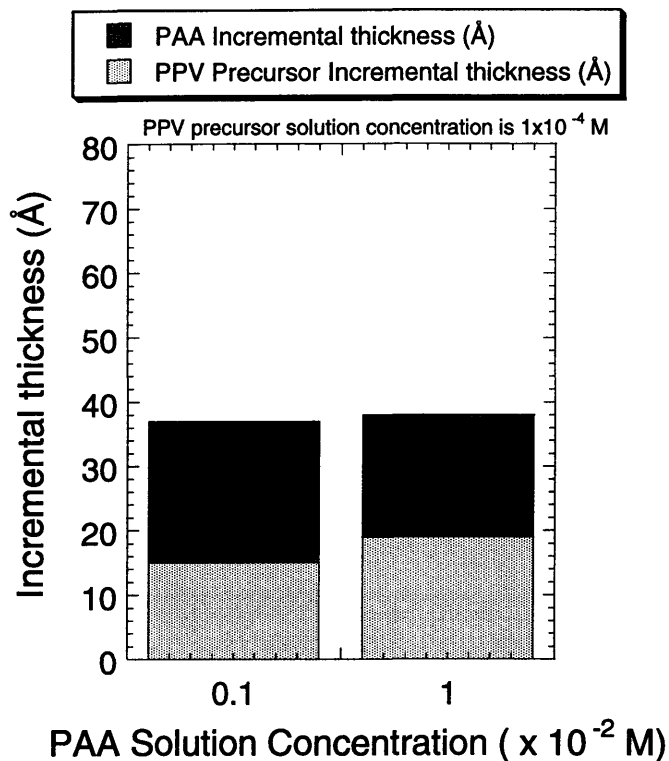
Figure 2-3 - Dependence of the incremental thickness values of PPV precursor and PAA on PAA concentration
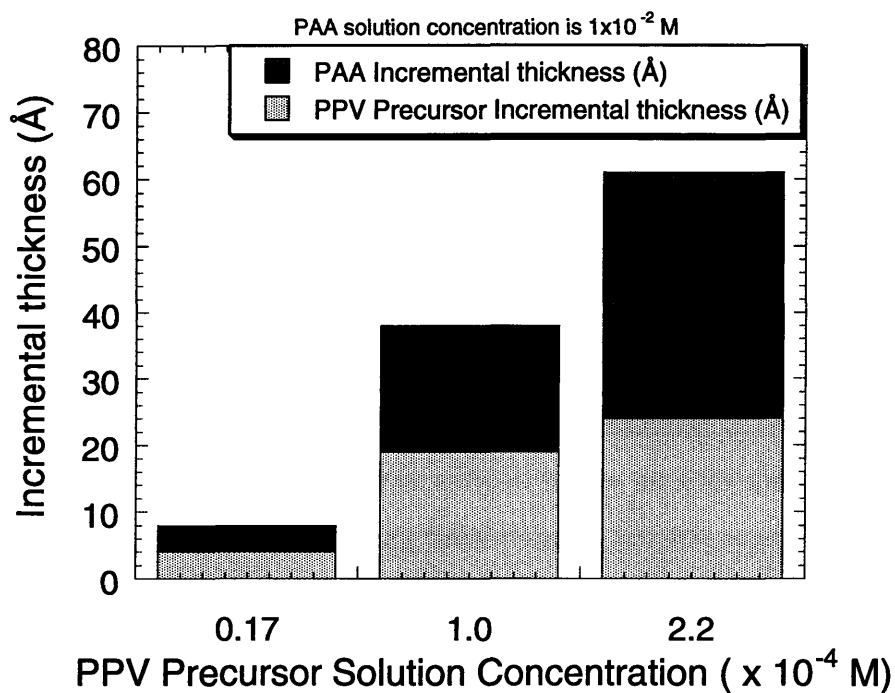
Figure 2-4 - Dependence of the incremental thickness values of PPV precursor and PAA on PPV precursor concentration
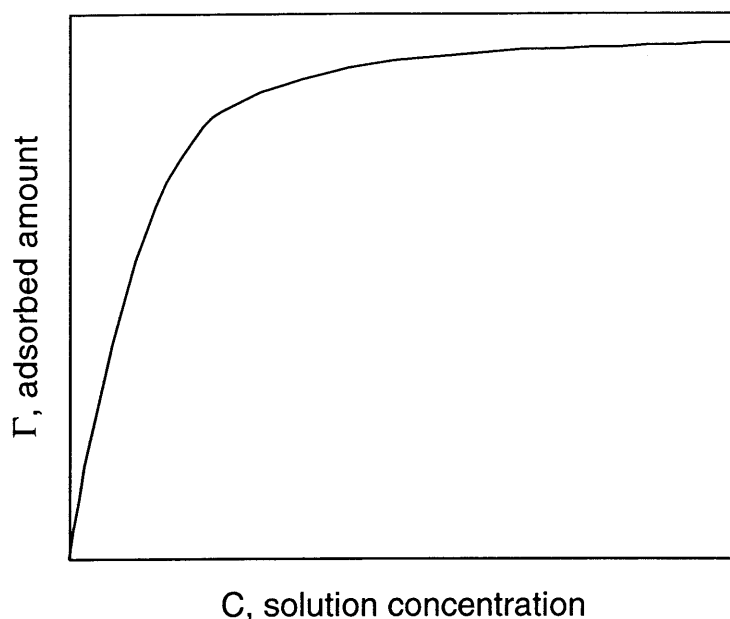
Figure 2-5 - Schematic of a generic adsorption isotherm

of 10^{-3} to 10^{-2} M, has no effect on the adsorption. We are therefore on the plateau region of the adsorption isotherm in which surface saturation has been attained. Since the surface is saturated, any change in the PAA concentration does not result in a net increase in the thickness. On the other hand, large changes in thickness were observed when the PPV precursor concentration was changed as shown in Figure 2-4. This implies that the PPV precursor adsorption is taking place in the steeply inclined region of the isotherm whereby complete surface saturation is not attained. Any change in the PPV precursor concentration results in a change in the degree of saturation and hence a change in thickness. It should be noted, however, that it is not only the PPV precursor incremental thickness that is changing as the PPV precursor concentration is changed. Interestingly, both of the incremental thickness values seem to follow the PPV precursor concentration. Since the PAA concentration is being held constant in these cases, it implies that the thickness of the adsorbing PAA layer is dependent upon the thickness of the previously adsorbed PPV precursor layer. A thicker underlying layer promotes a thicker layer of PAA to be adsorbed by virtue of the fact that there are more positive charges to which the PAA can attach. So it is seen that changing the thickness of one layer by changing its

concentration (the PPV precursor) drives a change in the thickness of the other layer (the PAA).

2.5 Solution pH effects

In addition to the concentration, the pH of the polyelectrolyte solutions that are used for sequential adsorption can play a major role in determining the resultant film structure. As discussed in Chapter 1, adjusting the pH of a weak polyelectrolyte solution allows one to control the charge density along the chain which in turn affects the conformation of the polymer in solution. By using the ellipsometric technique that was described above to measure thickness increments, we have looked at some of the effects that result from changing this charge density.

The effects of varying the pH of the polyelectrolyte solutions independently is shown in Figure 2-6. Three general trends can be discerned. First, as the pH of the PAA
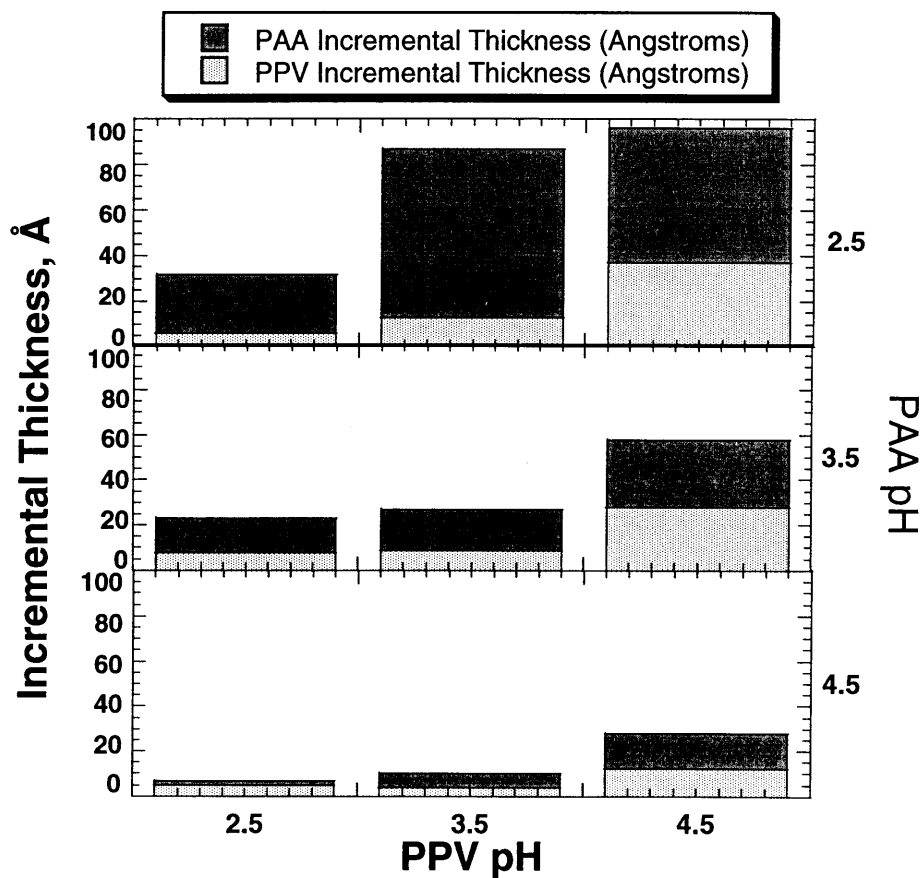
Figure 2-6 - pH matrix showing the dependence of the incremental thickness values of PPV precursor and PAA on solution pH

increases, its relative thickness contribution per bilayer decreases. The PAA is a weak polyelectrolyte for which an increase in the pH causes an increase in its degree of ionization (higher charge density). The result, shown schematically in Figure 2-7, is to create more electrostatic repulsion between charges causing the chain to adopt a more extended conformation. In turn, this tends to give thinner layers upon adsorption due to the chain's ability to lay flat on the surface. On the other hand, as the pH of the PPV precursor increases, its relative thickness contribution per bilayer increases. The PPV precursor acts like a salt in the sense that the ionic groups, which render it water soluble, are completely dissociated. Consequently the degree of ionization, and hence the conformation in solution, are essentially independent of the pH, unlike PAA. However, the degree of ionization of the previously adsorbed PAA layer is still free to change with pH, as shown in Figure 2-8. A larger pH in the PPV precursor solution causes the charge density of the surface, which is composed of PAA chains, to increase and promotes more adsorption of the PPV precursor. The third point concerns an effect previously observed in the above section on the concentration dependence of the thickness. Here again, the
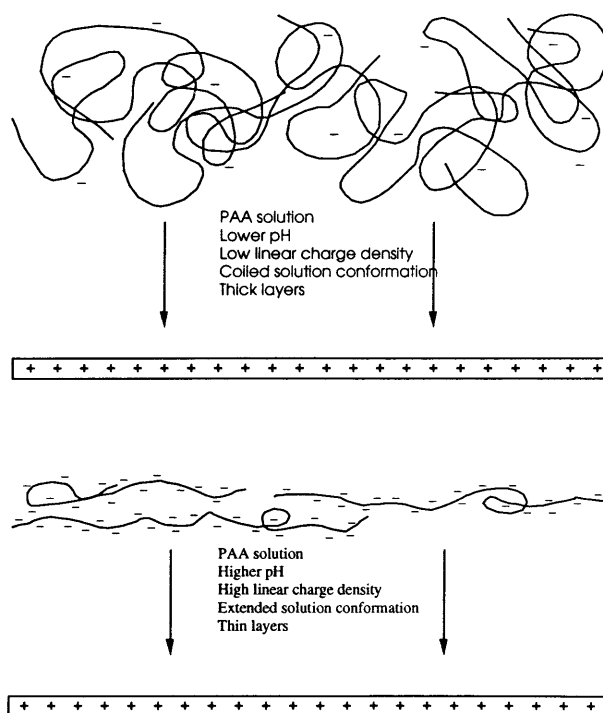
Figure 2-7 - The influence of PAA solution pH during film growth

PPV precursor solution
Lower pH
Low surface charge density from PAA
Thinner PPV precursor layers

PPV precursor solution
Higher pH
Higher surface charge density from PAA
Thicker PPV precursor layers
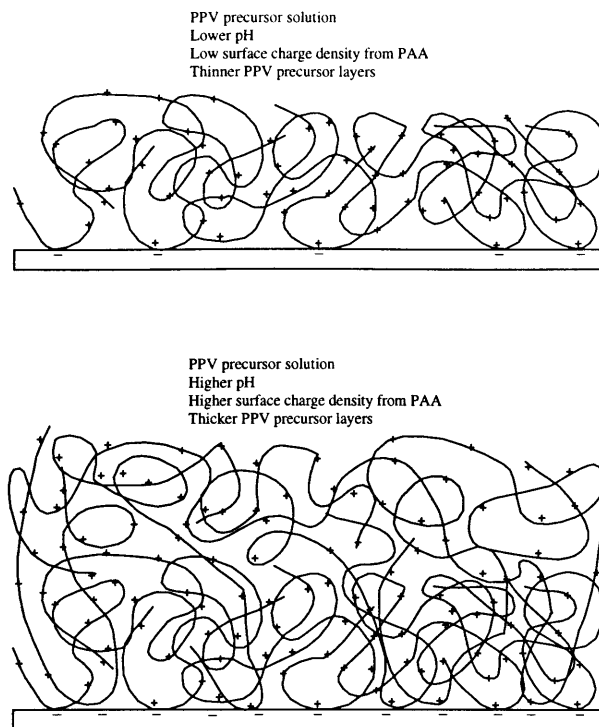
Figure 2-8 - The influence of PPV precursor solution pH during film growth

thickness of an adsorbing layer is dependent on the underlying layer thickness. That is to say, a thickness change in the PPV precursor layer due to a changing pH drives a simultaneous thickness change in the PAA layer. Similarly, a thickness change in the PAA layer due to a changing pH drives a simultaneous thickness change in the PPV precursor layer. Apparently, a thicker underlying layer promotes a thicker adsorbing layer by creating more potential sites of attachment, as well as by creating a rougher surface.

A slightly larger pH window is shown in Figure 2-9 but with both solutions maintained at the same pH value, as in the diagonal of the matrix shown in Figure 2-6. Based on previous arguments, as the pH of both solutions are increased, the PAA thickness contribution should decrease due to its forming a more extended conformation in solution, while the PPV precursor contribution should increase (or reach a plateau) due to an increase in the surface charge density. This is indeed what is observed in Figure 2-9 up to a pH of about 4.5. Beyond this, the thickness contribution from both components
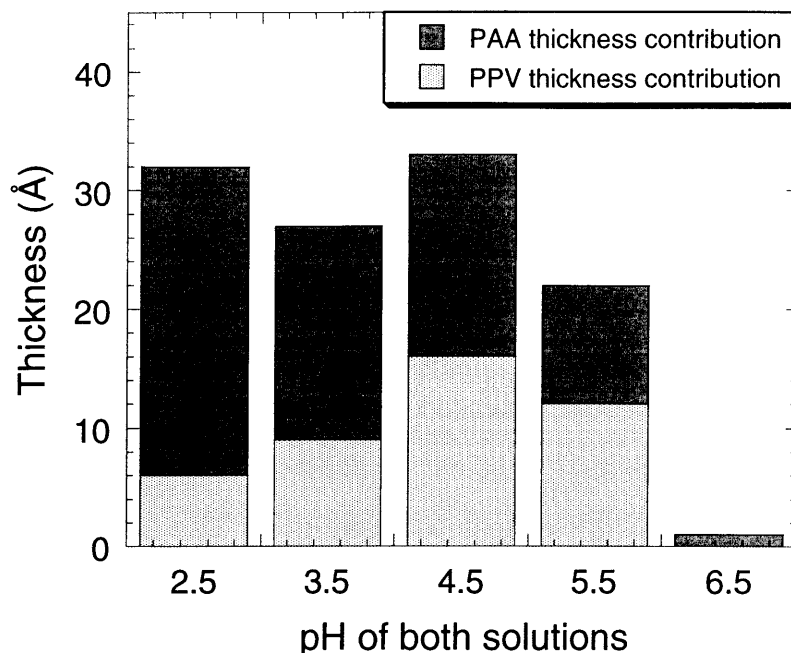
Figure 2-9 - Dependence of the incremental thickness values of PPV precursor and PAA on solution pH with both solutions maintained at the same pH value

decreases, and at a pH of 6.5 the bilayer thickness is miniscule. In order to reconcile this observation, another explanation must be invoked. As a reminder, this system is made up of a polycation (PPV precursor) which is highly charged independent of pH, and a weak acid (PAA) whose charge density changes with pH. At low pH, the PAA chain is weakly charged and it forms a layer with many loops and tails due to its coiled conformation in solution. Relatively little PPV precursor is adsorbed to the PAA at this low pH due to its low charge density. As the pH of both solutions increase, the charge density of the PAA increases and causes more PPV precursor to be adsorbed. Free energy considerations dictate that at still relatively low charge densities, the polycation will try to maximize its conformational entropy by going down in a relatively loopy, and hence thick, conformation. As the pH, and hence the charge density, continue to increase, the enthalpic contribution will eventually take over. A more energetically favorable situation is created when the two polymers form one-to-one contact ion pairs in extended chain conformations resulting in a very thin bilayer and the observed transition in the thickness as shown schematically in Figure 2-10. Essentially, at high pH values, the system is

PPV precursor solution
Fairly high pH
Fairly high surface charge density from PAA
Thick PPV precursor layers

PPV precursor solution
Still higher pH
Very high surface charge density from PAA
Thin PPV precursor layers
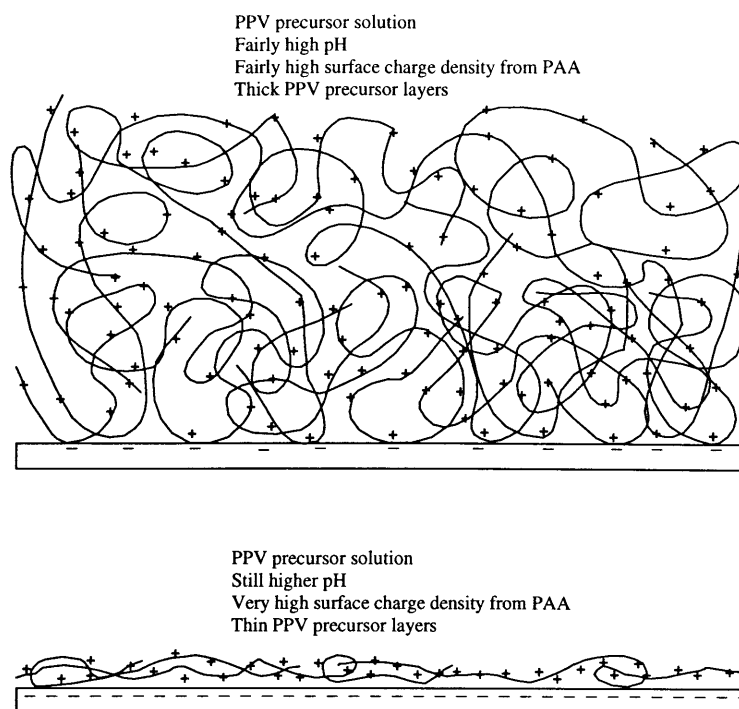
Figure 2-10 - Influence of solution pH at high PAA charge densities (high pH)

behaving as two highly charged macromolecules, comparable to films made with both a strong acid (polyanion) and a strong base (polycation). This requirement is met for films made of sulfonated polystyrene (SPS) and poly(allylamine hydrochloride) (PAH), both of which are fully charged independent of pH in the region of interest, and whose structures are shown in Figure 1-1. It is known that for this system, very thin bilayers with extended chain conformations do indeed form[63-65]. It is in this manner in which the above films of PAA and PPV precursor are behaving.

In the normal pH range of deposition where this thickness transition does not occur, the pH of the solutions determines the degree of ionization of the PAA. Only those groups on the PAA chain that are charged contribute to the deposition process. So if a relatively low pH of both solutions is chosen, then few of the carboxylic acid groups on the PAA will be ionized during the deposition to form ion pairs with the PPV precursor. This results in a high concentration of free carboxylic acid groups left in the film that are not bound to the PPV precursor. These can then be activated after the deposition process is complete by submerging the entire film into water adjusted to a high

pH. This procedure will become important in the next chapter when discussing devices made from these films. Now, the effect of this post water treatment on the film thickness will be discussed. Figure 2-11 shows the total thickness of sequentially adsorbed films made with a PPV precursor pH of 4.5 and a PAA pH of 3.5 and afterwards treated to a pH adjusted water bath, at a pH as indicated in the figure, for 1 hour. The pH of the water bath was either adjusted down with HCl or up with NaOH. There is a large pH range from about 3 to about 9 over which the film thickness doesn't change appreciably. In this range, the degree of ionization of the PAA can change drastically but the film remains intact and of good quality. At both very high pH's and very low pH's the film thickness drops precipitously but it seems to drop faster at low pH's. At these low pH values, the HCl causes the PAA to lose most of its charge density by forming free acid groups with the Cl⁻ ion providing the necessary counter-ion to the PAH. So at a low pH, the macromolecules are no longer electrostatically bound to each other and could potentially re-dissolve back into the solution. On the other hand, at a high pH the PAA becomes fully ionized and so this breaking up of the film is not likely,
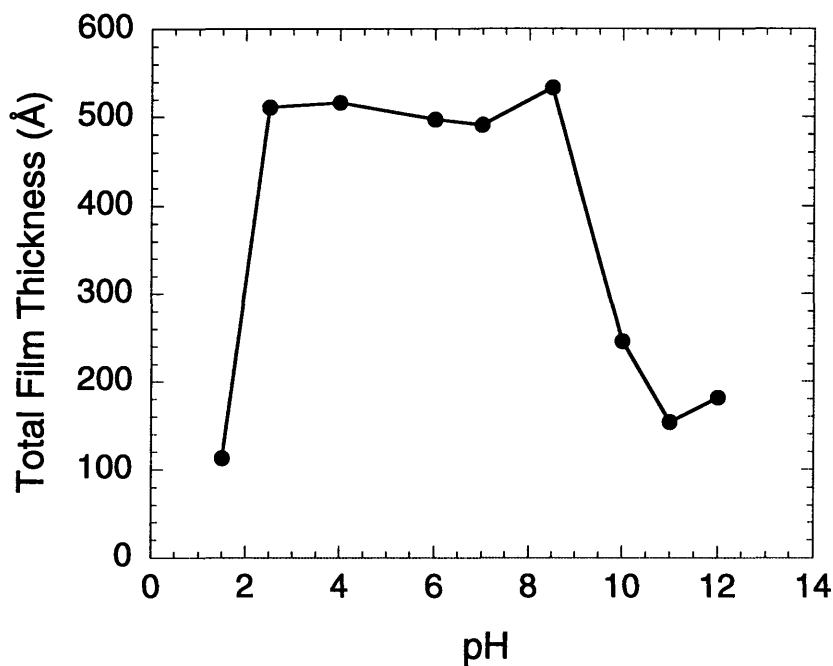
Figure 2-11 - PPV precursor/PAA film thickness after submerging it in water adjusted to the indicated pH for 1 hour

yet a decrease in the film thickness is still observed. In this range, the presence of the hydroxyl groups (OH⁻) from NaOH compete with the surface sites anchoring the film to the surface and eventually dominate resulting in a delamination of the film from the surface. Indeed this could also be the source of the decrease in film thickness even at low pH's where it seems that both mechanisms are possible.

2.6 Thermal Conversion Issues

Once the PPV precursor and PAA have been sequentially adsorbed onto a substrate, the film must be heated in order to convert the PPV from its precursor form into its conjugated form. This was done under vacuum in order to minimize any oxidative degradation that can occur if done under ambient conditions. When a spin coated film of pure PPV precursor is heated in vacuum, the chemical conversion proceeds with the elimination of tetrahydrothiophene and hydrogen chloride gas, as previously shown in Figure 1-3. The situation is a bit different, however, for sequentially adsorbed films. When the PPV precursor and the PAA are assembled, the charged groups on each of the polymers become ion pairs and most of the small counter-ions remain in solution, as shown in the first step of Figure 2-12. The PPV precursor now effectively has a carboxylate counter-ion instead of a chloride, which is of importance when the film is heated to bring about thermal conversion. The influence of different counter-ions on the conversion characteristics of cast films of PPV precursor has been investigated by previous workers[66]. They have shown that precursor films with halide counter-ions (F⁻, Cl⁻, and Br⁻) are fully converted by 200°C, but those with an acetate counter-ion (i.e. CH_3COO^-) require temperatures up to 350°C for complete elimination. The case of the sequentially adsorbed layers considered here is similar to that for the acetate ion in that both have a carboxylate group as the counter-ion. However, a fundamental difference here is that upon conversion, the acid group is forced to remain in the film by virtue of the fact that it is covalently bonded to the PAA chain, as shown in the second step of Figure 2-12. Tetrahydrothiophene is still eliminated, but now the charged carboxylate ion reacts to form a carboxylic acid group (neglecting the possible

M = H or Na

MCl (solution)
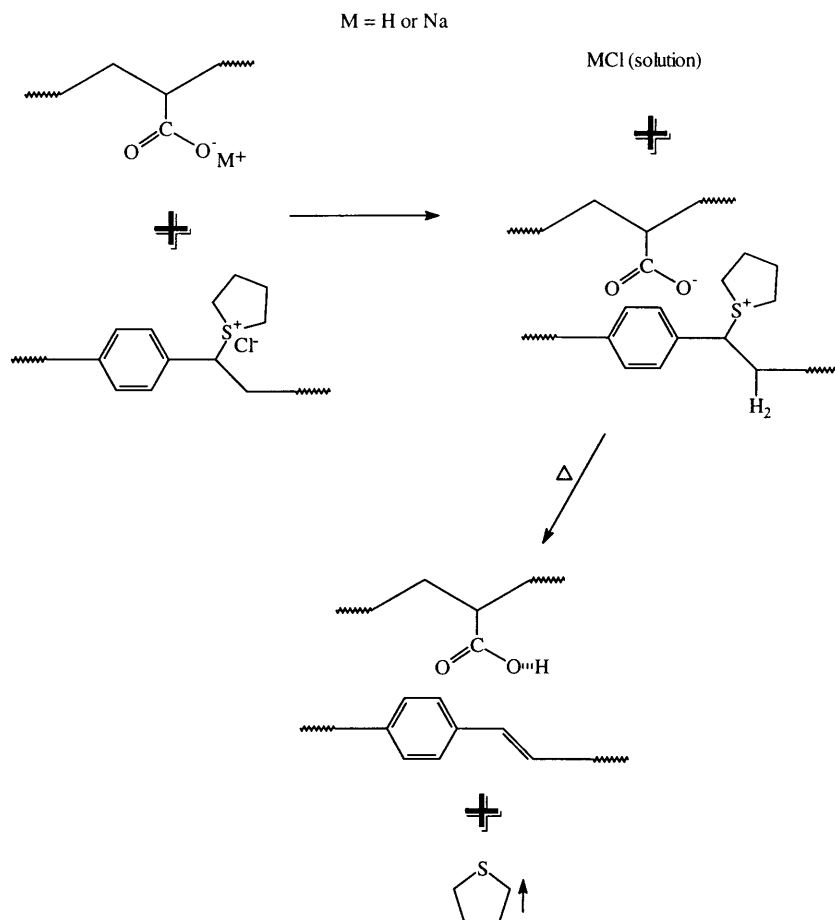
Figure 2-12 - Schematic of the sequential adsorption and then thermal conversion of PPV precursor and PAA

formation of dimers) that is still tethered to the polymer backbone. A small amount of HCl, however, may still be formed due to any repeat units of the PPV precursor that are not ion paired with the PAA.

Upon conversion, tetrahydrothiophene and any residual water are driven out of the film and this can cause a net decrease in the film thickness. Figure 2-13 shows the total film thickness before and after conversion for 20 bilayers of PPV precursor and PAA under conditions where the PAA pH is held constant at 3.5 and the PPV precursor pH is varied from 2.5 to 4.5. In the pH matrix of Figure 2-6, this corresponds to the center row. The pre-conversion thickness values are different from each other just because they each have different bilayer thickness values but the same number of bilayers were put down in each case. Upon conversion, however, we can calculate a
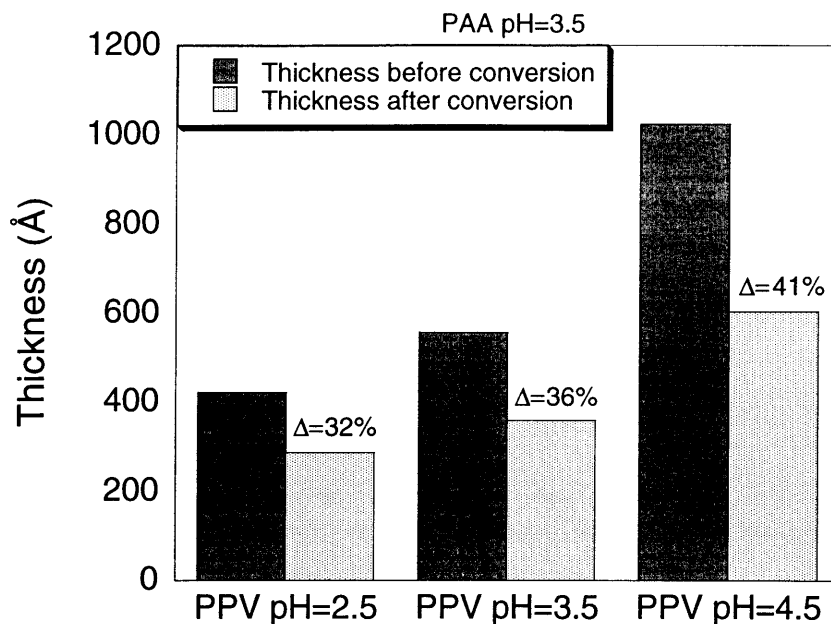
Figure 2-13 - Thickness change upon conversion of PPV/PAA films

percent shrinkage of the film and relate this back to the individual bilayer thickness. It can be seen, then, that as the PPV precursor pH increases, the film shrinks more. This could be attributed to a number of things including the fact that a higher PPV precursor pH causes a slightly higher percentage of PPV precursor in the film. The film is composed of approximately 35% PPV precursor for the (PPV pH/PAA pH)=(2.5/3.5) combination and it increases to about 48% for the (4.5/3.5) combination. Since it is this component which is losing a major constituent of its structure upon conversion (i.e. tetrahydrothiophene), it stands to reason that the more of this material present in the initial structure, the more shrinkage there will be. There are most likely other contributions to the variation in shrinkage such as slight density variations and differing degrees of swelling, however the variation in shrinkage is not very large, hovering around 35-40%, and it is difficult to draw any definitive conclusions.

The effect that the conversion temperature has on the absorption spectra of these sequentially adsorbed films is shown in Figure 2-14 for a 20 bilayer film of PPV and PAA converted under vacuum for 11 hours at a range of temperatures - note that the film

0.8

0.7

0.6

0.5

Absorbance (a.u.)

0.4

0.3

0.2

0.1

0

300   350   400   450   500   550

Wavelength (nm)

— ⊖ — 140°C
— ▫ — 170°C
— ◇ — 230°C
— × — 260°C
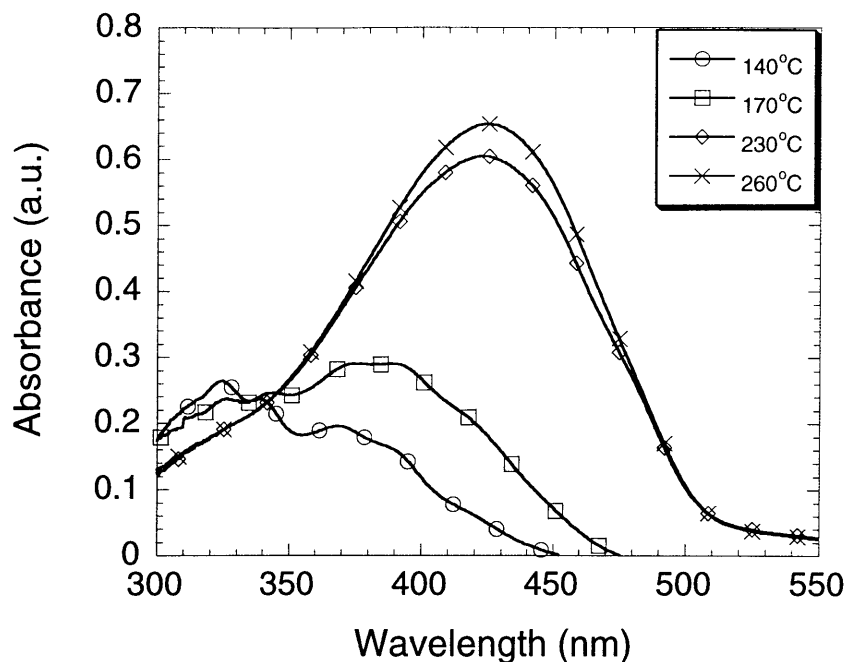
Figure 2-14 - Absorption spectra of PPV/PAA films converted at the indicated conversion temperature for 11 hours

covered both sides of the substrate and hence all absorption values are about doubled. In the unconverted film (not shown) there is no absorption peak in the visible region because there is no extended conjugation. As the conversion temperature is increased, the absorption peak shifts to lower energies (longer wavelengths) as well as increasing in intensity. The intensity increases because at low temperatures, not all of the precursor material gets converted. Higher temperatures result in a higher degree of conversion until the material becomes fully converted, at which point the intensity becomes approximately constant. It can be seen that relatively high temperatures are required to get complete conversion of the precursor. The peak also shifts to lower energies upon increasing the conversion temperature due to an increase in the conjugation length. As the length over which the π electrons are delocalized increases, the bandgap of the material decreases. Enthalpy considerations favor a longer conjugation length because of the resulting lower energy configuration as compared to the nonconjugated structure, however entropic effects limit it by tending to break the conjugation at an average critical length. So as the conversion temperature is increased and more precursor material gets converted, the

conjugation length increases to a certain critical length resulting in a shifting of the absorption peak to longer wavelengths.

2.7 Summary

It has been clearly demonstrated that the conditions of the dipping solutions, such as pH and concentration, used to build up these films significantly influence the resultant film structure. Over a PAA concentration range of 10^{-2} M to 10^{-3} M, it has been shown that the bilayer thickness is relatively insensitive to the PAA concentration. However, because a much more dilute PPV precursor concentration was required for viscosity reasons, the bilayer thickness was shown to be highly sensitive to its concentration. Furthermore, the PAA, being a weak polyelectrolyte, exhibits a pH dependent charge density and this is responsible for the variation in bilayer thickness that is observed as the pH of the solutions is varied. A higher PAA solution pH causes the PAA to adopt a more extended chain conformation in solution and results in a thinner PAA incremental thickness. However, a higher pH in the PPV precursor solution results in an increase in the surface charge density, due to the previously adsorbed PAA layer, and this causes a thicker PPV precursor incremental thickness. As the charge density of the PAA continues to increase with pH, however, a point is reached whereby a transition in the bilayer thickness to very small values is observed. Above this charge density, the system behaves as two fully charged macromolecules which tend to adopt relatively extended chain conformations in solution and form one-to-one contact ion pairs on the surface creating very thin bilayers.

3. LIGHT EMITTING DEVICE CHARACTERISTICS OF PPV/PAA SEQUENTIALLY ADSORBED POLYELECTROLYTE MULTILAYERS

3.1 Introductory remarks

The sequential adsorption of poly(p-phenylene vinylene) (PPV) precursor and poly (acrylic acid) (PAA) discussed in detail in the previous chapter, can now be used to create light emitting devices (LEDs). As these devices now have an extra component in them (namely PAA) as compared with pure spin coated PPV devices, the mechanism of device operation could be, and is, different. It is the purpose of this chapter to explore the fabrication and characterization of these devices and to understand the effects that the sequential adsorption process imparts on the performance of organic light emitting devices.

By carrying out the adsorption process on Indium-Tin Oxide (ITO), a thin transparent electrode, heating to bring about thermal conversion of the PPV precursor, and subsequently thermally evaporating aluminum on top as the opposite electrode, a sandwich-type device architecture is obtained as has already been shown in Chapter 1, Figure 1-7. If a DC voltage is applied between these two electrodes (forward bias = ITO+/Al-), electrons and holes, which are injected at opposite electrodes, can recombine with each other to emit a photon and produce light through the transparent ITO.

In order to understand how these materials emit light, it is necessary to understand the optical properties of the thin polymer films from which they are made. The absorption and photoluminescence (PL) spectra for a PPV sequentially adsorbed film (with PAA) is shown in Figure 3-1. The absorption band is centered at about 420 nm and when the film is excited by light of this wavelength, some of the absorbed energy is re-emitted as radiation of a lower energy, as shown in the photoluminescence spectra of the same figure. This so-called Stokes shift between the absorption and photoluminescence spectra is widely observed in organic materials and is due to the Frank-Condon principle.
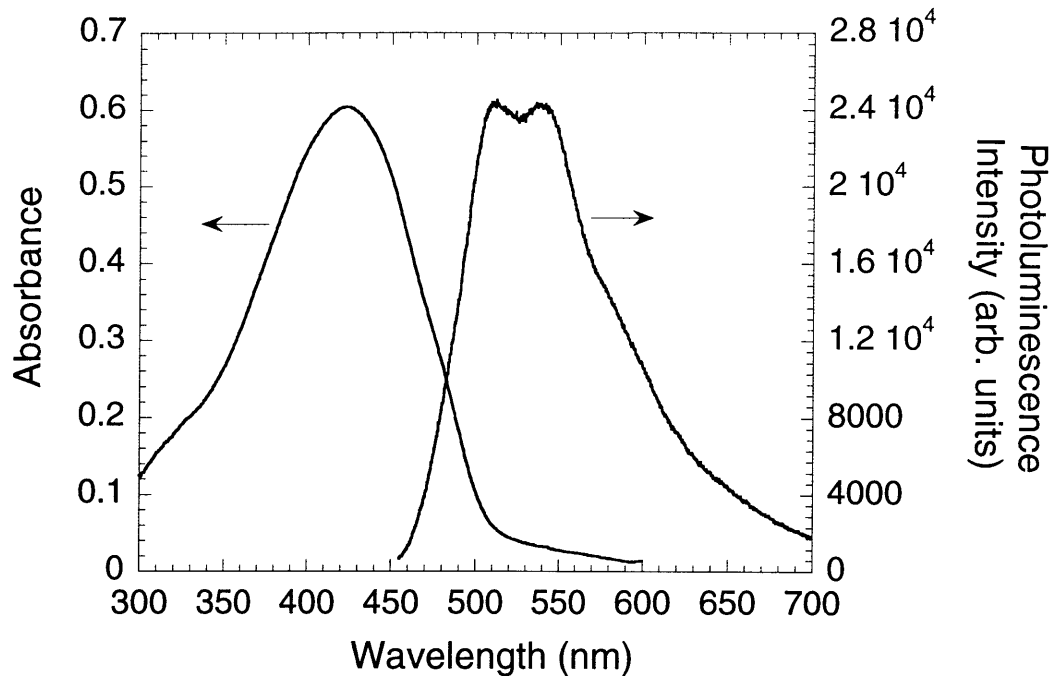
Figure 3-1 - Absorption and Photoluminescence spectra of a PPV/PAA film

Simply put, the response time of electrons is much faster than that of their respective nuclei (because of mass differences). When a molecule absorbs a photon, the electrons quickly respond causing an electronic transition, as reflected in the absorbance spectra, but the nuclei respond much slower. Consequently it is only after the electrons have redistributed that the nuclei have time to relax into a lower energy vibrational state. Emission from this lower vibrational level of the electronically excited state is of lower energy than the initial transition resulting in the observed Stokes shift. In electroluminescence, charge carriers are electrically injected into the material instead of being created by an optical transition. However, the photoluminescence and electroluminescence spectra in general, and for PPV in particular, are frequently very similar indicating that the same excited state species is responsible for both. Because there is little overlap between the absorption and electroluminescence spectra, we can create LEDs with little self absorption.

3.2 Experimental

Light emitting devices were fabricated by sequentially adsorbing layers of PPV precursor and PAA onto ITO coated glass. The conductive ITO was deposited (sputtered) by Donnelly Applied Films onto a glass substrate to give a thin film with a sheet resistance that was less than 15 Ω/square. It was then patterned, using standard photolithographic techniques, and cut by DCI, Inc. to give 2"x1" glass substrates with several ITO stripes that were 3 mm wide and several thousand angstroms thick. The ITO coated glass substrates were then cleaned before use according to the following procedure. They were sonicated for 15 minutes in a 3:1 solution of H_2O:Lysol^{TM} and then in pure H_2O. They were then dried and again sonicated for 15 minutes in each of the following solvents: 1,1,1-Trichloroethane, Acetone, and Methanol. Finally the substrates were rinsed with pure water before use. The polyelectrolyte solutions were made and the sequentially adsorbed layers were prepared in accordance with the procedures described in the experimental section of the previous chapter. The top aluminum electrode was thermally evaporated at a base pressure of at least $2x10^{-6}$ torr, through a shadow mask to create aluminum stripes which were 2 mm wide and several thousand angstroms thick. They were oriented perpendicular to the ITO stripes and so the completed structure consists of a "grid" pattern of intersecting ITO and aluminum stripes with each active pixel being 3mm x 2mm.

The current-voltage characteristics of these devices are measured with a Keithly model 230 programmable voltage source in series with a Hewlett Packard model 34401A multimeter. "Forward bias" corresponds to a positive ITO electrode (the anode) and a negative aluminum electrode (the cathode). A silicon photodiode connected to a Newport model 1830-C optical power meter collects the light output from the face of the device. All of this is completely automated and controlled by a computer using a program written in Labview which communicates to the equipment through GPIB connections. In addition, because devices typically deteriorate if they are tested in air, all testing was done in a glove box that is purged with dry nitrogen and effectively maintained to be free of both moisture and oxygen.

The external quantum efficiency, defined as the ratio of the total number of photons emitted to the total number of charge carriers injected, was calculated as follows. The total number of carriers/second that are injected into the device can be calculated by dividing the measured current by e, the electronic charge. The optical power meter detects the light coming from the device in units of watts (or fractions thereof). If the simplifying assumption is made that all of the photons have a wavelength of 530 nm, approximately the center of the luminescence spectra, the total number of photons/second can be obtained by dividing the measured power by $h\nu$ where h is Planck's constant and ν is the frequency of the radiation. This, however, only gives the total number of photons that impinged on the photodiode. A correction factor must be made that takes into account the fact that photons are emitted in all directions from the front face of the device and that they are not all collected by the photodiode. Greenham *et al.*[67] have shown that the emission of light from the surface of these thin film devices is approximately Lambertian. That is to say that the intensity of light is largest in the direction that is perpendicular to the surface and decreases approximately as the $cos\theta$ where θ is the angle with respect to the surface normal. Furthermore, they have shown that the total flux of light leaving the front face of the device, F_{ext}, is given by

$$F_{ext} = \int_{0}^{\pi/2} 2\pi L_0 \cos\theta \sin\theta d\theta = \pi L_0$$

where L_0 is the flux of light per unit solid angle leaving the device in the forward direction (i.e. at $\theta = 0$). However, the photodiode is only 1cm in diameter and it is placed approximately 1.2cm from the surface of the device. The only light that it collects is that which exits the surface at an angle that is less than about 23° with respect to the normal. This forms a cone of light and any light emitted outside the cone is not detected by the photodiode. Therefore in terms of the above equation, the amount of light that is detected, F_1, is

$$F_1 = \int_{0}^{\theta_1} 2\pi L_0 \cos\theta \sin\theta d\theta = \pi L_0 \left[1-\cos^2\theta\right]_{0}^{23°} = 0.159\pi L_0$$

which means that only about 16% of the total amount of light emitted from the front face of the device is detected. Consequently the external quantum efficiency is given by

$$\eta_{ext}(\%) = \frac{(0.159)(P/h\nu)}{(I/e)}$$

The absorption spectra of these films were measured in a Cary 5E Spectrophotometer which scanned the wavelength of the incident radiation using a monochromator. The photoluminescence characteristics were measured on a Spex Fluorolog in which the source of the radiation was from a Xenon lamp. This broadband radiation was first passed through a monochromator that was set at the wavelength corresponding to the peak absorbance of the film. The photoluminescent radiation was then directed towards a CCD camera which detected the entire spectra simultaneously.

3.3 Effects of PPV/PAA film preparation conditions on device performance

As previously discussed, the thickness of a film can easily be controlled in the sequential adsorption process simply by adjusting the number of bilayers that are deposited. It was shown in Chapter 2, Figure 2-1 that the film grows linearly with an increasing number of bilayers. The effect that this increase in film thickness has on device characteristics for PPV/PAA films is shown in Figure 3-2. The conditions of deposition were such that the PPV precursor solution had a pH of 4.5 and a concentration of 10^{-4} M, while the PAA solution was at a pH of 2.5 and a concentration of 10^{-2} M. First, it can be seen that the turn-on voltage, that at which light begins to be emitted from the device, increases with an increasing number of bilayers (Note that the light output from the 5 bilayer device in this figure is present but is too small to be visible on this scale). In many models of device operation, a critical electric field in the device is required for the device to turn on. Thicker devices require a higher voltage to achieve a given electric field in the device and so the turn-on voltage increases with film thickness. In addition the maximum light output and the external quantum efficiency (photons emitted/electrons injected) also increase with an increasing number of bilayers. The increase in quantum efficiency can be seen by looking at the ratio of the maximum light output to the maximum current density for each device. Thicker devices have a lower current density and a higher light output, both of which give an increase in the quantum efficiency. The explanation comes by considering the position of the recombination zone of electrons and holes in these devices. In general, PPV devices are much better at
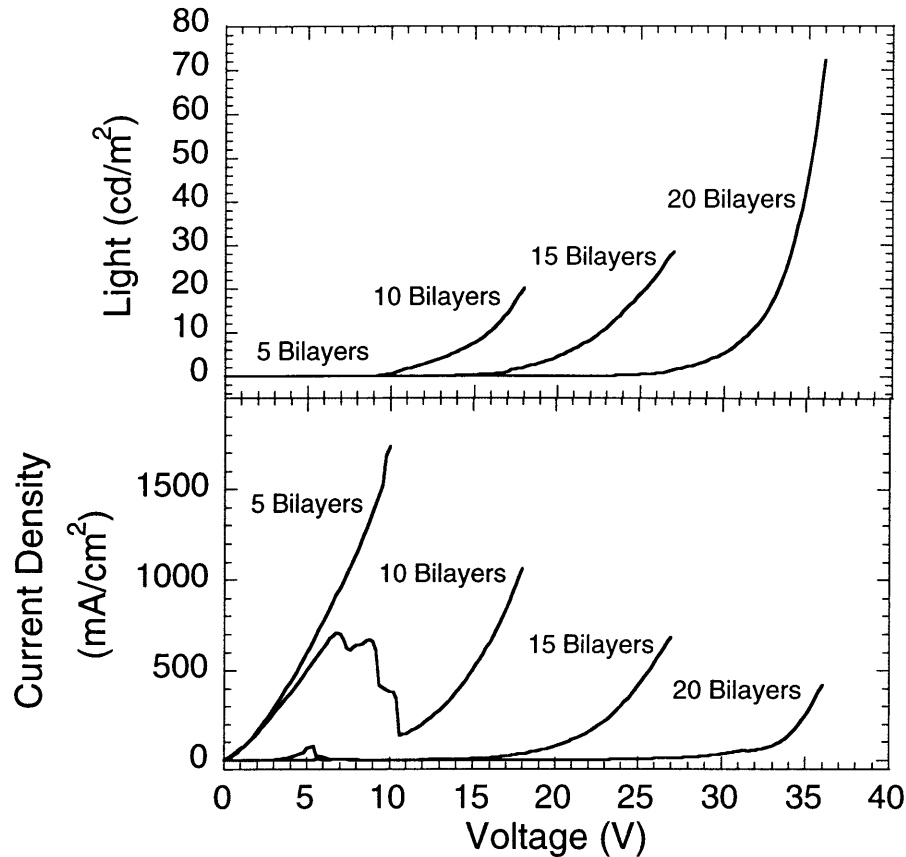
Figure 3-2 - Device characteristics for PPV/PAA films with a variable number of bilayers (see text for deposition details)

transporting holes than electrons and so in forward bias, the recombination zone is close to the aluminum electrode where there are surface states which can serve to quench the luminescence via nonradiative recombination pathways. As the device becomes thicker, several factors contribute to the increase in device performance. First, the number of holes that are transported across the device and reach the opposite electrode before recombining with an electron is a form of leakage current. By going to thicker films, the recombination zone is moved further away from the aluminum interface thereby decreasing the amount of leakage current passing through the device as well as reducing the amount of quenching that happens at that interface. Second, any current due to local defects such as pinholes in the device will also be reduced by going to thicker films. There is also an anomalous current spike in the 10 bilayer sample of Figure 3-2. Similar

observations have been made by other workers[68, 69] but its nature is not well understood. It is not always present, and may possibly be related to the quality of the electrode interfaces.

Changing the film structure by controlling solution pH, as discussed in detail in Chapter 2, can significantly affect the performance of light emitting devices made from these films. From the pH matrix of Figure 2-6, it is seen that films made with a PPV precursor pH of 4.5 and a PAA pH of either 2.5 or 3.5 differ significantly in total bilayer thickness but only slightly in relative composition. The (4.5/2.5) system has an average composition of about 39% PPV precursor and is almost twice as thick as the (4.5/3.5) case which is itself composed of about 48% PPV precursor. Figure 3-3 shows the device characteristics in terms of light output vs. voltage and external quantum efficiency vs.
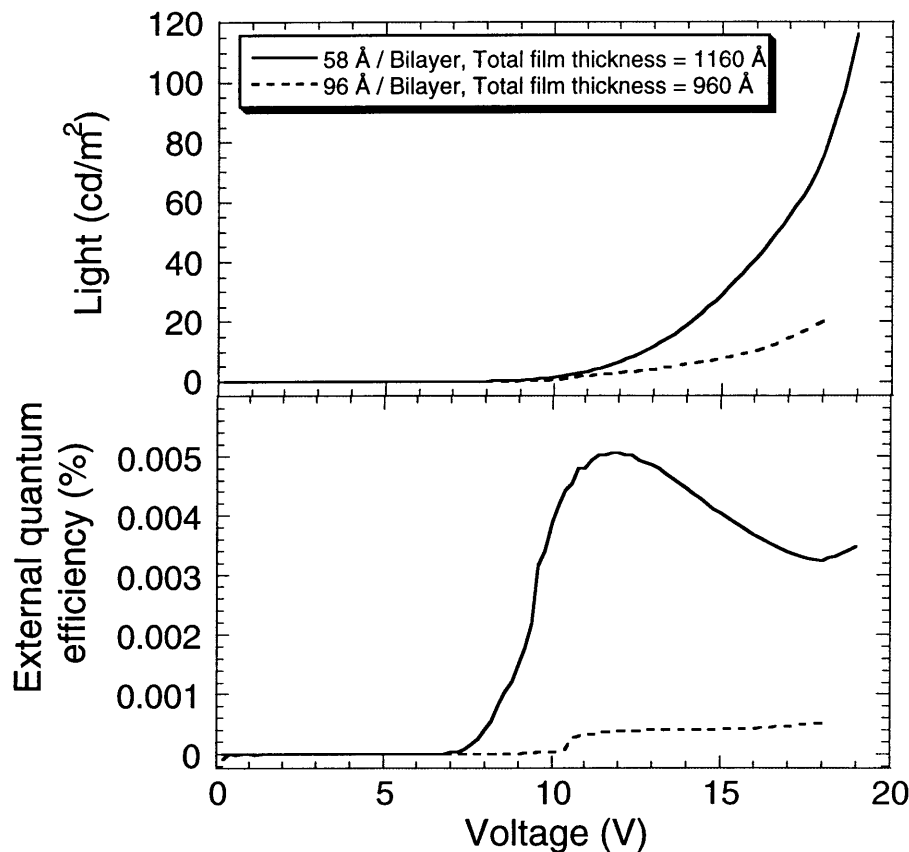
Figure 3-3 - Device characteristics for PPV/PAA films made at pH values of 4.5/3.5 (solid line) and 4.5/2.5 (dashed line) for the PPV precursor/PAA solutions

voltage for devices made with these two different film structures but with similar total film thicknesses. These films were converted at 230°C for 11 hours under vacuum prior to evaporation of the aluminum cathode. The devices made under the (4.5/3.5) pH conditions showed improved device performance both in light output and in external quantum efficiency. At its maximum at 18V, the light output for this system was about 4 times larger than that for devices made under (4.5/2.5) pH conditions. The efficiency on the other hand, increased by about 1.5 orders of magnitude at its maximum at 11V, but slowly decreased at higher voltages. The total bilayer thickness and its composition are the main differences between these two film structures. The bilayer thickness undergoes a much larger change than the composition and is probably the primary reason for the improved device performance. The thicker bilayer structure likely has a less interpenetrated structure with thicker regions of PAA separating the PPV, leading to poorer device performance.

The conditions under which the film is heated to promote thermal conversion can also play a major role in determining the device performance. It is known that the conversion conditions used for pure spin coated PPV precursor is very important in determining device performance and has consequently been the source of a lot of research. Similarly, the conditions used to convert these sequentially adsorbed layers based on PPV are expected to be very significant, albeit slightly different, due to the presence of the counter polymer used to build up the film. Figure 3-4 shows the absorption and photoluminescence (PL) spectra of a 20 bilayer film of PPV and PAA converted under vacuum for 11 hours at a range of temperatures (note that the film covered both sides of the substrate and hence all absorption and PL values are about doubled). As discussed in the previous chapter, in the unconverted film (not shown) there is no absorption peak in the visible region because there is no extended conjugation. As the conversion temperature is increased, the absorption peak shifts to lower energies (i.e. longer wavelengths) as well as increases in intensity. The intensity increases because not all of the precursor material gets converted at low temperatures. Higher temperatures result in a higher degree of conversion until the material becomes
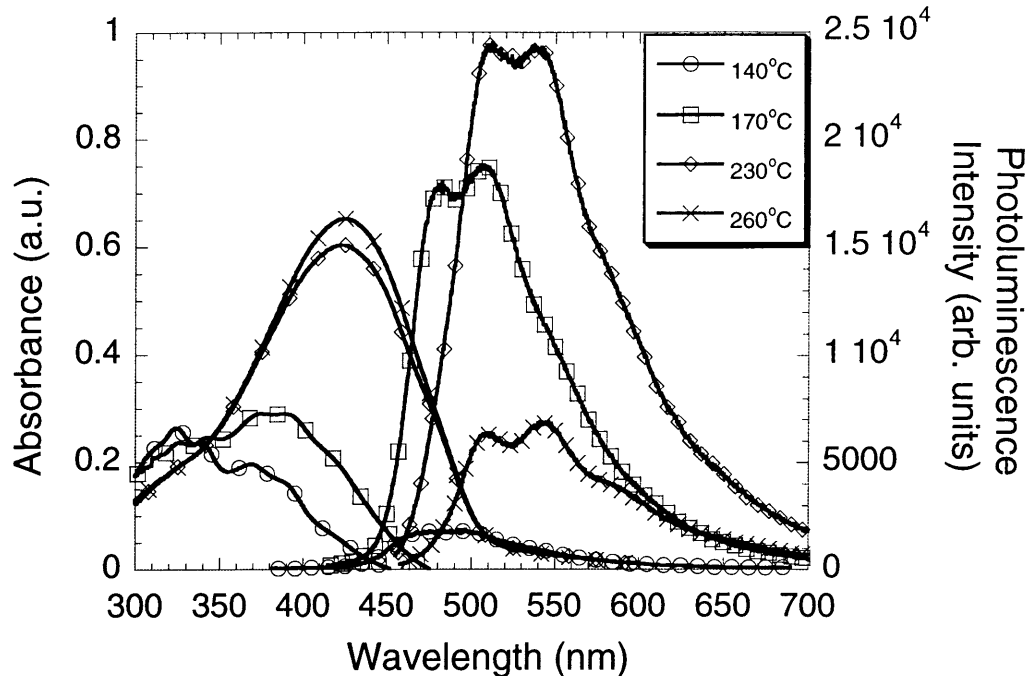
Figure 3-4 - Absorption and Photoluminescence spectra of PPV/PAA films converted at the indicated temperature for 11 hours - the pH of the PPV precursor/PAA solutions used to make the films was 4.5/3.5

fully converted, at which point the intensity becomes approximately constant. The peak also shifts to lower energies upon increasing the conversion temperature due to an increase in the conjugation length. As the length over which the π electrons are delocalized increases, the bandgap of the material decreases. Enthalpy considerations favor a longer conjugation length because of the resulting lower energy configuration as compared to the non-conjugated structure. Entropic effects, however, limit it by tending to break the conjugation at an average critical length. So as the conversion temperature is increased and more precursor material gets converted, the conjugation length increases to a certain critical length resulting in a shifting of the absorption peak to longer wavelengths. The same shifting due to this conjugation length effect happens in the photoluminescence spectra as shown in Figure 3-4. However, the PL intensity goes through a maximum and starts to decrease after $230°C$ which indicates a decrease in the PL quantum efficiency. At elevated temperatures, degradative effects come into play. Other workers[70] have shown that the PPV can react with oxygen to produce carbonyl

groups along the backbone which then act to quench the luminescence and hence decrease the quantum efficiency. Higher temperatures cause more oxidation and therefore more quenching. At still higher temperatures the polymer itself may start to degrade.

Surprisingly then, the device characteristics given in Figure 3-5 show a dramatic improvement with temperature even up to 300°C. In this figure, the maximum light output and external quantum efficiency continuously increase as the conversion temperature is raised from 260°C to 300°C. It can be seen that for a conversion temperature of 300°C, the maximum light output from the device is greater than 1000 cd/m^2 with an estimated external quantum efficiency of 0.04% (as a reference point, the brightness of an average computer screen is about 50-100 cd/m^2). For a pure spin coated
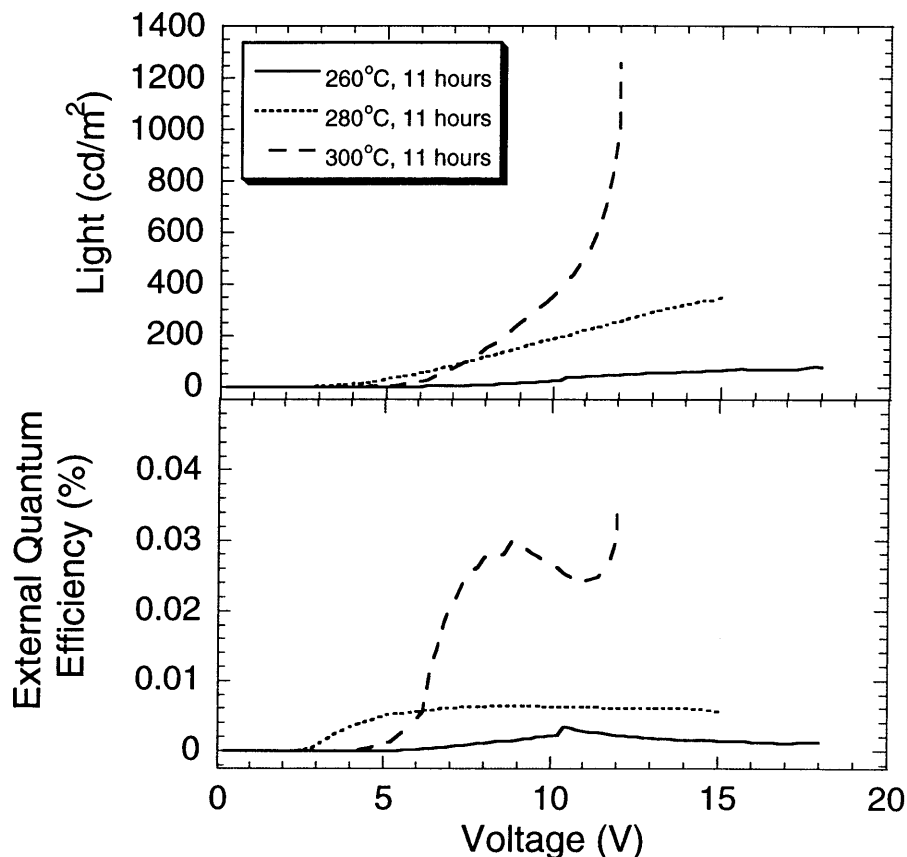
Figure 3-5 - Device characteristics for PPV/PAA films converted at the indicated temperature - the pH of the PPV precursor/PAA solutions used to make the films was 4.5/3.5

PPV film with an aluminum cathode and an ITO anode[71-73], a maximum brightness of only about 10 cd/m^2 is typically reported, significantly less than that obtained here. This result, together with the observation that the photoluminescent quantum efficiency decreases with increasing conversion temperature, implies that another mechanism must be active and responsible for the improved performance in these devices, as discussed in the next section.

3.4 Mechanism of Device Operation

Some insight into the mechanism of device operation can be obtained by examining the temporal response of a device under a constant DC applied bias. Figure 3-6 shows the behavior over time of the current density, light output, and external quantum efficiency of a PPV/PAA device under an applied bias of 10V. The voltage on this device was initially scanned from zero up to 10V two times and after this, it was held constant at 10V to get the results shown in the figure. The current density, light output, and efficiency all increase with time until they reach a maximum, but after this they begin to slowly decrease (not shown). The light output starts out at about 10 cd/m^2 and increases by more than 1.5 orders of magnitude. The current density, however, only increases by a factor of about 3, while the external quantum efficiency increases by a factor of about 20. This behavior, which will be referred to as charging the device, is not observed in films of pure PPV. Recently, as discussed in Chapter 1, an electrochemical mode of operation of thin film light emitting devices has been reported and various models have been put forth[74-85]. These light emitting electrochemical cells (LECs) are typically made by spin coating a film from a common solution containing the luminescent polymer or its precursor (e.g. PPV), additional salt (e.g. $Li^+CF_3SO_3^-$), and an ion conducting polymer (e.g. PEO). A transient response like that observed in Figure 3-6 is attributed to ion motion under the application of an electric field[79, 80, 82]. In this vein, it should be emphasized that the sequentially adsorbed films presented here are not comprised of pure PPV. Rather, the counter polymer that was used to build up the film, namely the PAA, contains carboxylic acid groups that get incorporated into the structure and can play an important role in device operation.
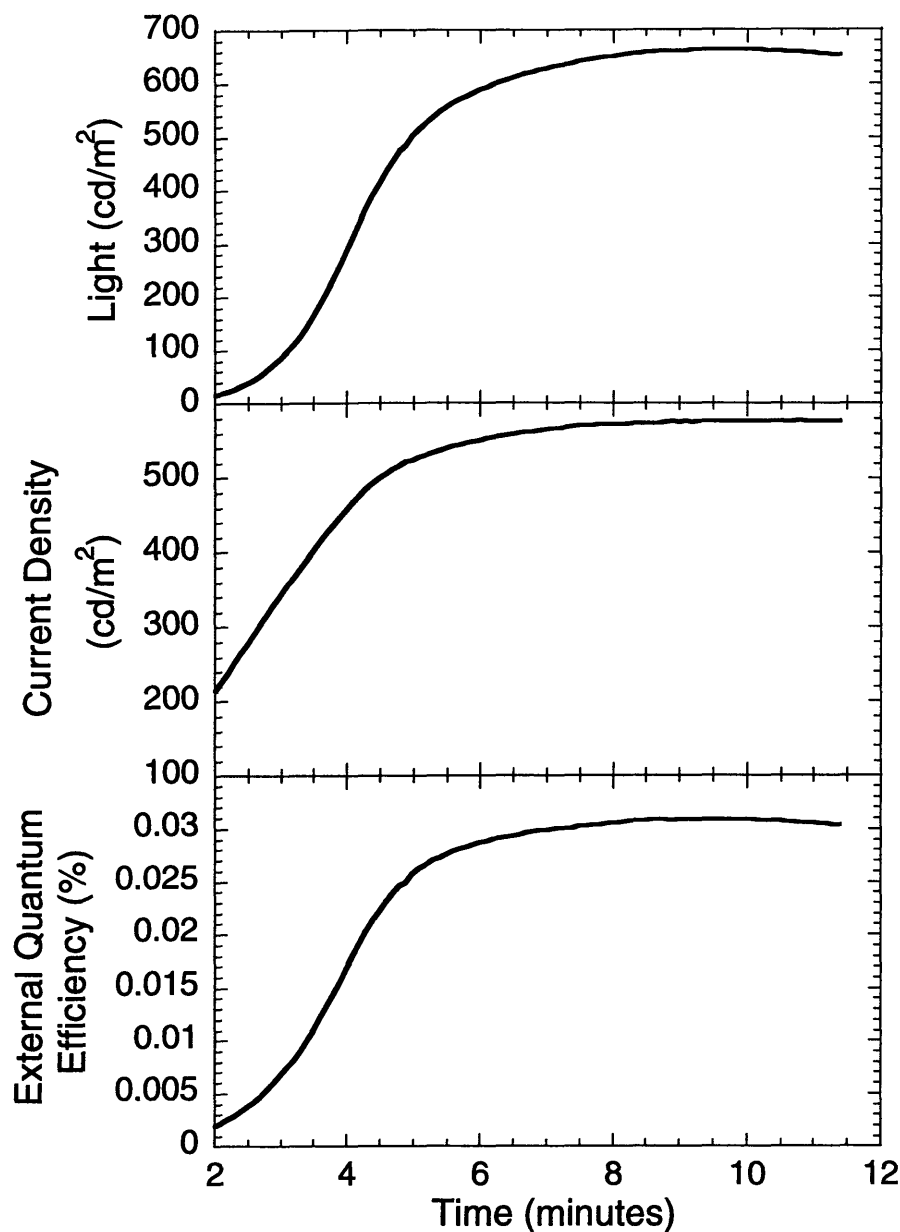
Figure 3-6 - Charging behavior of a PPV/PAA device at 10V - the pH of the PPV
precursor/PAA solutions used to make the film was 4.5/3.5

When a spin coated film of pure PPV precursor is heated in vacuum, the chemical conversion proceeds with the elimination of tetrahydrothiophene and hydrogen chloride gas, as previously shown in Chapter 1, Figure 1-3. As discussed in the previous chapter, the situation is a bit different for sequentially adsorbed films. When the PPV precursor and the PAA are assembled, the charged groups on each of the polymers form ion pairs

and most of the small counter-ions remain in solution as previously shown in Chapter 2, Figure 2-11. The PPV precursor now effectively has a carboxylate counter-ion instead of a chloride, which is of importance when the film is heated to bring about thermal conversion. Schlenoff[86] has shown that precursor films with an acetate counter-ion (i.e. - CH_3COO^-) require temperatures up to 350°C for complete elimination, a temperature much higher than that required for the usual Cl^- counter-ion. The sequentially adsorbed layers, having a carboxylate group as the counter-ion, thus require a higher conversion temperature to achieve complete elimination and good device performance as shown in Figure 3-5. This is emphasized by the fact that when a lower conversion temperature was used, the aluminum electrode formed "bubbles" on its surface during device operation. In this case, because the film was not completely converted, further conversion occurred upon resistive heating of the device during operation and the volatile elimination products caused the resultant damage to the aluminum electrode.

A fundamental difference here, however, is that upon conversion, the acid group is forced to remain in the film by virtue of the fact that it is covalently bonded to the PAA chain. This also has been previously shown in Figure 2-11. Tetrahydrothiophene is still eliminated, but now the charged carboxylate ion reacts to form a carboxylic acid group (neglecting the possible formation of dimers) that is still tethered to the polymer backbone. In essence, then, the converted film is composed of an undoped semiconducting polymer, namely PPV, surrounded by carboxylic acid groups attached to the PAA chains. The degree of ionization of these groups will be dependent on the chemical makeup of the matrix as well as the applied bias. In general, however, the weak carboxylic acid can dissociate into carboxylate anions and protons which can then move under an applied field to give the time dependent characteristics shown in Figure 3-6.

If the applied voltage is scanned from zero up to some maximum forward bias voltage, and then back to zero again, a positive hysteresis is typically observed in both the measured current (I-V curve) and light output (L-V curve). This corresponds to the time dependent charging behavior just discussed and shown in Figure 3-6. If consecutive
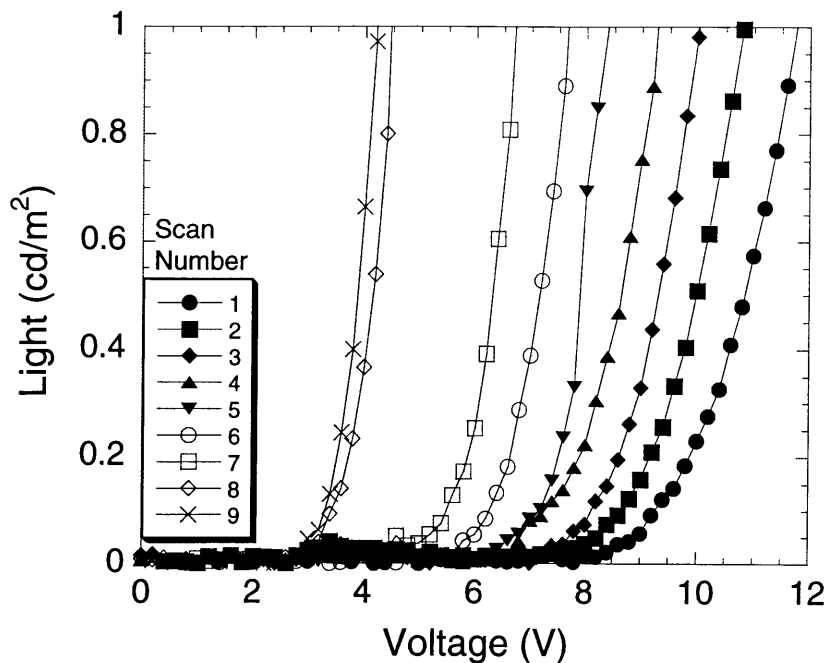
Figure 3-7 - Light-Voltage curves showing the decrease in turn-on voltage as the device is consecutively scanned - the pH of the PPV precursor/PAA solutions used to make the film was 4.5/3.5
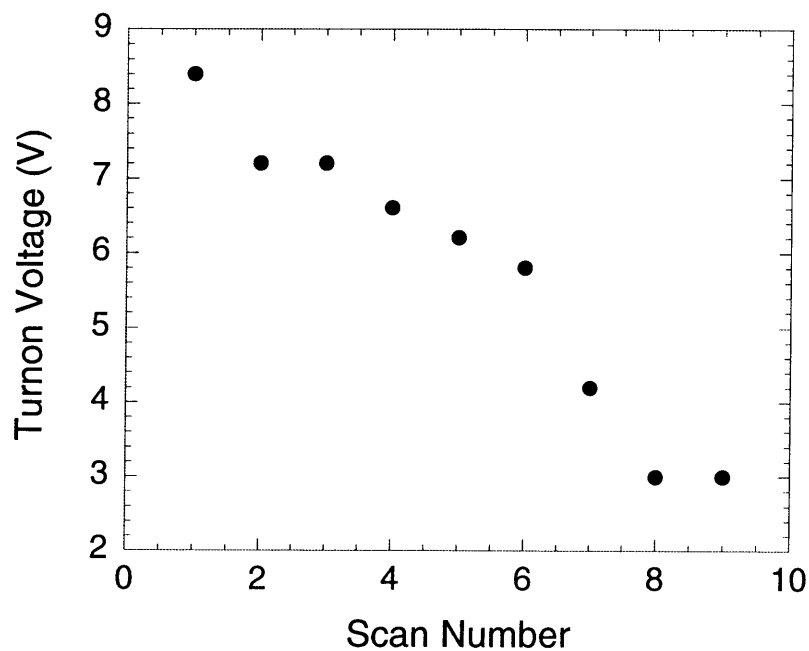
Figure 3-8 - Dependence of the turn-on voltage of PPV/PAA films on scan number - the pH of the PPV precursor/PAA solutions used to make the film was 4.5/3.5

voltage scans are now performed, the resultant L-V curves are shown in Figure 3-7. As more scans are performed on the device, it becomes more highly charged and a decrease in the turn-on voltage is observed. The actual value of the turn-on voltage as the device is scanned consecutively is shown in Figure 3-8. It starts at about 8.5V for the initial scan, but then it decreases until it reaches about 2.5V to 3V where it remains even upon further scanning.

A proposed mechanism of device operation depends upon the presence of mobile ions in the film. Figure 3-9 shows an ideal case of how the ions can redistribute in a sequentially adsorbed film of PPV and PAA. Physically, only the cations are mobile because the carboxylic acid groups are attached to the PAA chain. However, under an applied bias, as the protons move toward the cathode (aluminum, negatively charged) they leave behind carboxylate anions which can still move towards the anode (ITO, positively charged) by the redistribution of the cations. The situation is analogous to electron and hole movement in inorganic semiconductors in which physically only the electrons are mobile. Effectively, however, the holes (absence of electrons) are considered to be mobile positive carriers. Similarly, both cations and anions will be

$M^+ = H^+$ or Na^+
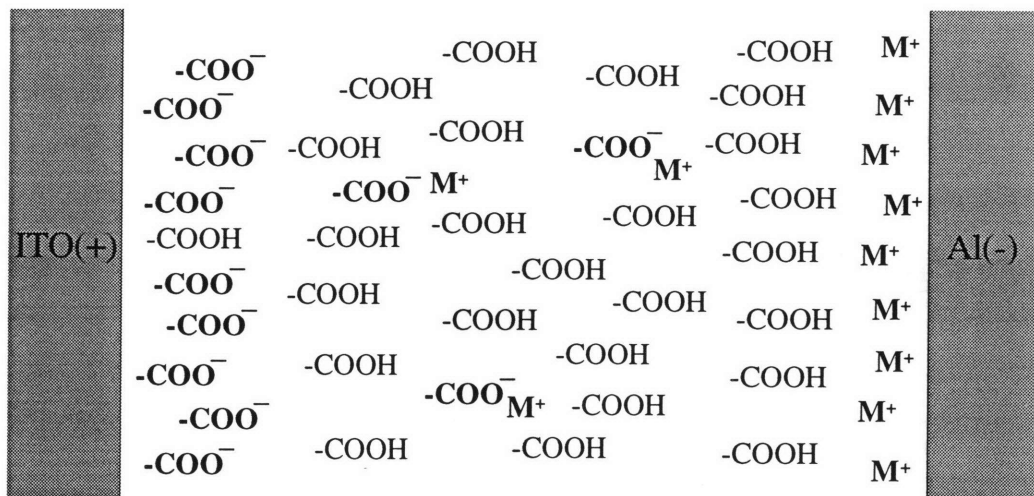
Figure 3-9 - Schematic of the distribution of ions in a PPV/PAA film under an applied bias

driven towards their respective electrodes by the applied voltage. This, in turn, creates a space charge or double layer at each interface which can significantly affect the injection characteristics of electrons and holes.

In Figure 3-10, the charge density distribution, energy band diagram, and electric field distribution are shown for a typical LED and LEC under forward bias. In part (a) of
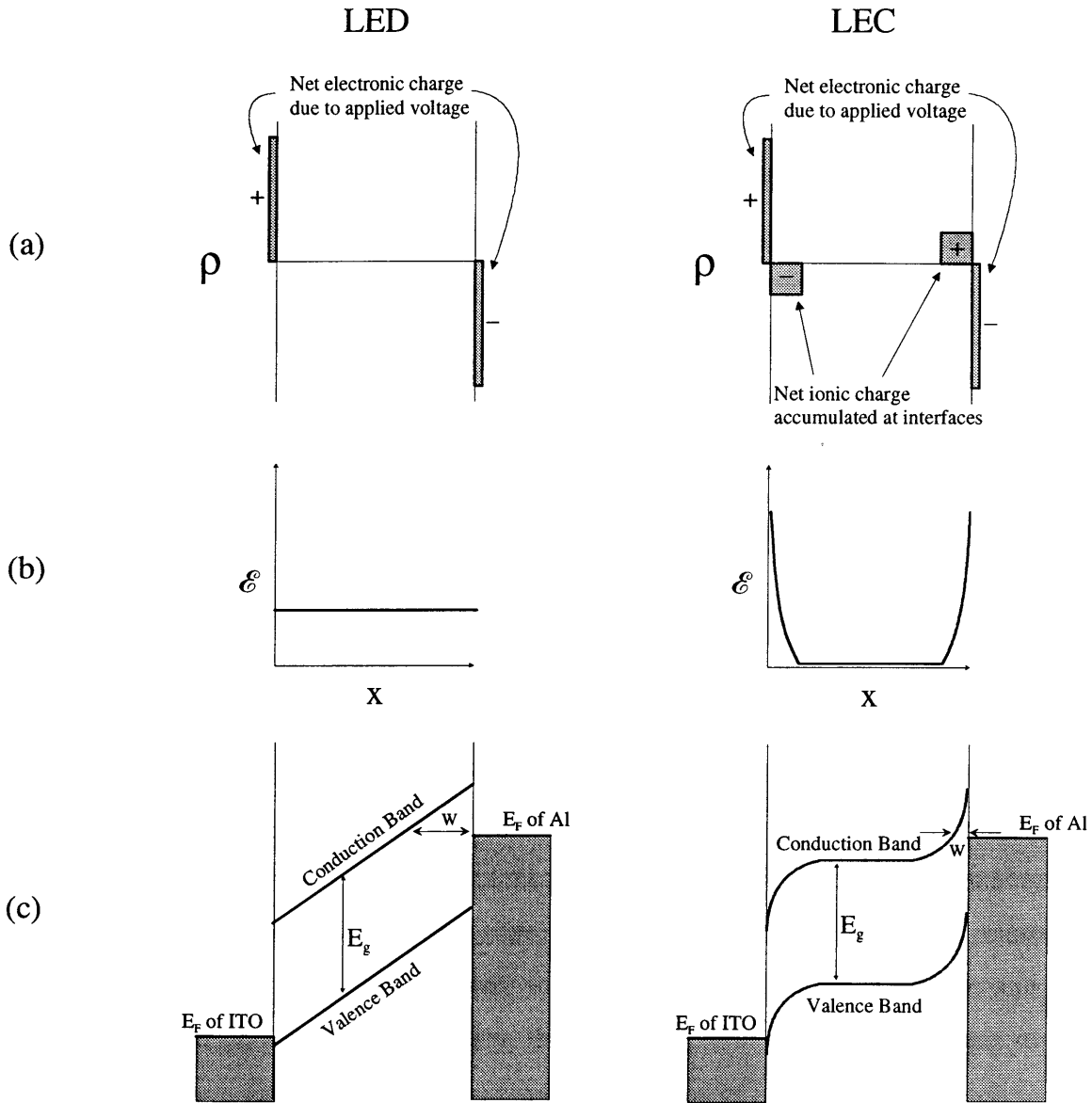
Figure 3-10 - Comparison between the (a) charge density distribution, (b) electric field distribution, and (c) band diagram of an LED and an LEC

the figure, for the case of the LED, there are no ions present in the film and the bandgap is sufficiently large so that the concentration of thermally generated carriers is negligibly small. Therefore the charge on the electrodes due to the applied voltage is not compensated by any charges in the film. For the case of an LEC, as was just discussed, ions are present and can move to the electrodes to counterbalance the charge on the electrodes. Therefore for an LED, there is a constant electric field in the device which is equal to the applied voltage divided by the thickness of the device as shown in Figure 3-10(b). For an LEC, however, since the ions are counterbalancing the charge on the electrodes, all of the electric field is concentrated at the interfaces and no field is present in the bulk of the film. The effect that all this has on the energy levels is shown in Figure 3-10(c). In a normal LED, electrons tunnel through the triangular barrier, of width W, to get injected into the film. A higher electric field, which is effectively equal to the slope of the energy bands, results in a decrease in the barrier width and consequently more electrons being injected. In an LEC, the effect of the ions is to produce a very large electric field at the interface and consequently a significant narrowing of the barrier to injection. Therefore, the slow charging response that was observed in the temporal response of the device shown in Figure 3-6 corresponds to the ions moving to their respective electrodes. The decrease in the turn-on voltage as the extent of this charging increases, as was shown in Figure 3-7 and Figure *3-8*, is due to a decreasing barrier to carrier injection as the ions build up at the interface.

The effect of this charging process on the overall device characteristics is shown in Figure 3-11. Before this charging process begins to occur, the total light output and external quantum efficiency are low, and the turn-on voltage relatively high, in analogy to a device made with pure PPV. In this case, the barrier to electron injection is related to the energy difference between the work function of the aluminum electrode and the conduction band of the PPV. Similarly, the barrier to hole injection is related to the difference between the ITO electrode and the valence band of PPV. It is well known, and can easily be seen by comparing the work functions of aluminum and ITO with the conduction and valence bands of PPV, that the barrier to hole injection is smaller than the barrier to electron injection. Consequently many more holes are injected into the device

than electrons. Some of the holes can then pass through the device without recombining with an electron (leakage current) and the recombination primarily occurs at the aluminum-polymer interface. As the device becomes charged and the barrier to injection as well as the turn-on voltage decrease, the current density increases by factor
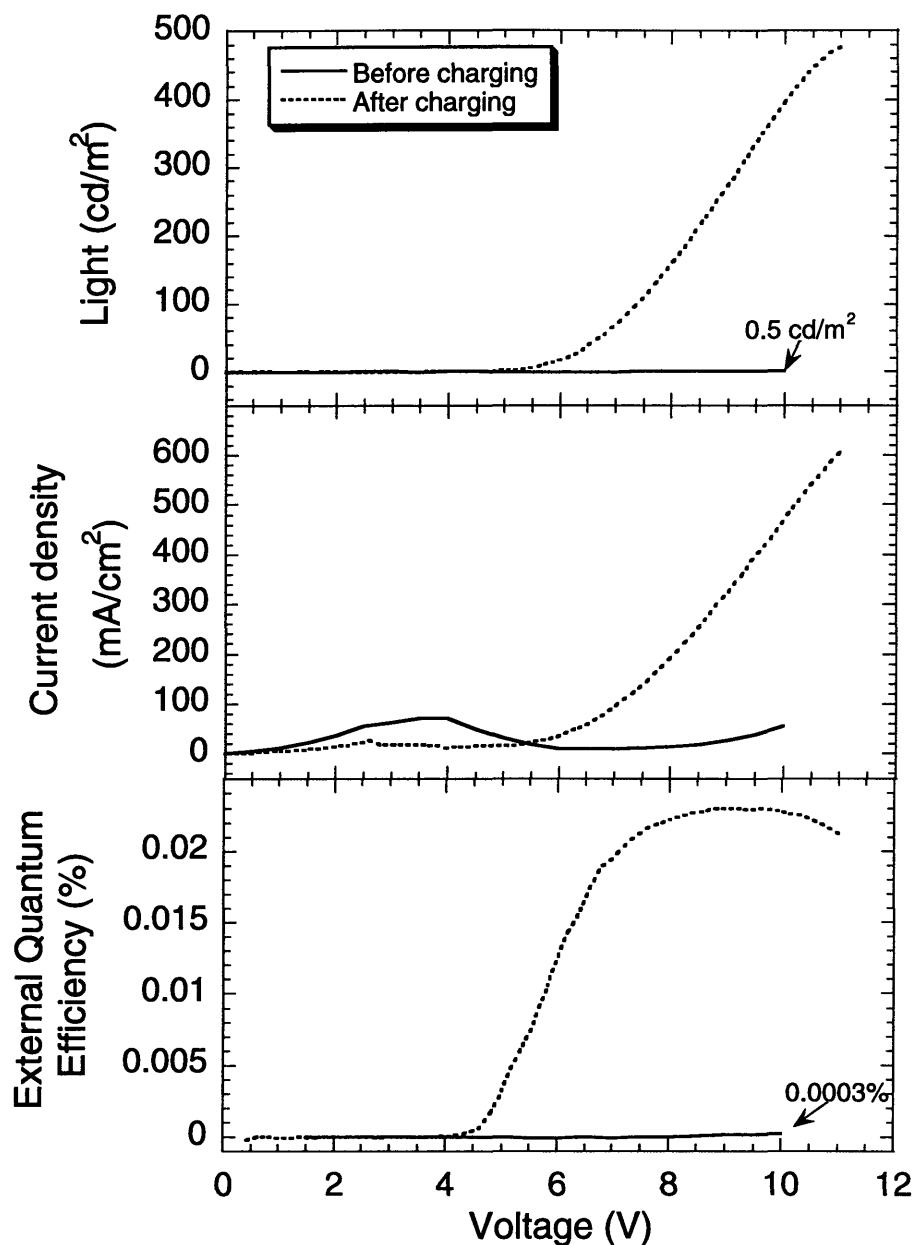
Figure 3-11 - Device characteristics for PPV/PAA films before and after charging - the pH of the PPV precursor/PAA solutions used to make the films was 4.5/3.5

of about 8 in this case. Simultaneously, however, the light output increases by 2 to 3 orders of magnitude and the external quantum efficiency increases by almost 2 orders of magnitude. As the ions move to the interfaces and the barriers to injection decrease, the number of electrons injected starts to approach the number of holes injected. In other words, a better balance of carriers is achieved which results in more carriers recombining to give a higher light output. Furthermore, less leakage current now flows through the device resulting in a higher external quantum efficiency. When the barriers to injection become negligibly small, then the rate of injection of electrons and holes should be equal and the I-V characteristics are no longer dominated by the interfaces, but rather by the bulk. It is interesting to note, however, that this improvement in device performance with charging is relatively irreversible. The device characteristics taken 12 hours after removal of the voltage were similar to those just described after the device was charged. However, a small amount of charging was again observed after the 12 hours suggesting the possible relaxation of the ions after the voltage was removed.

If these results are compared to recent reports for spin coated LECs, it is seen that the external quantum efficiency (after charging) is about an order of magnitude less than that reported by deMello *et al.*[82] However, the difference between the efficiency before and after charging for these PPV/PAA layers is about two orders of magnitude and this is close to the difference between the LED and LEC reported by deMello *et al.* The difference likely lies in the concentration of mobile ions that are present in the films. The values reported for the spin coated LECs were for an ionic concentration of about 10^{20} cm^{-3}, however in these PPV/PAA sequentially adsorbed layers, a much lower concentration is likely present.

In a normal LED based on PPV, rectification behavior is observed whereby little or no current and light are detected in reverse bias [ITO(-), aluminum(+)]. In such a case, electrons would have to be injected from the ITO into the conduction band of the PPV, and holes from the aluminum into the valence band. Such a situation is very energetically unfavorable as is seen by comparing the energy differences between the Fermi levels of ITO and aluminum to the conduction and valence bands of the PPV, respectively (see Figure 3-10(c)). In devices made from sequentially adsorbed layers of PPV and PAA,

however, light and current are observed in both forward and reverse biases as shown in Figure 3-12. It should be noted that in this figure, separate devices were used for the forward and reverse bias tests to eliminate any effects due to charging.

Before charging, light and current are still detected in reverse bias, implying that some level of charging is present even at short times, however a maximum reverse bias light output of only 1 cd/m^2 is observed. As the device becomes charged, a decrease in the turn-on voltage as well as an increase in both the light output and the current density, as described above, are seen in both forward and reverse bias. Since the presence of ions decreases the barrier to injection by concentrating the electric field at the interfaces, the injection characteristics become independent of the electrode work function and both forward and reverse bias current and light are observed. In effect, the band bending that
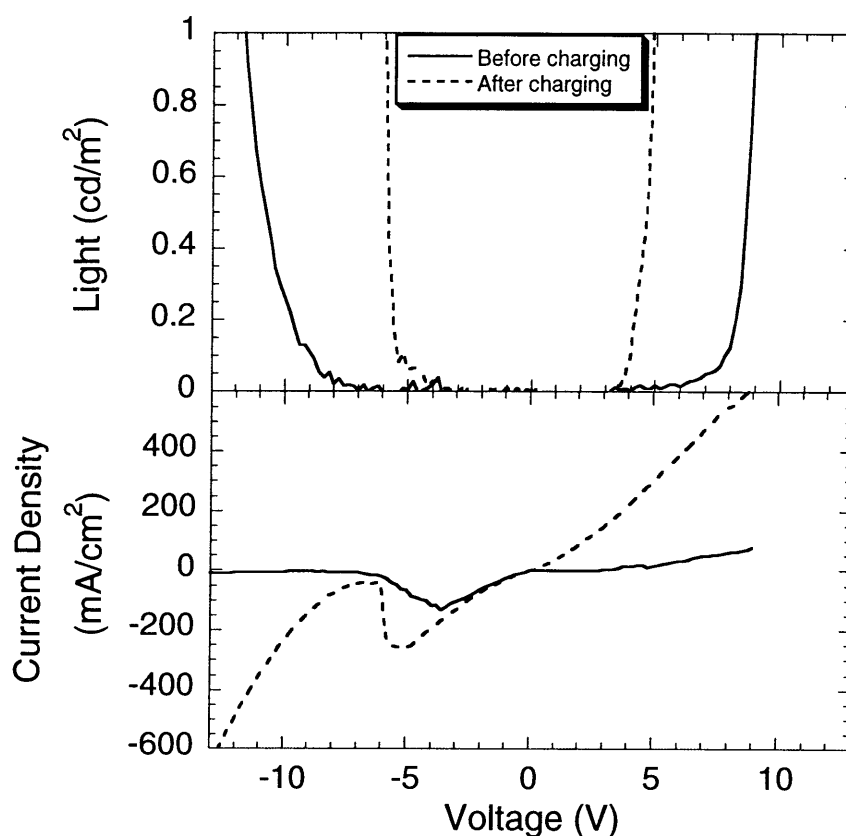
Figure 3-12 - Forward and reverse bias characteristics for a PPV/PAA film before and after charging - Forward and reverse bias scans were performed on separate devices - the pH of the PPV precursor/PAA solutions used to make the films was 4.5/3.5

occurs at each interface sufficiently reduces the barrier so that the injection characteristics become independent of the relative energy levels. However, it should be noted that the device characteristics are not completely symmetrical in forward and reverse biases. In general, the turn-on voltages for reverse bias behavior are generally higher than the corresponding forward bias case. Furthermore, the light output in reverse bias is usually lower than that in forward bias. In Figure 3-12, the maximum light output in forward bias after charging was about 350 cd/m^2 and that for the reverse bias case was 60 cd/m^2, both at 13V. This may be related to the ionic conductivity in these films. No additional salt ions or ion transporting polymer was added to these films, as is typical for LECs based on spin coated systems. As such, the concentration of ionic species as well as their mobility will be of prime importance in the operation of these devices. This was
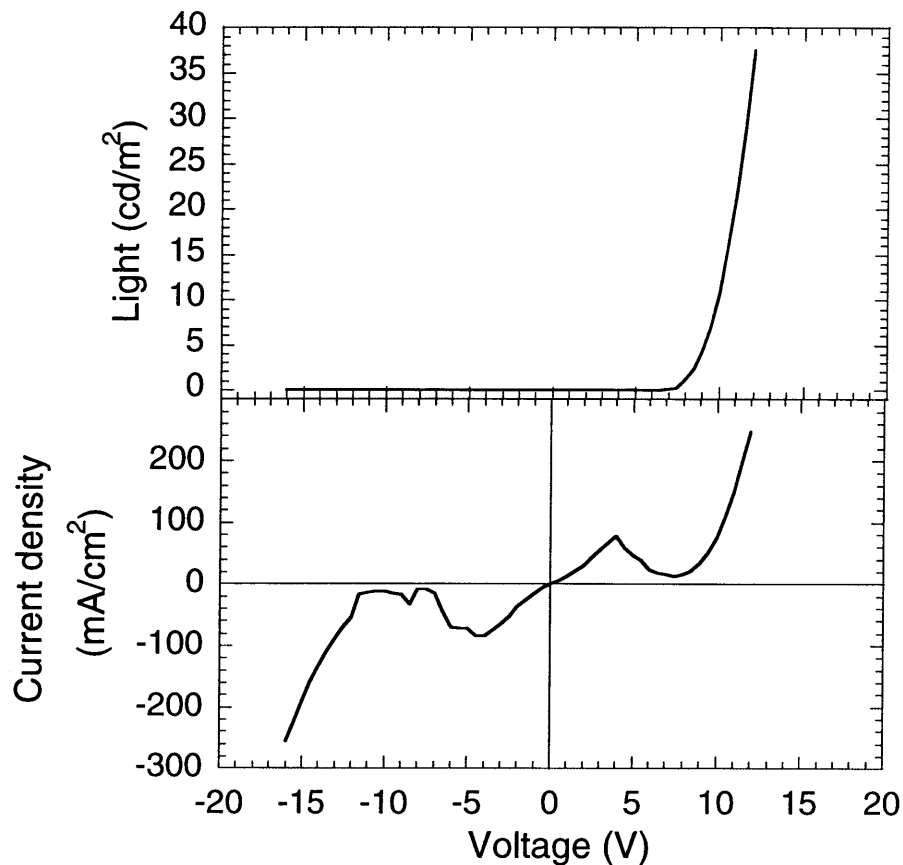
Figure 3-13 - Forward and reverse bias characteristics for a PPV/PAA film after charging under a forward bias - the pH of the PPV precursor/PAA solutions used to make the films was 4.5/3.5

one of the prime motivating factors underlying the study of ionic conductivity issues in sequentially adsorbed films presented in the next chapter.

An interesting effect occurs if a device is charged in forward bias and then tested in reverse bias, as shown in Figure 3-13. As expected, light and current are observed in the forward bias. However, in reverse bias, no light is detected but current is still observed. This type of testing has not been extensively explored and its behavior is not completely understood. It is possibly related to the kinetics of reversing the formation of the space charge layers, but this speculation has not been substantiated.

3.5 Modification to the PPV/PAA device structure

Ionic conductivity appears to play a crucial role in the operation of these devices. It is believed that during the sequential adsorption process, most of the small counter-ions associated with the charged groups on each polymer are displaced in favor of forming ion pairs between the groups attached to the polymer as shown in the first step of Figure 2-11. However since the PAA is a weak acid, the degree of ionization of the carboxylic acid groups depends upon pH. Therefore before conversion, the film not only has charged carboxylate anions paired with the PPV precursor, but also unpaired free carboxylic acid groups. Indeed, this is the very effect that controls the pH dependent bilayer thickness presented in Chapter 2. If the film is made at a pH where a significant number of free acid groups are incorporated into the film, then immersing it into water at a high pH after the adsorption process is complete will cause these free acid groups to ionize. If there is any salt present, an ion exchange reaction can occur to incorporate these cations into the film. Furthermore, since the entire film is swelled by water, it is very likely that in addition to the ion exchange reaction occurring, excess salt in the form of both cations and anions are incorporated into the film. This procedure was done for a number of salts and the I-V and L-V results are shown in Figure 3-14 for several such systems. In general the device characteristics for films with added salt were quite inferior to those films without. Lower light output, higher operating voltages, and poorer device stability were observed for films with added salt.
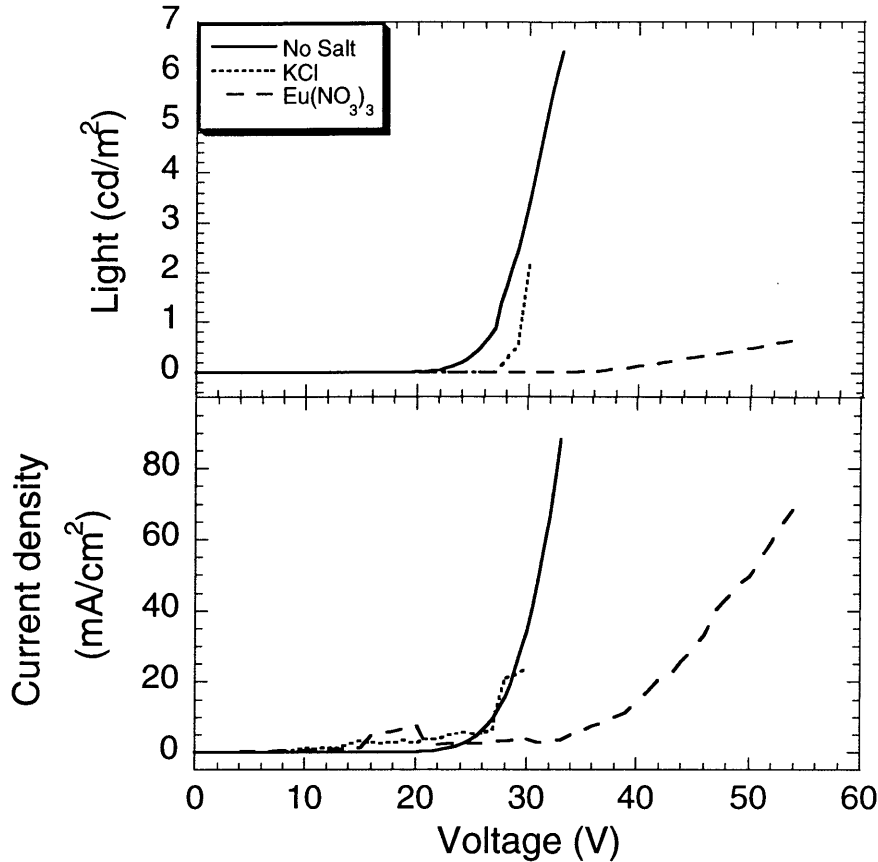
Figure 3-14 - Device characteristics for PPV precursor(pH 4.5)/PAA(pH 3.5) films that were dipped into the indicated aqueous salt solutions for 1 hour before thermal conversion

Part of the explanation may come from examining the absorption and photoluminescence spectra for these and other films with added salt as shown in Figure 3-15. The decrease in intensity and blue shifting of the absorption spectra when salt is added suggests that added salt tends to hinder the conversion of the PPV precursor, resulting in a less converted material (intensity decrease) and a smaller conjugation length (blue shift). However, these changes are insufficient to fully account for the quenching observed in the photoluminescence when salt is added to these films. In chemically doped conjugated polymers, the dopant ions tend to quench the photoluminescence by providing sites for non-radiative recombination and it is believed
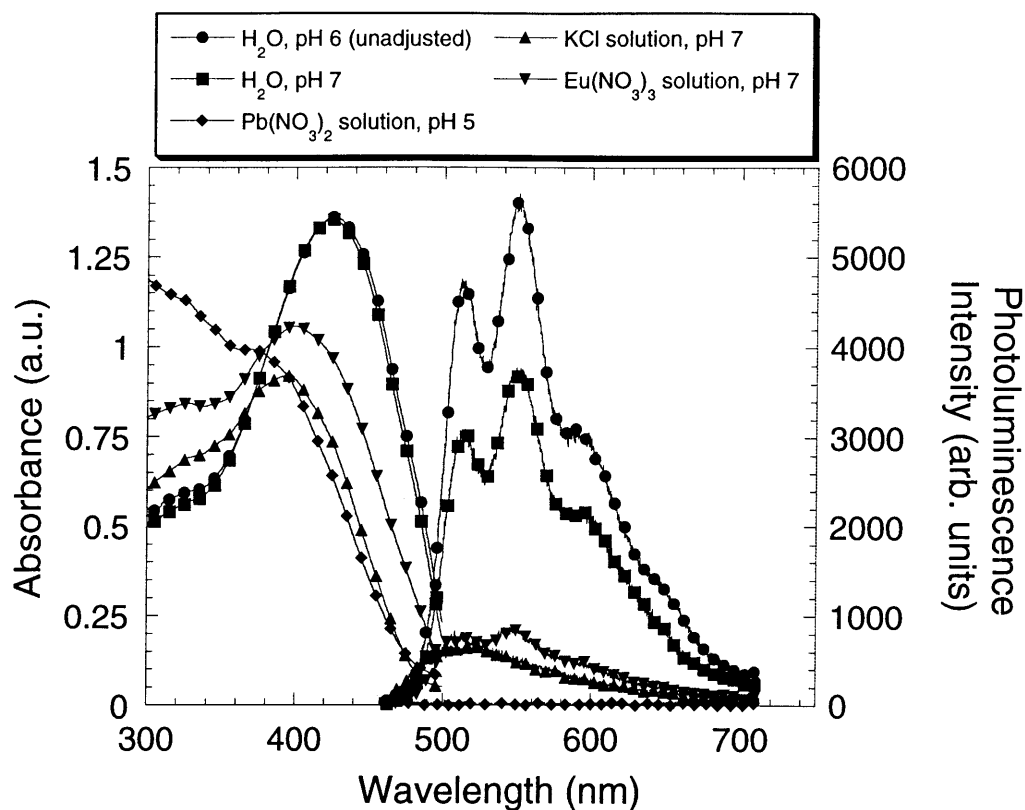
Figure 3-15 - Absorption and Photoluminescence spectra for PPV precursor(pH 4.5)/PAA(pH 3.5) films that were dipped into the indicated aqueous salt solutions for 1 hour before thermal conversion

that the added salt ions are acting similarly here. It is interesting to note, however, that in typical LECs made by spin coating, this quenching effect is not generally observed[82]. The source of the discrepancy is not well understood.

One of the advantages of the sequential adsorption technique is that it affords molecular level control over the film architecture. Layers that are tens of angstroms thick can be manipulated and deposited onto the surface. It has recently been found by Rubner *et al.*[87, 88] and others[89] that a thin electronically insulating layer in between the active light emitting layer and the cathode (aluminum in this case) tends to increase the device efficiency. Figure 3-16 shows the device performance when thin insulating layers of PAH and PAA (structures shown in Chapter 1) are sequentially adsorbed onto a PPV/PAA light emitting platform. The figure shows light output versus current density
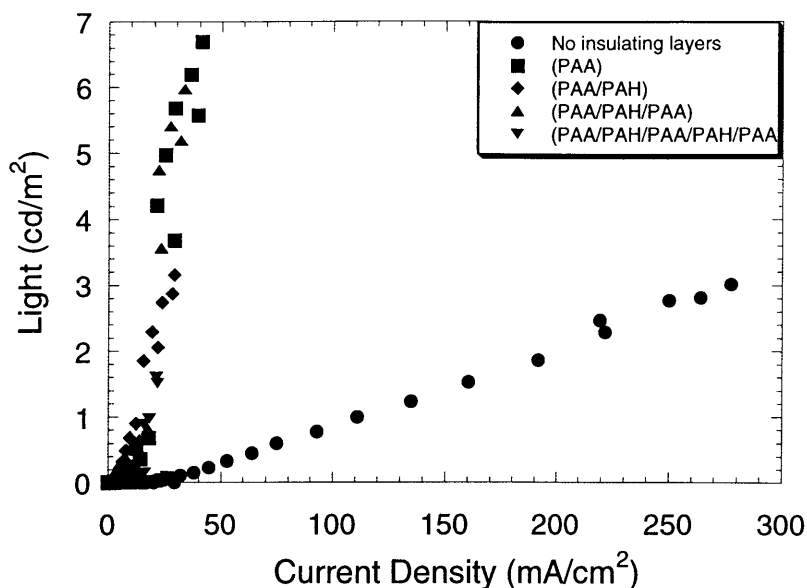
Figure 3-16 - Device characteristics for PPV/PAA films with thin insulating layers at the aluminum interface

with voltage as the implicit variable. The slope of the graph is directly proportional to the efficiency of the device. Even one monolayer of insulating material is sufficient to increase the efficiency by about 14 times. Then as the insulating layer becomes thicker, the total current density and light output decrease, but still the efficiency (i.e. slope) remains constant. Several factors could be responsible for this behavior which stems from the location of the recombination zone. As previously noted, the recombination zone in devices made from PPV is near the aluminum electrode due to the fact that many more holes are injected at the ITO contact than electrons at the aluminum, and that the hole mobility is slightly greater than the electron mobility. In general, the aluminum interface causes quenching of the excitons and so by moving the recombination zone away from the aluminum interface, the device efficiency increases. Others[89] have explained this phenomenon by considering that the barrier to electron tunneling decreases by having a large voltage drop across the insulating layer (i.e. large electric field). However, more work is needed to make any definite conclusions here.

3.6 Summary

In summary, it has been shown that light emitting devices based on PPV/PAA sequentially adsorbed layers behave quite differently than normal spin coated PPV devices. They show characteristic features which suggest an electrochemical mode of operation. A time dependent charging behavior was seen which resulted in an increase in the current density, but an even larger increase in both the light output and the external quantum efficiency. A light output of greater than 1000 cd/m^2 (about 10 times the brightness of a computer monitor) was observed which is significantly higher than that typically reported for films of pure PPV with an aluminum cathode and an ITO anode. The turn-on voltage was also shown to decrease from about 8V to about 3V in forward bias upon charging. In reverse bias, a similar increase in the light and current, and a decrease in the turn-on voltage, was also observed. These results suggest that the mechanism of device operation is similar to a light emitting electrochemical cell (LEC). Ions present in the film can move under the influence of an applied field and build up at the interface, thus modifying the injection characteristics, and are responsible for the improved device performance.

4. DIELECTRIC PROPERTIES OF PAH/PAA AND PAH/SPS SEQUENTIALLY ADSORBED POLYELECTROLYTE MULTILAYERS

4.1 Introductory remarks

Sequentially adsorbed layers based on poly(allylamine hydrochloride) (PAH) with both poly(acrylic acid) (PAA) and sulfonated polystyrene (SPS), have been studied extensively in terms of their adsorption characteristics[90-100]. The chemical structures of these materials have been repeated for convenience in Figure 4-1. These materials are not electrically active like the conjugated materials described in previous chapters and the electrical characteristics of sequentially adsorbed layers made from them have not been studied in depth. They are, however, of interest for a number of reasons.

Poly(acrylic acid)
(PAA)

Poly(styrene 4-sodium sulfonate)
(SPS)

Poly(allyl amine hydrochloride)
(PAH)
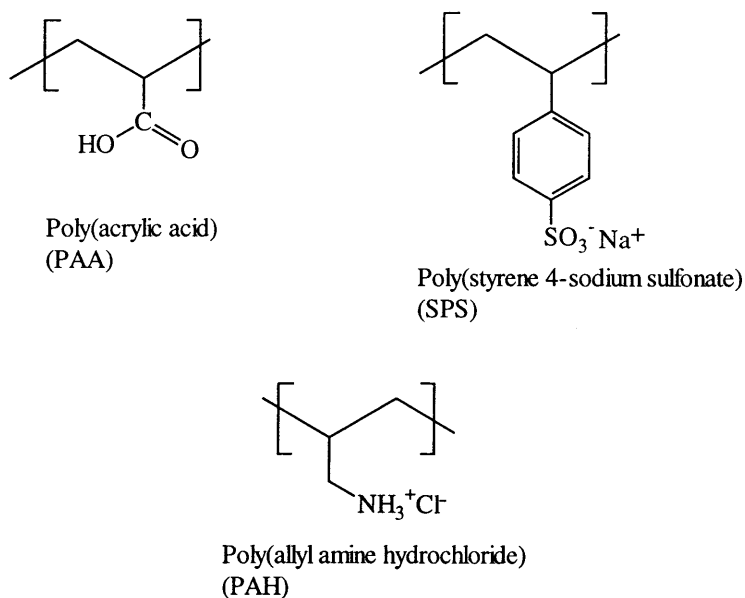
Figure 4-1 - Chemical structures of some typical polyelectrolytes

These materials are simple polyelectrolytes and the adsorption characteristics of the PAH/PAA system are qualitatively similar to those for the PPV precursor/PAA system described in previous chapters. The polyanion, PAA, is the same in both systems. It is a weak polyelectrolyte whose charge density can be controlled by changing the pH. The polycation, PAH, is similar to the PPV precursor in the sense that over the pH range

of interest, the polymer is fully charged and is essentially independent of pH. It has been shown that the ionic conductivity in films made for light emitting devices can be of great importance in determining their characteristics. For this reason, films composed of PAH and PAA can potentially act as a model system in which to understand the mechanism of ionic transport in these sequentially adsorbed layers. Furthermore, the electrical properties of these films are also of interest in their own right. As will be shown in this chapter, understanding the influence of preparation conditions on the electrical characteristics can be used to obtain a more fundamental understanding of the sequential adsorption process itself, which is still in its infancy.

These films may also be of interest in battery and fuel cell technology. For thin film batteries, solid polymer electrolytes have been extensively investigated. Solid electrolytes have certain desirable characteristics over liquid ones. Leakage of the electrolyte from the battery housing becomes a mute point and the fact that it is a solid means that it is structurally easier to make a smaller cell using conventional processing techniques. A longer shelf life and wider operating temperature range are also among the advantages of solid electrolytes[101]. Usually, however, solid electrolytes have a significantly lower ionic conductivity than liquid ones and this has been the impetus for a lot of research into increasing the conductivity of solid electrolytes. In addition, polymer electrolytes are generally preferred to other materials like glass or ceramics in the sense that they are flexible and more pliable and can better withstand any volume changes[101]. Again however, the conductivity issue plays a dominating role.

An important design criteria is the transference or transport number. In these materials, both cations and anions, as well as electrons, can contribute to the conductivity. The total conductivity is then just the sum of all these contributions, $\sigma_{TOTAL} = \sigma_1 + \sigma_2 + \sigma_3 + \cdots$. The transference number of a particular species is then just the fraction of the total that it contributes to the conductivity, $t_n = \sigma_n / \sigma_{TOTAL}$. Frequently the electronic conductivity is negligible and so only the cationic and anionic contributions are important[102]. For thin film, solid polymer electrolyte rechargeable batteries, a high cationic transport number is desired. The anion should remain immobile while the cation easily shuffles between the cathode and anode. Some of the most promising candidates

for these solid polymer electrolytes are polar polymers such as polyethers (i.e. poly(ethylene oxide) (PEO)), mixed with a lithium salt such as $Li^+CF_3SO_3^-$. The salt dissolves in the PEO which is then capable of transporting these ions. One of the problems, however, is that the $CF_3SO_3^-$ anion is not completely immobile and in fact can contribute significantly (in some cases greater than 50%!) to the overall ionic current[103]. One possible solution is to make use of polyelectrolytes whereby the anions are attached to the polymer chain, rendering them immobile, and the associated cations would have a transference number of 1. Unfortunately, these polyelectrolytes are usually glassy and brittle in the absence of solvent and very low ionic conductivities are observed for the pure materials which is presumable due to extensive ion pairing. The idea of a cationic transference number of 1, however, is very tempting and attempts have been made to improve their conductivity. The blending in of plasticizers such as poly(ethylene glycol) (PEG) has been shown to significantly enhance the conductivity[104, 105]. Taking this a step further, plasticizing groups can be copolymerized with the polyelectrolyte to enhance the conductivity[106].

Candidates other than PEO-like materials have been looked at for use as the matrix polymer. Polyelectrolyte complexes are formed when a polycation and a polyanion are mixed together in solution. They have been studied for years in the field of ion exchange membranes. Due to the attractive electrostatic interaction between polycation and polyanion, they complex together and precipitate out of solution. The complex that is formed is a polar matrix which is capable of dissociating ion pairs into free cations and anions and could therefore act as an electrolyte when mixed with a salt[107]. It is interesting to note that this scenario is very similar to the sequential adsorption of oppositely charged polyelectrolytes which is essentially the controlled formation of a polyelectrolyte complex. Other types of complexes have also been studied where, for instance, hydrogen bonding provides the requisite attractive force between polymers[108, 109].

It is the goal of this chapter, then, to examine the electrical (impedance and dielectric) characteristics of sequentially adsorbed layers of the aforementioned materials. This will lead to a better understanding of the nature of the sequential adsorption process.

The information gained from this chapter can then additionally be used to further understand the mechanism of device operation described in previous chapters and to potentially help in creating more efficient light emitting devices. Furthermore, this initial research may also lead to some interesting developments in the field of solid polymer electrolytes.

4.2 Experimental

The poly(acrylic acid) (PAA) was purchased from Polysciences and it had a molecular weight of about 90,000. It was received in the form of a 25% aqueous solution and it was diluted with pure water to obtain the desired concentration for sequential adsorption. The poly(sodium 4-styrenesulfonate) (SPS) as well as the poly(allylamine hydrochloride) (PAH) were obtained from Aldrich in solid form and both had a weight average molecular weight of approximately 70,000. Solutions were made by dissolving the polymer in water to obtain the desired concentration. All of the above solutions were filtered through 2.5 micron filter paper and their pH was adjusted as described previously. The polymers were then sequentially adsorbed onto an ITO electrode with the subsequent thermal evaporation of an aluminum electrode in accordance with the procedures described in the experimental section of the previous chapters.

Impedance and dielectric measurements were carried out on a Solartron model 1260 Impedance/Gain-Phase Analyzer which has a frequency range of $10\mu Hz$ to 32MHz. The instrument was controlled by a computer through the use of a program called Zplot created by Scribner Associates, Inc. In most cases, the AC amplitude was 10mV but no DC bias was applied. The data was obtained as real and imaginary impedance values and were transformed into the dielectric domain according to the equations given in chapter 1. Film thickness values were measured with Tencor surface profiler using a 5mg stylus force. Data analysis, including the simulation runs described in the chapter, were done using the ZView program made by Scribner Associates, Inc.

The devices were tested in one of two specially made sample chambers. Most of the measurements were performed in a chamber which had the capabilities of being evacuated or purged with a flowing gas. The temperature was constantly monitored by a type-K thermocouple placed in close proximity to the sample itself. The thermocouple

was connected to a Eurotherm programmable temperature controller which heated the chamber resistively. In most cases, pure Argon was purged through the chamber during testing, however for the cases in which the samples were exposed to a humid environment, the Argon was first bubbled through water before flowing through the sample chamber. For the case when the samples were heated above a temperature of about 110°C, testing was performed in a separate sample chamber. In this case, the sample was placed in a quartz tube which was then heated in a tube furnace. Again, the temperature was monitored by a type-K thermocouple and the chamber was purged with Argon during device heating and testing.

4.3 Results

4.3.1 Basic Device Behavior and Modeling

The same device architecture that was used to create light emitting devices was again used here. Sequentially adsorbed layers were built up on an ITO electrode and an aluminum electrode was then thermally evaporated on top. The impedance (dielectric) characteristics were then measured as a function of frequency, as described in Chapter 1. Figure 4-2 and Figure 4-3 show the typical type of response that is exhibited by films of PAH and PAA. For the purposes of illustration, these figures show the response at about 108°C, under flowing Argon, for films that were sequentially adsorbed at a pH of 3.5 in both solutions. Figure 4-2 plots the data in the dielectric domain and shows the real (dielectric 'constant', ε') and imaginary (dielectric loss, ε'') components of the relative permittivity. These devices typically exhibit two loss peaks, one at high frequency and one at low. The large value of ε' at low frequencies is indicative of ions moving under the influence of the applied field and building up at the interface. The same data can be examined in the form of a complex plane plot, or a Cole-Cole plot, in the impedance domain (-Z'' vs. Z') and is shown in Figure 4-3. It shows a semicircular arc at high frequencies which overlaps with a low-frequency 'spike' that is close to a vertical line (note that the arrow indicates the direction of increasing frequency).
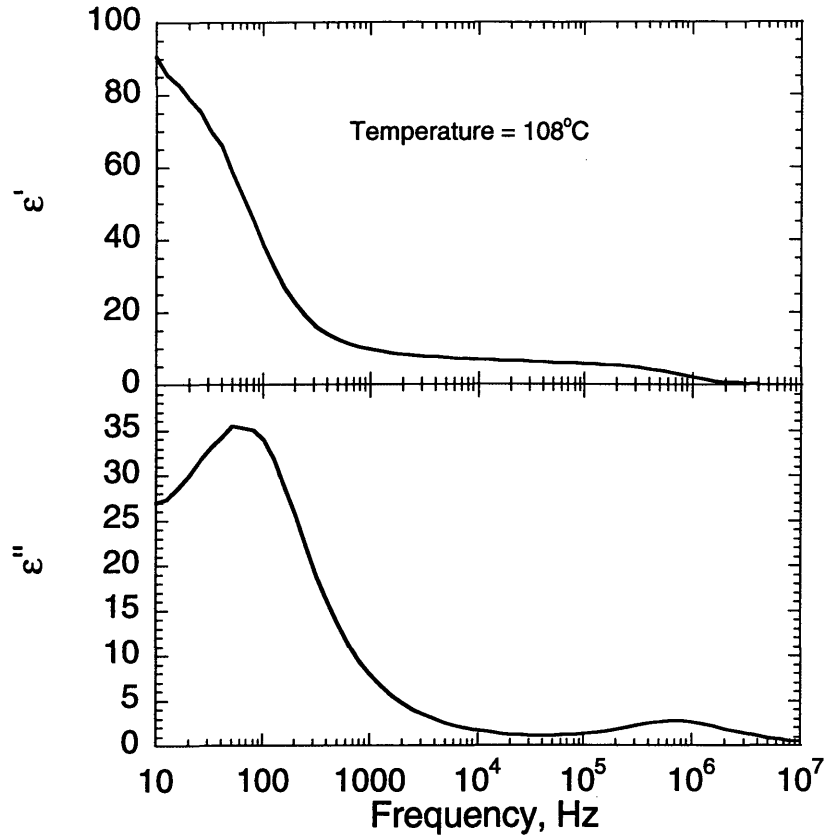
Figure 4-2 - Dielectric characteristics at 108°C of a PAH/PAA film made at a pH of 3.5 for both solutions
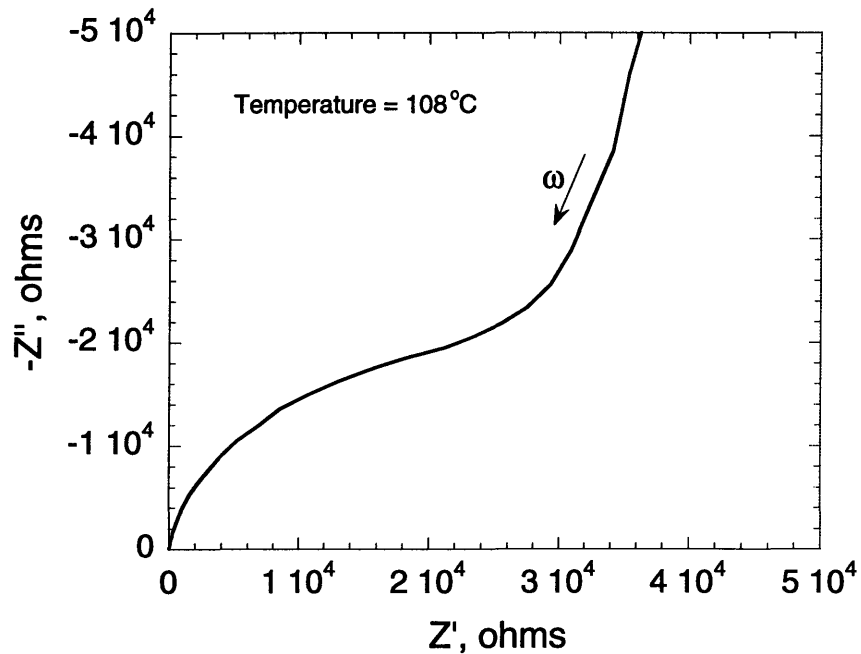
Figure 4-3 - Impedance characteristics at 108°C of a PAH/PAA film made at a pH of 3.5 for both solutions - The arrow indicates the direction of increasing frequency
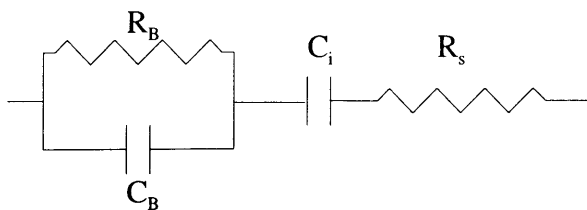
R_B = Bulk Resistance
C_B = Bulk Capacitance
C_i = Interfacial (Double Layer) Capacitance
R_S = Series Resistance

Figure 4-4 - Proposed equivalent circuit

This type of response is typical of an ion conducting polymer film sandwiched between two ion blocking electrodes. The electrodes are considered blocking because they are inert and do not take part in any electrochemistry. Furthermore, no ions can cross the interface and enter into the electrode. The electrodes 'block' the ions from any further movement. Also, it is assumed that the electronic conductivity is negligible in these films. The response can then be modeled by an equivalent circuit of the type shown in Figure 4-4. Under an applied bias, ions can be transported through the film and this process is represented by a bulk resistance (R_B). Simultaneously the material can polarize, as it would in the absence of any long range ion motion, and this gives rise to a bulk capacitance (C_B). Since these two processes can physically occur at the same time, R_B and C_B are combined in parallel in the equivalent circuit. As the ions move toward the electrodes, they start to pile up at the interface since the electrodes are blocking and do not allow any ions to pass. The charge on the metal electrode is counter-balanced by the charge on the ions in the film. This is a so-called double layer of charge whose behavior is similar to a parallel plate capacitor with a plate spacing on the order of the thickness of the interfacial layer. This is then modeled as an interfacial (or double layer) capacitance (C_i) in the equivalent circuit. Since the interfacial layer thickness is generally a very small value, C_i is usually quite high compared to C_B. The response of the bulk of the film (R_B-C_B in parallel) is physically in series with this interfacial capacitance and this is reflected in the series combination in the equivalent circuit. The final component in the equivalent circuit is a series resistance. This represents any residual resistances of the

leads and/or contacts, most notably the ITO resistance, that could not be eliminated from the measurement.

The ideal electrical response of this equivalent circuit is shown in Figure 4-5 and Figure 4-6 for two different values of R_B. It can be seen that the overall response of the equivalent circuit shows similar characteristics to the measured data. Looking first at the dielectric response in Figure 4-5, two separate loss peaks can be distinguished. At low frequencies, ε' reaches a high value that is related to the ions building up at the interface, and its value is determined by the interfacial capacitance. As the frequency is increased, the first of the two transitions is observed, and the frequency about which it is centered decreases with an increase in the value of R_B. At still higher frequencies, ε' approaches a plateau and its value is effectively determined by C_B (assuming that C_i is much greater than C_B, which is usually the case). The transition at high frequencies is just due to the electrode and/or contact resistances, R_S, which are in series with the effective capacitance of the film. This artificially causes ε' to go to zero in the region above this high-frequency transition. Indeed, it is observed that if the resistance of the ITO is systematically decreased, by decreasing the length of the ITO electrode, this peak shifts out to higher frequencies (not shown). In the limit when the series resistance goes to zero, this peak would not be present. However, since each cell that was tested differs slightly in their series resistance (due to variability in ITO resistance, aluminum resistance, etc.) this electrode effect could not be subtracted out with any true degree of accuracy. Consequently, since this loss peak is merely due to the test cell setup, it gives no vital information about the polymer film or the interface and so for the remaining discussion it will be ignored.

Turning now to the ideal impedance response of the equivalent circuit, in Figure 4-6, an increase in the value of R_B results in an increase in the diameter of the semicircle. In fact, the diameter of the semicircle is equal to the value of R_B and so by experimentally measuring this diameter, and knowing the thickness and area of the sample, the resistivity (and conductivity) of the film can be determined. The vertical spike is just due to C_i and so it is seen that this complex plane plot is just a superposition of the response of a
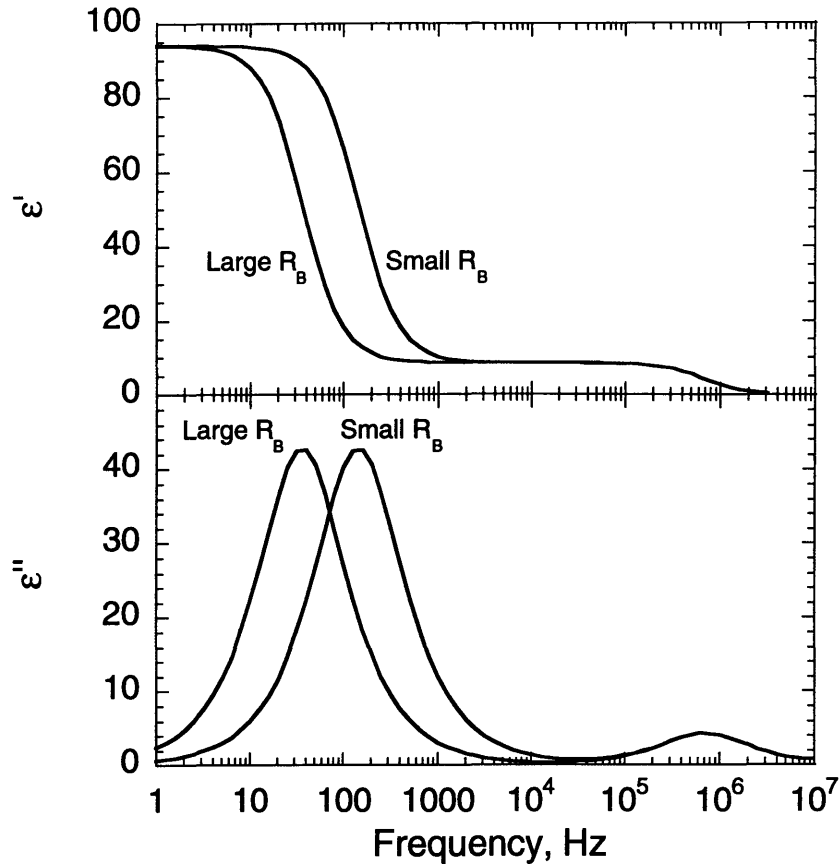
Figure 4-5 - Ideal dielectric characteristics of the proposed equivalent circuit
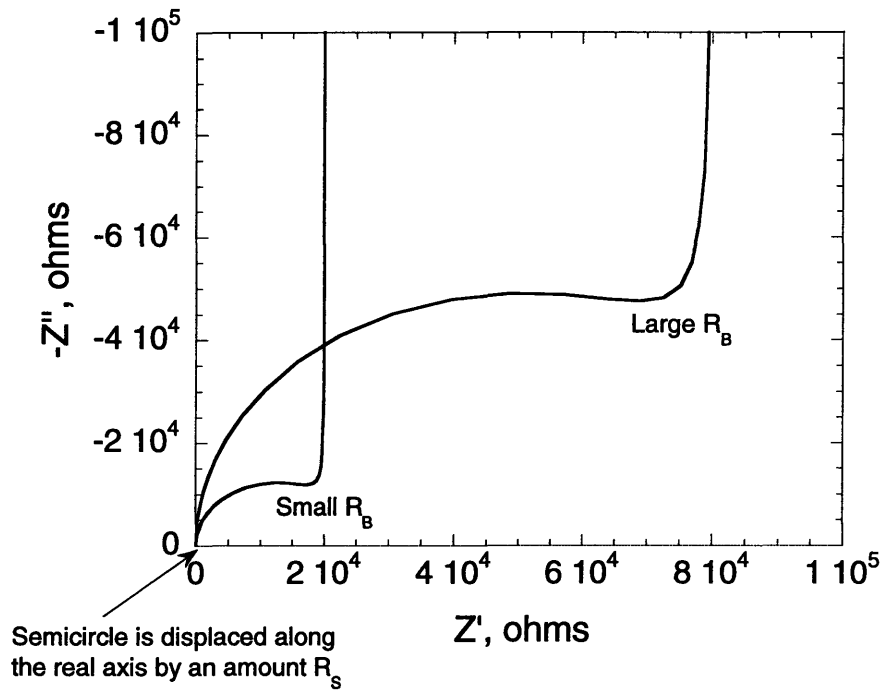
Figure 4-6 - Ideal impedance characteristics of the proposed equivalent circuit

parallel RC combination (R_B and C_B) together with the interfacial capacitance. In this graph, the series resistance, R_S, is manifested in a shifting of the entire curve along the real axis by a value equal to R_S.

4.3.2 PAH/PAA Films

4.3.2.1 Temperature Dependencies

Now that the basic response characteristics of the film are known, their temperature dependence can be studied. The dielectric and impedance characteristics were measured over the temperature range from 30°C to about 110°C for a PAH/PAA film that was sequentially adsorbed from solutions that were both set at a pH of 3.5. The sample was first heated to 110°C, while Argon was being purged through the sample chamber, in order to ensure that any residual water was removed from the film. The measurements were then taken as the film was cooled back down to room temperature. The dielectric characteristics in Figure 4-7 show that when the temperature of the film is lowered from 110°C, the loss peak shifts to lower frequencies. The dielectric 'constant' approaches a large value of about 100 at low frequencies which is attributed to ions moving to the interfaces and building up a space charge polarization. At higher frequencies, in the plateau region, this long range ion motion can no longer keep up with the alternating field and so ε' decreases to a value of about 5. The complex plane plot of the impedance in Figure 4-8 shows that as the temperature is decreased, the diameter of the semicircle systematically increases. Furthermore, at the highest frequencies, all of the curves converge and approach a value of 60 Ω on the real impedance axis. It is important to note that up to 110°C, this behavior is completely reversible in the sense that the film shows the same characteristics upon being reheated.

An increase in the film conductivity (decrease in R_B) is responsible for the decrease in the diameter of the semicircle in the complex plane plot of the impedance, as well as the shifting to higher frequencies of the dielectric loss peak. The higher temperature increases the mobility of the ions thus causing an increase in the conductivity. The calculated values of this conductivity as a function of temperature are
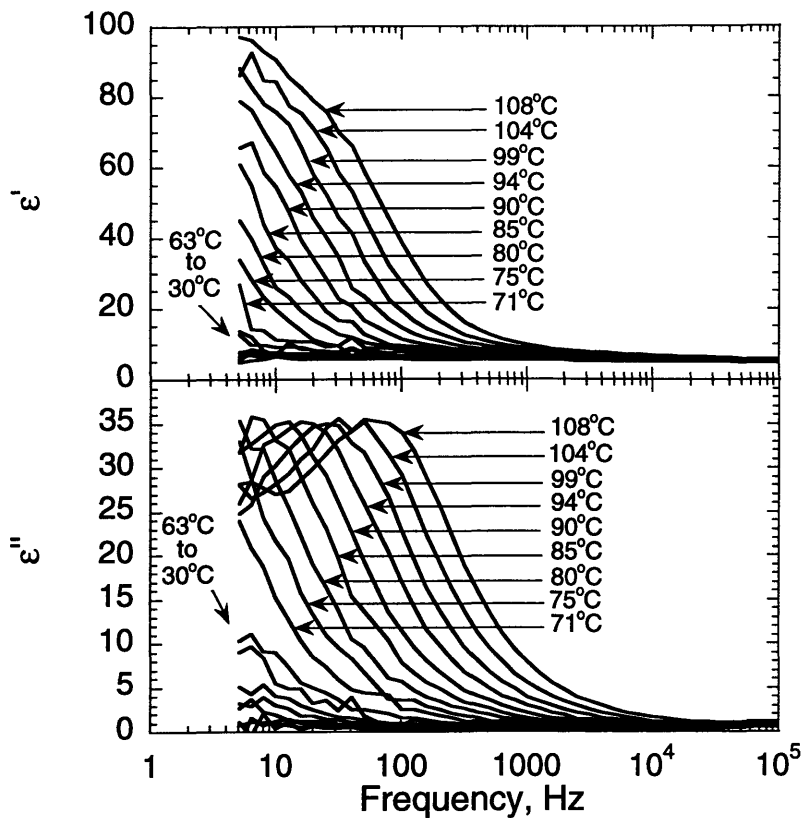
Figure 4-7 - Temperature dependence of the dielectric characteristics of a PAH/PAA film made at a pH of 3.5 in both solutions
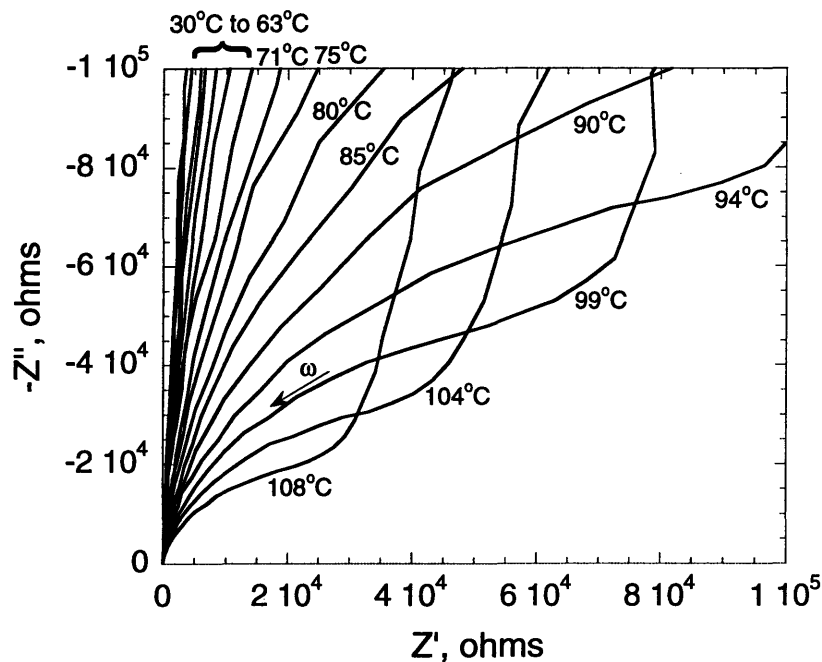
Figure 4-8 - Temperature dependence of the impedance characteristics of a PAH/PAA film made at a pH of 3.5 in both solutions

shown in the form of an Arrhenius plot in Figure 4-9. The conductivity in these films is quite low and ranges from about 1×10^{-12} S/cm at room temperature up to about 4×10^{-9} S/cm at 108°C. The data form a fairly straight line, which implies that the conduction is an activated process, with an activation energy of about 1 eV. This is typical of polymers below their glass transition temperature (T_g), however, ionically conducting polymers based on PEO and other PEO-like polymers typically operate above their T_g. These materials produce Arrhenius plots which have a negative curvature rather than forming straight lines. In such a case, significant segmental mobility of the polymer is present and conduction is believed not to be an activated process, but rather one in which the ions are swept along by the mobile polymer segments, the so called dynamic bond percolation model.

The species responsible for conduction could potentially be the small counter-ions that are initially associated with each polyelectrolyte (H^+ or Na^+ from PAA and Cl^- from PAH). However, it is generally believed that during the sequential adsorption process, most of the small counter-ions get swept out of the film in favor of the two
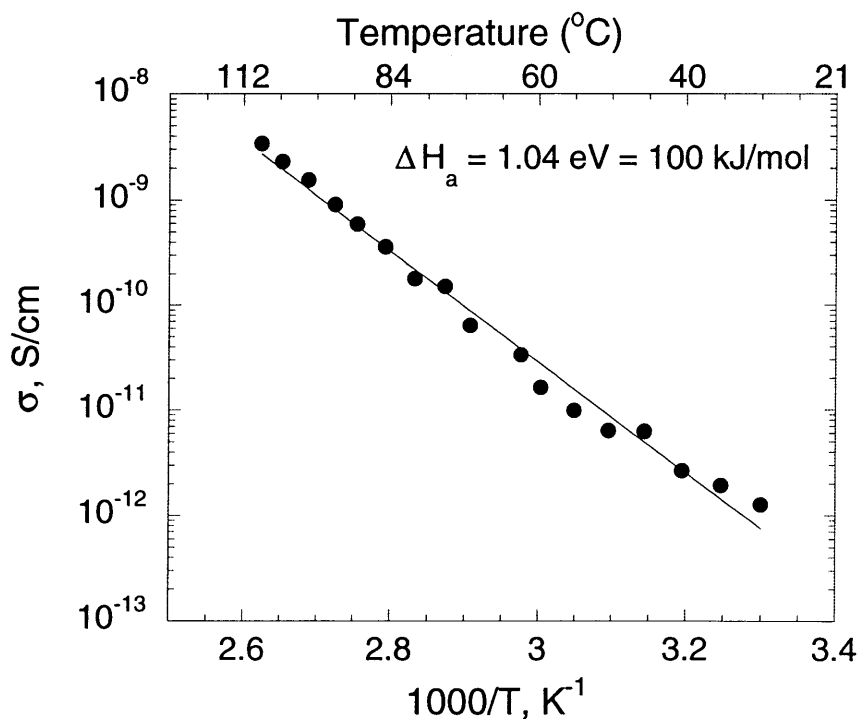
Figure 4-9 - Arrhenius plot of the conductivity of a PAH/PAA film made at a pH of 3.5 in both solutions

polyelectrolytes forming ion pairs[98, 100], an idea which will be discussed in more depth shortly. The polyelectrolytes themselves are immobile and cannot contribute to the conductivity. However the PAA, being a weak polyelectrolyte, can change its degree of ionization with pH. A larger pH causes more of the carboxylic acid groups to become ionized, while a lower pH causes less. The PAH, on the other hand, is fully charged in the pH regime that is typically of interest. In the multilayer film, it has previously been shown by Yoo et. al.[92] that under the pH conditions used to deposit these films (a pH of 3.5 in both solutions), about 50% of the functional groups of the PAA still exist as the free carboxylic acid. This is due to the fact that only the charged groups participate in the sequential adsorption process. The free acid groups remaining in the film can donate a proton (H^+) which can then move and give rise to the observed conductivity. PAA could indeed be acting as a proton conductor[110, 111] as evidenced in Figure 4-10 and Figure 4-11 which show the dielectric characteristics and temperature dependent
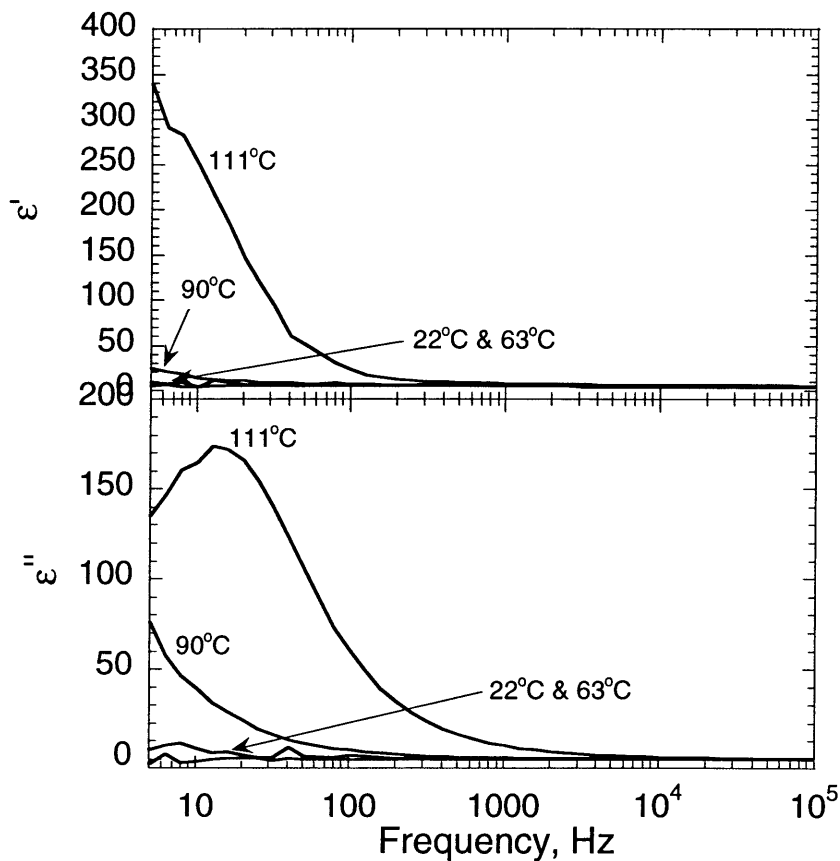
Figure 4-10 - Dielectric Properties of a thin film of poly(acrylic acid)
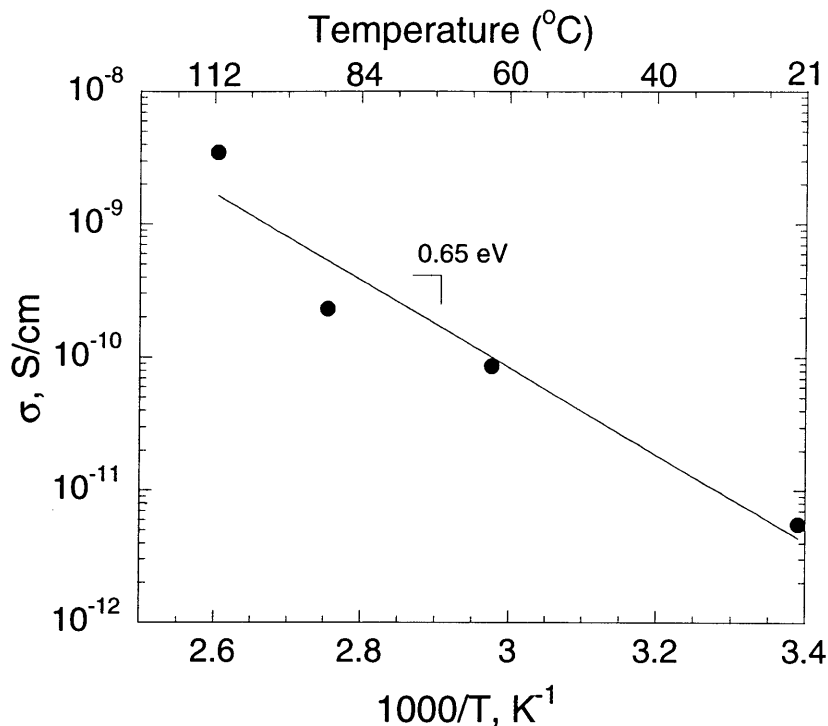
Figure 4-11 - Temperature dependent conductivity for a thin film of poly(acrylic acid)

conductivity, respectively, of a thin film of pure PAA (acid form, not the salt). For these measurements, a 25% aqueous solution of PAA was diluted to a 4% solution with 2-methoxyethanol which was then used to spin coat a thin film. As shown in Figure 4-10, the dielectric constant for a pure spin coated film of PAA achieves values significantly higher than that observed for the PAH/PAA sequentially adsorbed film (Figure 4-7) for a similar temperature. Furthermore, Figure 4-11 shows that the ionic conductivity of a pure PAA film is higher than that for the PAH/PAA film (Figure 4-9) and that it exhibits a large temperature dependence. These results suggest that in the PAH/PAA sequentially adsorbed film, there are either fewer carriers, or they have a lower mobility, than in the pure PAA film. This issue will be further addressed in the next section.

The PAH/PAA sequentially adsorbed films were also heated to temperatures greater than 110°C to examine the effects of elevated temperatures on their properties. Films of PAH and PAA, made at a pH of 3.5 in both solutions, were heated under flowing Argon and their dielectric properties were measured. In this case, the samples were tested as the temperature was increased so as to reveal any irreversibility brought about by the

elevated temperatures. Up to about 175°C, the behavior is the same as that shown previously in Figure 4-7 and Figure 4-8. An increase in temperature causes the loss peak, which is associated with the movement of the ions to the interface, to shift to higher frequencies. At higher temperatures, several other things begin to occur as shown in Figure 4-12 for the temperature range of 206°C to about 406°C. Both ε' and ε'' begin to increase at frequencies lower than the loss peak, but in addition, the loss peak itself shifts to lower frequencies. The irreversibility of this behavior is indicated in Figure 4-13 which provides a comparison of the characteristics of this film before and after it was heated up to 406°C and cooled back down. Before this conditioning, ε' is around 5 at room temperature, but there is a large increase in both ε' and ε'' due to ionic motion at 125°C (note that the scale is blown up here for clarity). After the film was heated to
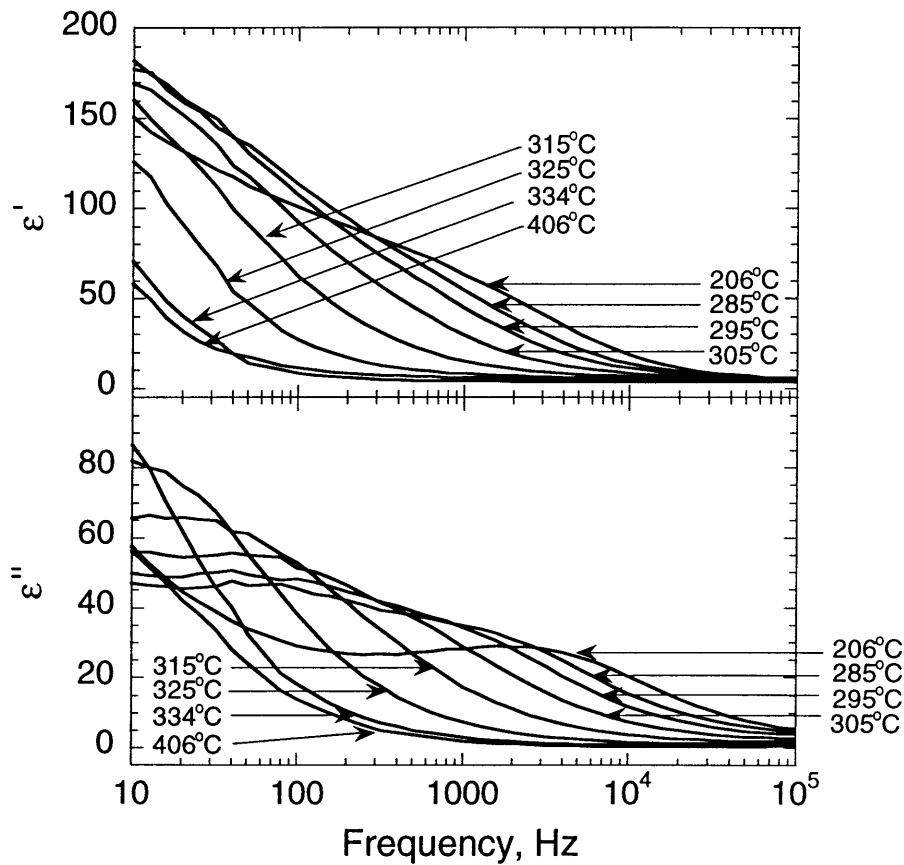
Figure 4-12 - Dielectric characteristics from 206°C to 406°C for a PAH/PAA film made at a pH of 3.5 in both solutions

406°C and cooled back down, there is no such increase in ε' or ε'' upon reheating to 125°C. Furthermore, this high temperature conditioning has decreased the bulk dielectric 'constant' from about 5 to about 3. This irreversible change in the film characteristics can be explained by considering the reaction between carboxylic acids and amines to produce an amide bond at elevated temperatures. The carboxylate groups on the PAA that are associated with ammonium groups on the PAH can react to produce a chemically cross-linked film. However, the free acid groups that are present in the film should, for the most part, remain intact. Figure 4-12 shows that during the initial heating to elevated temperatures, the dielectric loss peak that was attributed to ion motion shifts to lower frequencies. Apparently, the amidation reaction that occurs at elevated temperatures effectively cross-links the film and decreases the mobility of the ions in the film such that
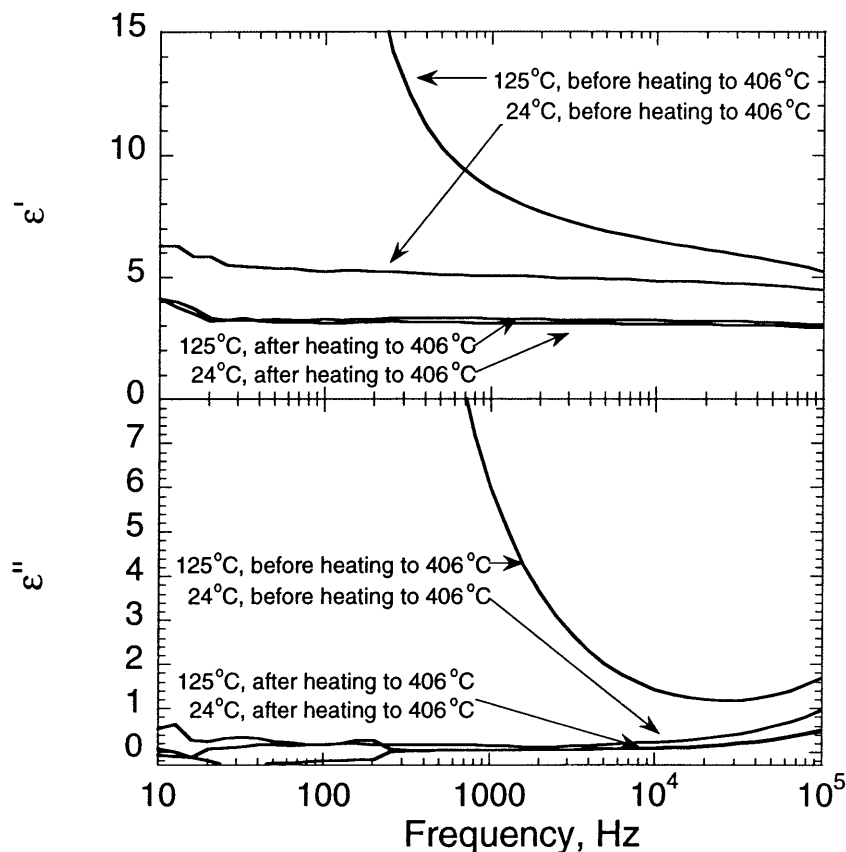
Figure 4-13 - Dielectric characteristics upon reheating of a PAH/PAA film made at a pH of 3.5 in both solutions

higher temperatures are required to move them. Furthermore, this would explain the decrease in the bulk dielectric 'constant' from 5 to 3 that occurs upon heating the film to 400°C, as shown in Figure 4-13. The less polar amide groups, as compared to the carboxylate and ammonium ions, cause the film to have a lower bulk dielectric constant. The cause for the increase in the intensity of ε' and ε'' at low frequencies is not completely understood but it but it seems to be due to an increase in the number of carriers that can move to the interfaces.

The possibility that this irreversible change was due to the loss of chemically bound water was examined by allowing the sample to equilibrate under ambient laboratory conditions (i.e. relatively high humidity) and then re-testing the device. This would have permitted the film to re-absorb any water that was lost at high temperature. However, the same behavior as that shown in Figure 4-13 was observed indicating that loss of any chemically bound water was not responsible for the observed behavior. In addition, this type of cross-linking effect in films of PAH and PAA has recently been reported by other workers and the formation of amide bonds at elevated temperatures has indeed been confirmed by infrared spectroscopy[112].

4.3.2.2 pH Dependencies

In addition to the temperature causing large changes in the observed dielectric characteristics, the conditions under which the films are prepared can also have dramatic influences on their behavior. When films of PAA and PAH are deposited, the pH that both solutions are set at can significantly influence the resultant film structure. A thorough investigation of this effect has been performed by Rubner *et al.*[91-93]. The key idea is that one of the components is a weak polyelectrolyte whose charge density varies with the pH. The effects of changing the pH of these solutions on the deposition process are qualitatively similar to the case for PAA and PPV precursor discussed in Chapter 2. When the pH is increased from an initially small value, keeping the pH of both solutions the same, more of the carboxylic acid groups on the PAA become ionized while the PAH remains fully charged. This results in the PAA adopting a more extended chain conformation in solution which translates into thinner layers of PAA adsorbing onto the

surface. The increase in the charge density of the PAA as the pH increases is further manifested in a change in the PAH thickness. In this case, the PAA is already on the surface and so now an increase in its degree of ionization results in a higher surface charge density which promotes more adsorption of the PAH. So the overall effect of increasing the solution pH in both solutions is the decrease the PAA incremental thickness and increase the PAH incremental thickness. This generally results in a net increase in the total bilayer thickness. From previous work of Rubner and Shiratori[93], the thickness increment that a layer of PAH and PAA contribute to the total film thickness is given in Figure 4-14 for the case when both solutions are set at the same pH. It shows that in region I, as the pH increases from 2.5 to 4.5, the PAA incremental thickness does indeed decrease, and the incremental thickness of the PAH increases. In region II, however, an increase in both the PAA and PAH incremental thickness is observed which is believed to be related to the surface roughness of the film. The PAH incremental thickness becomes sufficiently rough so as to drive a thickness increase in the associated
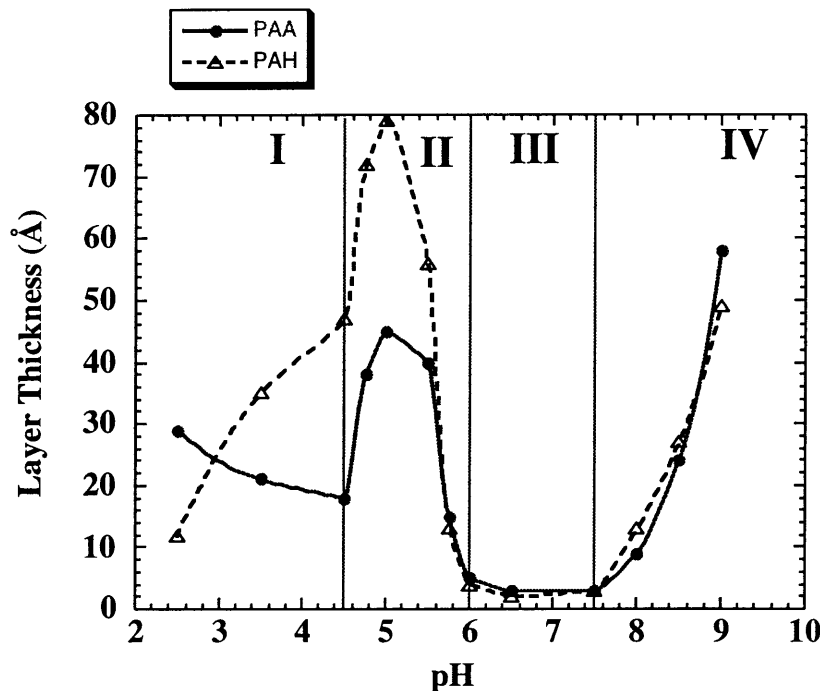
Figure 4-14 - Incremental thickness values of PAH and PAA keeping both solution pH's constant. Data from Rubner and Shiratori[93].

PAA layer, despite the fact that the PAA would prefer to form a relatively thin layer. A further increase in pH results in the thickness decreasing to very small values in region III. When the PAA reaches a certain critical charge density, it becomes more energetically favorable for the PAH and PAA molecules to form one-to-one contact ion pairs in extended chain conformations and this results in the formation of very thin bilayers. A transition is observed such that between a pH of 6.0 and 7.5, the thickness of a bilayer is very small. At these pH values, the PAH/PAA system is behaving as two highly charged polyelectrolytes in analogy to the PAH/SPS system that will be described below. In region IV, the PAA is fully charged but now the charge density of the PAH varies with pH. As the pH increases, the PAH becomes deprotonated and hence it becomes less ionized. In effect, then, the observed thickness transition is repeating itself with the roles of the polyelectrolytes being reversed.

The electrical characteristics of PAH/PAA films in region I, II, and III of Figure 4-14 were measured in an attempt to more fully understand the nature of the sequential adsorption process. PAA and PAH were both sequentially adsorbed at a concentration of $10^{-2}M$, based on the repeat unit molecular weight. The pH of both solutions was equal and set to three different values. A pH of 3.5 corresponds to a relatively low degree of ionization of the PAA and an estimated bilayer thickness of approximately 56Å. Increasing the pH to 5.0 results in a larger degree of ionization of the PAA and an increase in the bilayer thickness to about 124Å. This pH regime is just before the onset of the thickness transition. Pushing the pH to 6.5 increases the degree of ionization of the PAA past its critical value and so the bilayer thickness takes on very small values in this regime. The total film thickness for each of these films was 1155Å, 1176Å, and 692Å for the pH 3.5, 5.0, and 6.5 cases, respectively.

All three of these films show the same qualitative temperature dependence as that shown previously for the pH 3.5 case (Figure 4-7 and Figure 4-8) and the calculated values of the conductivity as a function of temperature are shown in the form of an Arrhenius plot in Figure 4-15 for all three cases. The pH 5.0 and 6.5 cases show very similar conductivities over the entire range of temperatures measured, ranging from
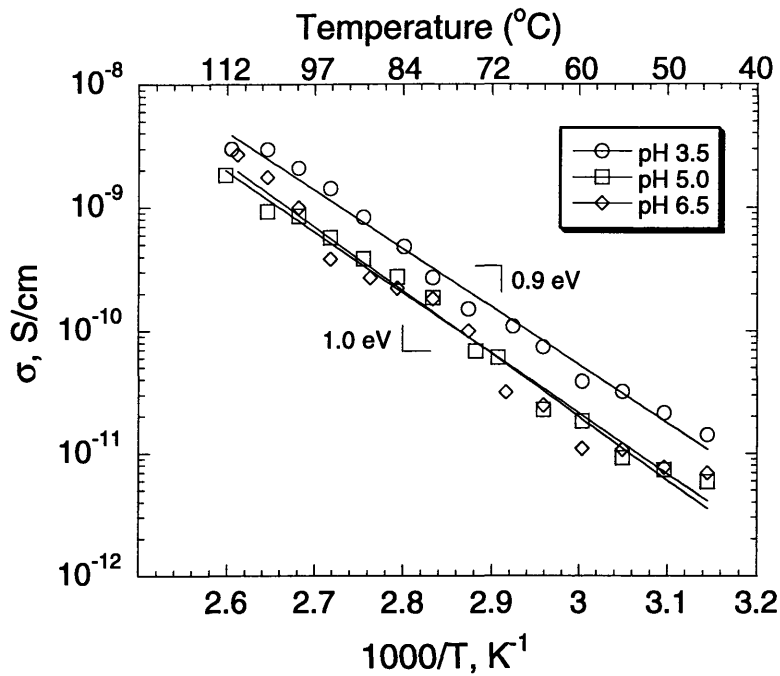
Figure 4-15 - Arrhenius plot of the conductivity of PAH/PAA films sequentially adsorbed at the designated pH value in both of the solutions
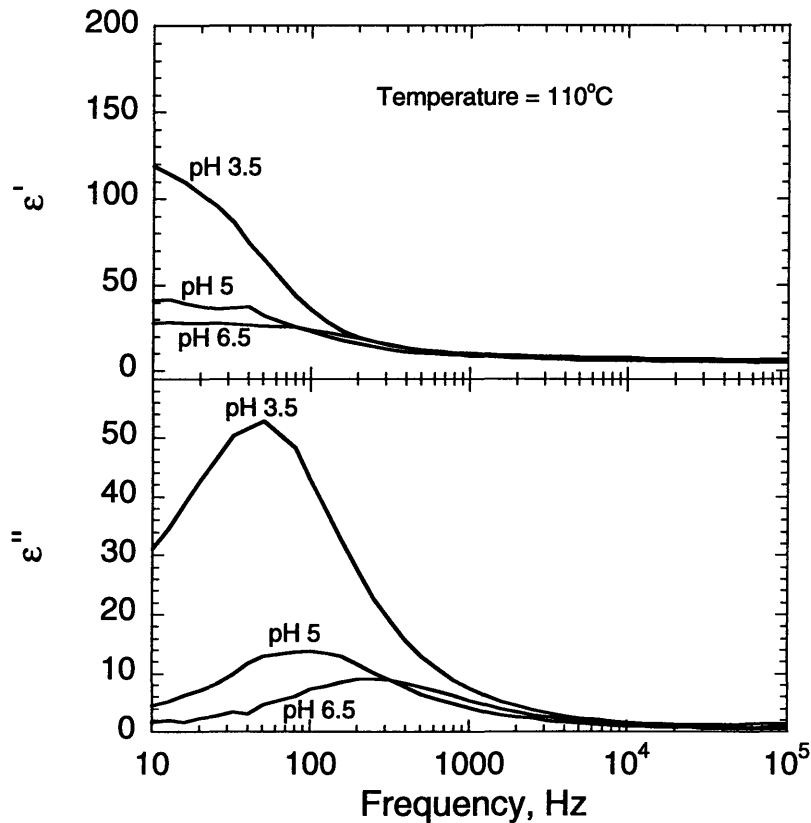
Figure 4-16 - Dielectric characteristics at 110°C of PAH/PAA films sequentially adsorbed at the designated pH value in both of the solutions

about 2×10^{-12} S/cm at room temperature to about 2×10^{-9} S/cm at about 110°C, despite the fact that they have quite different bilayer thickness values. The conductivity values for the pH 3.5 case are of similar magnitude but seem to be slightly larger than the others. All three films have an activation energy close to 1 eV. A clearer insight can be obtained from the data by looking at it in the dielectric domain, as shown in Figure 4-16 for each of these films at a temperature of about 110°C. In this figure, the effective dielectric 'constant' at low frequencies is significantly greater in the pH 3.5 case than for either of the other two cases. The films made at the two higher pH values have similar low-frequency dielectric 'constants' with perhaps the pH 5.0 case tending to slightly higher values.

These results reflect the fact that as the solution pH is increased, the PAA exhibits a higher degree of ionization. This results in more of the carboxylate groups taking part in the adsorption process which leads to both a more highly ionically cross-linked film as well as to the presence of fewer free acid groups in the final film. The increase in the density of ionic bonds can decrease the mobility of the small ions. However, the decrease in the free acid concentration can effectively decrease the carrier concentration if proton conductivity plays a major role. So it is seen that a higher solution pH can lead to fewer charge carriers being present, as well as to a decrease in their mobility, and these effects then translate into a lowering of both the effective dielectric 'constant' and the ionic conductivity. It should be noted, however, that even at a pH of 6.5, the film still exhibits appreciable conductivity and the low-frequency dielectric 'constant' is still significantly higher than its 'bulk' value. This implies that even when the molecules pair up to form very thin bilayers, all of the small counter-ions are not eliminated in favor of forming polymer-polymer ion pairs. In a later section, these results will be compared to those for layers of PAH and SPS, two fully charged macromolecules, and similar conclusions will be drawn.

4.3.2.3 Post Sequential Adsorption Treatment

It is interesting to consider the fact that there are free acid groups present in the PAH/PAA film after it has been sequentially adsorbed. These groups are not associated with the PAH and so there exists the potential to make use of them after the film has been

created. If a film containing free acid groups is submerged into an aqueous salt solution at a high pH, these groups become ionized and an exchange reaction can occur with the salt ions in solution. If a salt such as NaCl is present, for example, then the sodium carboxylate ($-COO^-Na^+$) can be formed. The dielectric characteristics for such a case at 110°C is shown in Figure 4-17 for PAH/PAA films that were sequentially adsorbed with a pH of 3.5 in both solutions. After the films were made, they were submerged for 1.5 hours into $10^{-5}M$ NaOH aqueous solutions, of differing NaCl

		σ, S/cm
A	Control, pure water	4×10^9 S/cm
B	$10^{-5}M$ NaOH	4×10^9 S/cm
C	$10^{-5}M$ NaOH and $5 \times 10^{-3}M$ NaCl	3×10^9 S/cm
D	$10^{-5}M$ NaOH and $5 \times 10^{-2}M$ NaCl	7×10^{10} S/cm
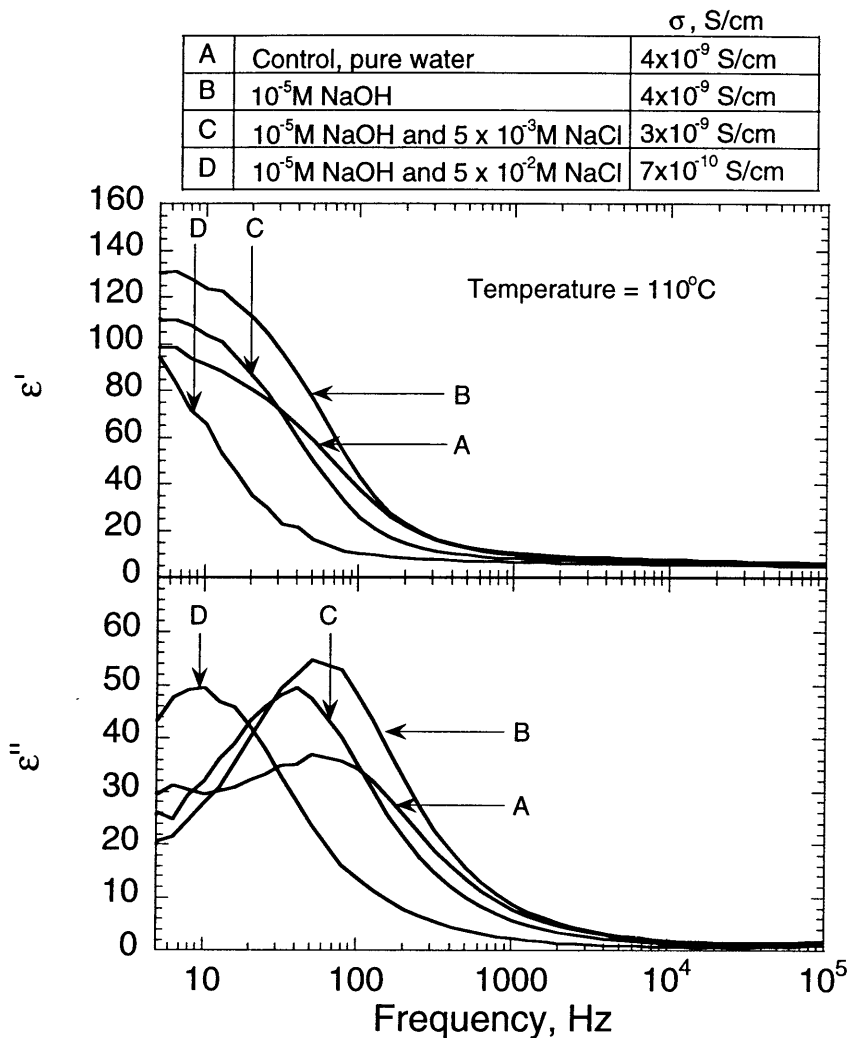
Figure 4-17 - Dielectric characteristics at 110°C for PAH/PAA films dipped into aqueous salt solutions for 1.5 hours after sequential adsorption - A pH of 3.5 was used in both solutions for the sequential adsorption process itself

concentrations which had a pH of about 8 to 9. The figure indicates that the conductivity, as calculated from the complex plane plot of the impedance, decreases as the concentration of salt increases. This is also reflected in the dielectric characteristics whereby the overall trend is to shift the loss peak to lower frequencies with an increase in the salt concentration. However, all of the samples that have been dipped in the higher pH solution have larger values of ε' and ε'', as compared to the control, implying the presence of more mobile species. So despite the fact that more carriers are being introduced, the conductivity of the film decreases. This is an effect that is frequently observed in polymer electrolytes based on PEO:salt mixtures in which the decrease in conductivity with increasing salt content is usually attributed to an increase in the glass transition temperature. This causes a stiffening of the matrix which significantly decreases the mobility of the ions and this more than compensates for the increase in their concentration. A similar effect may be responsible for the decrease in conductivity seen here.

In addition, subtle variations in the properties could be due to the fact that the free acids are being replaced by sodium carboxylate groups. In the former case protons are the conducting species, while in the latter it is sodium ions, and protons are generally observed to have higher mobilities than other ions due to their small size. It should also be noted that while the acid groups can indeed form the sodium carboxylate, there is nothing prohibiting both Na^+ and Cl^- ions from swelling the film and so both types of ions can be present. All of these possibilities make for a very complicated system.

4.3.2.4 Effects of Moisture

In addition to changing the ionic conductivity by controlling the number of ions that are present, a way to increase the conductivity of thin polymer films is through the use of plasticizers. In solid polyelectrolyte films, it is the strong ion pairing that occurs between the macro-ion (i.e. the ionized polymer) and the small counter-ion that gives rise to their glassy and brittle nature as well as to the low values of the conductivity. Plasticizing the matrix with a compatible, low molecular weight solvent can have the effect of breaking up this association. For the PEO:salt systems, propylene carbonate or ethylene carbonate are commonly used. For polyelectrolytes, however, water is usually

the solvent of choice as evidenced in ion exchange and fuel cell membranes[101]. Here, the effect that a humid environment has on the electrical properties of sequentially adsorbed layers of PAA and PAH is examined and the results are shown in Figure 4-18 and Figure 4-19. These films were again adsorbed with the pH of both the PAA and PAH solutions set at 3.5, and the total film thickness was about 900Å in the dry state. The complex plane plot of the impedance shows that there is a dramatic 5 order of magnitude increase in the conductivity (from 3×10^{-12} S/cm to 2×10^{-7} S/cm) brought about by hydrating the film. Furthermore, the dielectric 'constant' increases to a large value of about 325 in the hydrated state, a number which is indicative of ions building up at the interface. All of these values were based on a measured film thickness of about 900Å in the dry state. It has been shown recently, however, that the thickness of sequentially adsorbed layers of PAH and SPS can increase by as much as 18% when they are hydrated[98, 100]. Any increase in the film thickness brought about by hydration would cause an increase in the calculated conductivity and dielectric 'constant' by the same factor. Consequently all of the values reported here for the hydrated films can be considered to be lower estimates.

The reason for these large increases is mainly attributed to a solvation effect. The water solvates the ions in the film and can cause an increase in both the effective concentration of carriers as well as their mobility. These values can be compared to a dielectric 'constant' of about 110 and a conductivity of 4×10^{-9} S/cm for similar films that were heated to 110°C in a dry environment, as shown previously in Figure 4-7 and Figure 4-8. Heating the film as well as exposing it to moisture both increase the conductivity, but the latter does so much more effectively by breaking up the ion pairs. In addition, the final value of the low-frequency dielectric 'constant' is significantly higher when the film is hydrated ($\varepsilon' = 700$) than when it is heated to 110°C ($\varepsilon' = 100$). This implies that in these PAH/PAA films, moisture not only acts to increase the mobility of the ions by plasticizing the matrix, but it also increases their concentration by causing more of the free acid groups to become ionized.
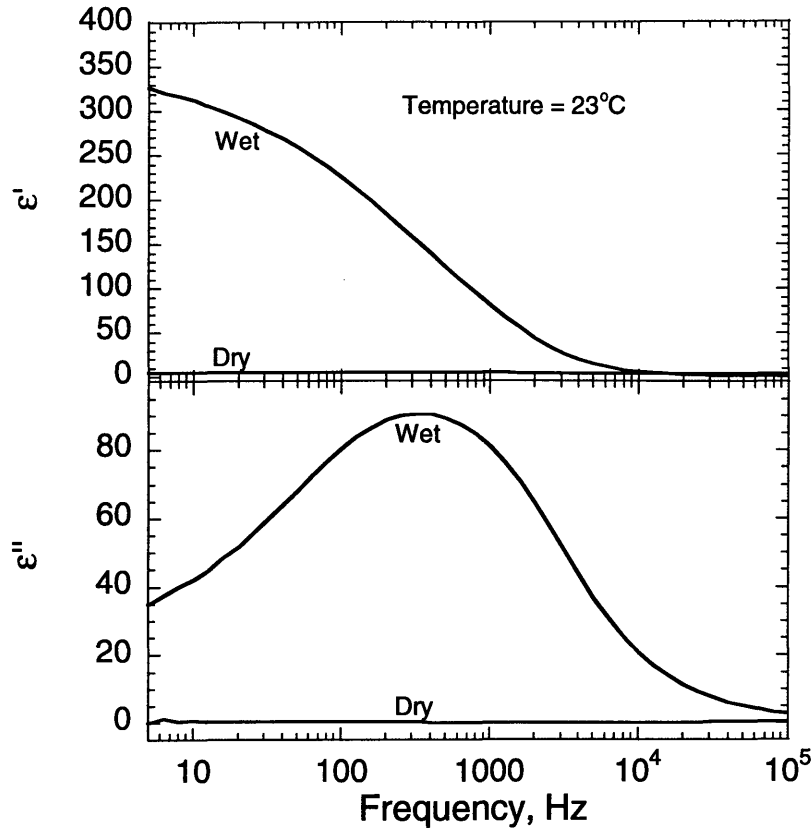
Figure 4-18 - Effect of a humid environment on the room temperature dielectric characteristics of a PAH/PAA film made at a pH of 3.5 in both solutions
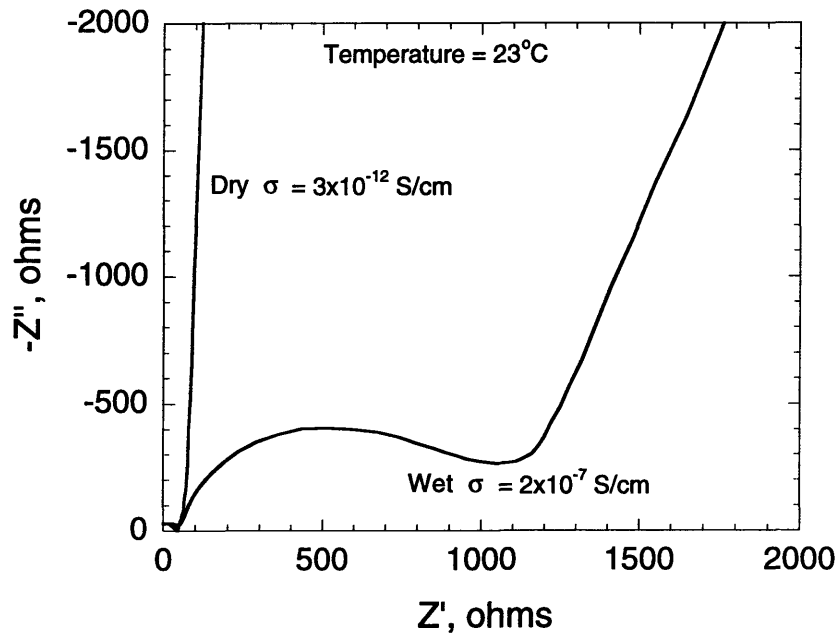
Figure 4-19 - Effect of a humid environment on the room temperature impedance characteristics of a PAH/PAA film made at a pH of 3.5 in both solutions

4.3.3 PAH/SPS Layers

4.3.3.1 Temperature Dependencies

The previous section dealt with the behavior of sequentially adsorbed layers of a fully charged polyelectrolyte (PAH) together with one whose charge density can vary with the pH (PAA). In this section, however, the behavior of two fully charged polyelectrolytes will be examined. The polycation is the same that was used in the previous section, namely PAH. The polyanion is sulfonated polystyrene (SPS) which, being a much stronger acid than PAA, is also fully charged under the pH conditions that are typically used. The structures of these polymers have been shown in Figure 4-1.

Both the SPS and the PAH tend to form more extended chain conformations in solution due to the electrostatic repulsion of like charges along the chain. So when they are sequentially adsorbed together, they can each lie flat on the surface, forming polymer-polymer contact ion pairs, and therefore create very thin bilayers. Frequently, a salt such as NaCl is added to the solution which effectively shields the charges along the polymer chain from each other. This shielding reduces the amount of electrostatic repulsion and thereby causes the chain to adopt a more coiled conformation in solution which, in turn, makes for thicker bilayers.

Films of PAH/SPS were made both with and without added NaCl in the solutions used for sequential adsorption, and at a pH of 3.5 for both solutions. For the films made without adding any salt into the solution, a very thin bilayer thickness of approximately 2 Å/bilayer was observed, as expected. When salt was added, a concentration of 0.1 M NaCl was used in both the PAA and the PAH solutions and this increased the bilayer thickness to about 16 Å/bilayer. In both cases, 75 bilayers were deposited which gave a total film thickness of close to 1200Å and 150Å for the cases with and without salt, respectively.

Figure 4-20 shows the dielectric response from 22°C to 350°C for the case when the PAH/SPS film was made without any added salt. The value of ε' continuously increases as the temperature is raised and it approaches a value of about 40 at low
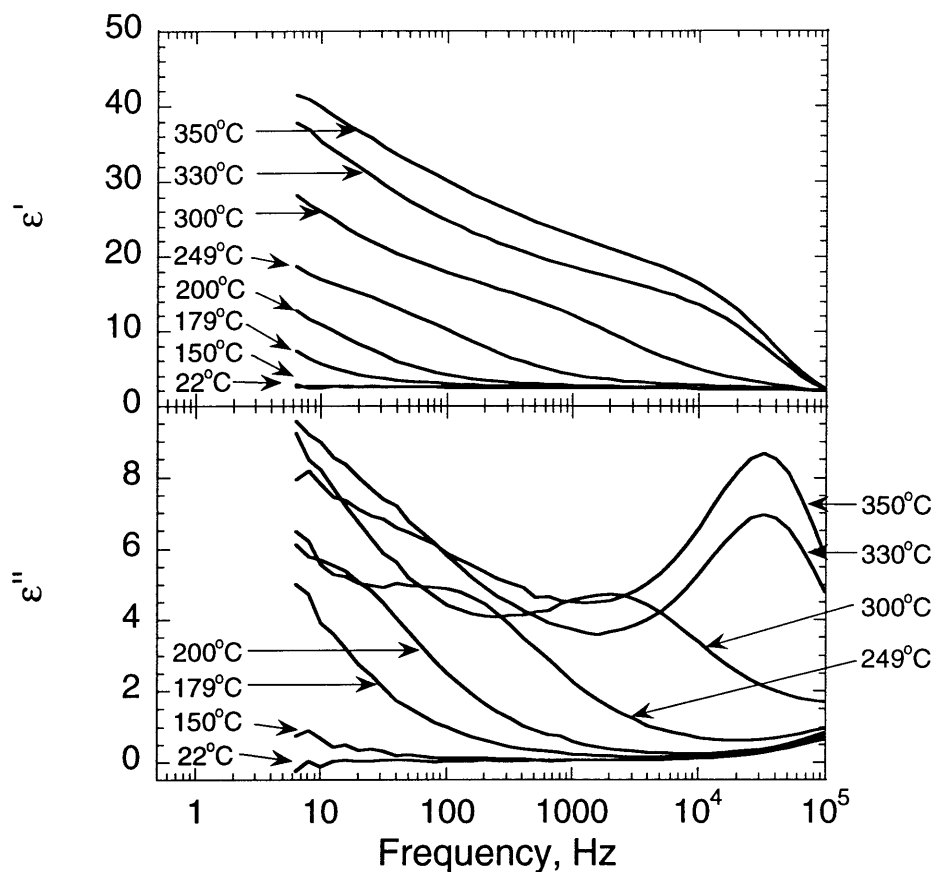
Figure 4-20 - Dielectric response of a PAH/SPS film made at a pH of 3.5 in both solutions with no added salt

frequencies and at 350°C. This large increase in ε' again implies the movement of ions to the interfaces, but now at significantly higher temperatures. This suggests that the sequential adsorption of two fully charged macromolecules does not result in the complete elimination of all the small ions from the film, but rather some residual amount of counter-ions are still retained in the film (Na^+ from SPS and Cl^- from PAH). The same behavior is observed for PAH/SPS films made with 0.1M NaCl added to both of the dipping solutions, as shown in Figure 4-21, but now the magnitude of ε' is even larger. At 350°C, ε' approaches a value of about 300 which is more than 7 times the value observed for the PAH/SPS film made without salt and at the same temperature. Assuming that the mobilities of the ions are the same in both cases, this would imply that there are more residual ions trapped in the film for the case when salt was added to the
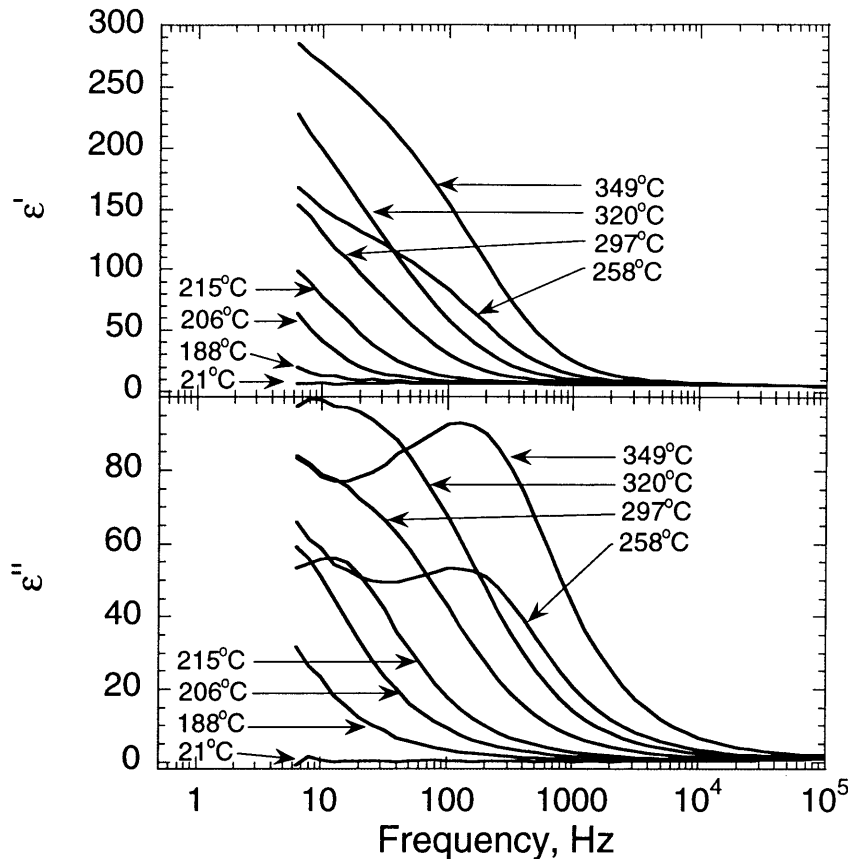
Figure 4-21 - Dielectric response of a PAH/SPS film made at a pH of 3.5 and with 0.1 M NaCl in both solutions

solutions. The additional ions could be a result of the salt that was added to the solutions becoming incorporated into the film. However, another possibility is that the PAH and SPS are forming fewer ion pairs with each other and so more of their small counter-ions remain in the film. It is difficult to determine, however, which one is predominant.

The effects of these ions is further reflected in the temperature dependence of the conductivity, as indicated in Figure 4-22. The linearity of the curves indicates that the conduction is an activated process with an activation energy close to 1.2 eV. For the film made with additional salt in the dipping solutions, the conductivity goes through a transition, after which it continues to increase with temperature. The source of this behavior is not completely understood at this time, but it may be due to the loss of bound water at high temperatures. In both cases, however, about a four order of magnitude increase in the conductivity was observed over the indicated temperature range.
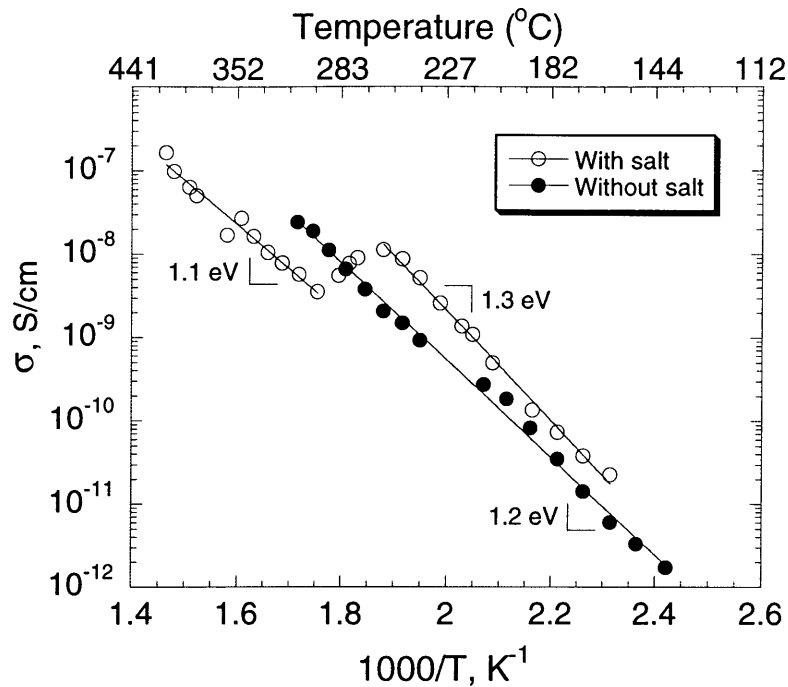
Figure 4-22 - Arrhenius plot of the conductivity of PAH/SPS films that were made with and without added salt in the dipping solutions - A pH of 3.5 was used for both solutions
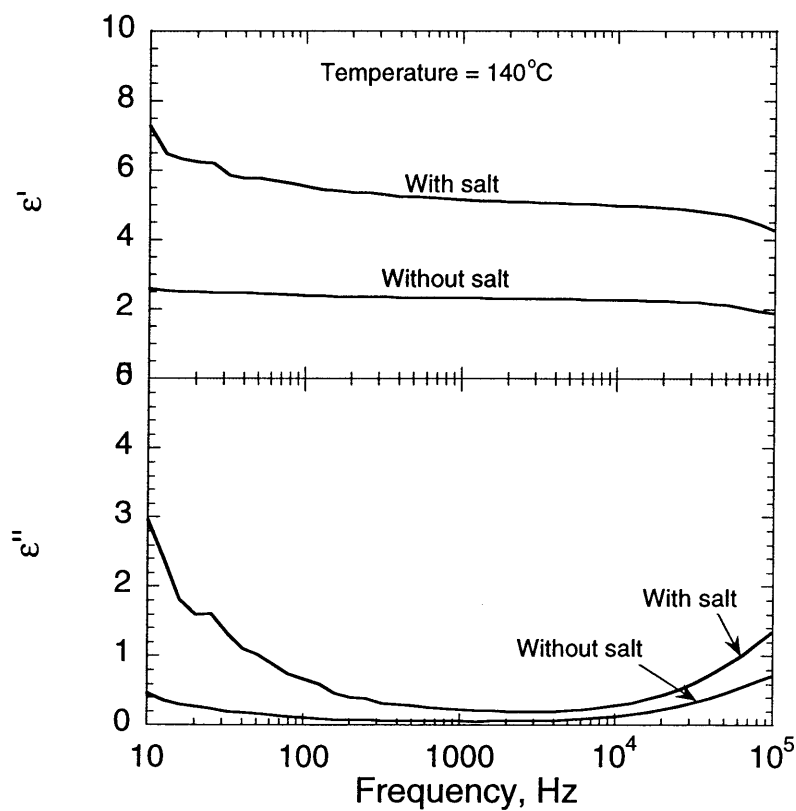
Figure 4-23 - Dielectric characteristics at 140°C for PAH/SPS films that were made with and without added salt in the dipping solutions - A pH of 3.5 was used for both solutions

The behavior of the film at temperatures below that required to get significant ion motion is shown in Figure 4-23. The figure only shows the response at 140°C, but the behavior is essentially the same down to room temperature. In this case ε', which represents the bulk dielectric 'constant', changes from about 2-3 to about 5-6 depending upon whether salt is added to the solution or not during sequential adsorption. Assuming that any interfacial or orientational polarization is negligible due to the high rigidity of the matrix, is seems plausible that an increase in the local, or atomic, polarization brought about because of the presence of a larger number of small counter-ions (Na^+ or Cl^-), is responsible for the increase in the bulk dielectric constant.

4.3.3.2 Effects of Moisture

Films of SPS and PAH were also exposed to a humid environment and their dielectric properties measured. The conditions of deposition for these films were the same as before. Namely, the pH of both solutions was set at 3.5 and in one case no extra salt was added to either solution, while in a second case 0.1M NaCl was added to both the SPS and the PAH solutions. The effect that moisture has on the room temperature dielectric characteristics is shown in Figure 4-24. In both cases, the low frequency dielectric 'constant' increases to large values upon hydration, however it is significantly higher in the case with added salt ($\varepsilon' = 500$) than without($\varepsilon' = 80$). In addition, both cases show at least a 4 order of magnitude increase in the conductivity when the film is hydrated. However, the conductivity of the film made with additional salt in the solutions is about 1 order of magnitude higher than that for the film made without. Note that the conductivities quoted in the figure for the dry state represent upper estimates because conductivities lower than this value for each sample could not be accurately measured.

The fact that these hydrated films have appreciable conductivity and a large dielectric constant at room temperature, even in the case when no additional salt was added to the solutions, reemphasizes that at least some of the small ions remain in the film after sequential adsorption. The increase in going from the dry to the hydrated state is much more pronounced in the case with salt added than without, implying the incorporation of
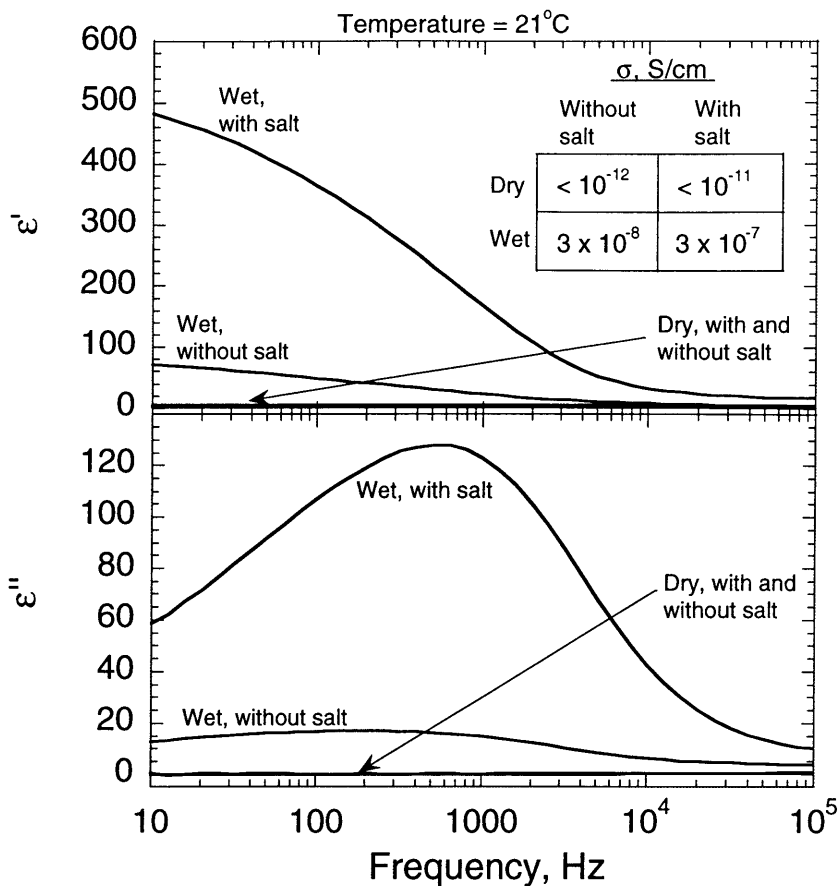
Figure 4-24 - Room temperature dielectric characteristics for a PAH/SPS film that was made with and without added salt in the dipping solutions - A pH of 3.5 was used for both solutions

more ions in the films made with salt. It is possible that the water is becoming hydrolyzed into H^+ and OH^- ions which could then contribute to the conduction process. However it is believed that the magnitude of the observed change in conductivity and dielectric 'constant' is much larger than could be explained by this effect.

4.4 Discussion and Summary

The results of the previous sections show that the impedance and dielectric characteristics of sequentially adsorbed layers can be used to obtain valuable insight into the nature of the adsorption process. Table 4-1 provides a summary of all the previous

Sample	Film	pH	Salt in dipping solutions?	Post Sequential Adsorption Treatment	Temperature(^{o}C)	Humidity	σ, S/cm	Max ε' (Low frequency)	Figure #
A1	PAH/PAA	3.5	no	none	25	dry	1×10^{-12}	(5)	Figures 4-5
A2	PAH/PAA	3.5	no	none	110	dry	4×10^{-9}	100	and 4-6
A3	PAH/PAA	3.5	no	none	25	wet	2×10^{-7}	325	Figure 4-13
A4	PAH/PAA	3.5	no	NaOH	110	dry	4×10^{-9}	130	
A5	PAH/PAA	3.5	no	NaOH + 5×10^{-3} M NaCl	110	dry	3×10^{-9}	120	Figure 4-12
A6	PAH/PAA	3.5	no	NaOH + 5×10^{-2} M NaCl	110	dry	7×10^{-10}	120	
A7	PAH/PAA	5	no	none	110	dry	2×10^{-9}	40	Figures 4-10
A8	PAH/PAA	6.5	no	none	110	dry	2×10^{-9}	30	and 4-11
A9	PAH/PAA	3.5	no	heat to 400°C then cool	25	dry	2×10^{-12}	(3)	Figure 4-8
A10	PAH/PAA	3.5	no	heat to 400°C then cool	125	dry	2×10^{-12}	(3)	
S1	PAH/SPS	3.5	no	none	25-140	dry	$< 10^{-12}$	(2)	Figures 4-14,
S2	PAH/SPS	3.5	no	none	260	dry	2×10^{-9}	25	4-16, and 4-17
S3	PAH/SPS	3.5	no	none	25	wet	3×10^{-8}	80	Figure 4-18
S4	PAH/SPS	3.5	yes	none	25-140	dry	$< 10^{-11}$	(5)	Figures 4-15,
S5	PAH/SPS	3.5	yes	none	260	dry	1×10^{-8}	160	4-16, and 4-17
S6	PAH/SPS	3.5	yes	none	25	wet	3×10^{-7}	500	Figure 4-18

**(x) means no loss peak was observed

Table 4-1 - Summary of conductivity values and low-frequency ε' values for PAH/PAA and PAH/SPS films

sections by quoting the conductivity of the samples, made and tested under the indicated conditions, as well as their dielectric 'constant' at low frequencies. The values quoted for ε' are effectively the maximum that the sample displayed under the indicated conditions. If the value is in parentheses, it indicates that no dielectric loss peak was observed under those conditions and so it essentially represents its bulk value. Otherwise, it is reflective of ions building up at the interface.

It has been shown (samples A1 and A2 in the table) that increasing the temperature of PAH/PAA films up to $110°C$ leads to large changes in their conductivity as well as in their dielectric characteristics. The max value of ε' increases to about 100 at elevated temperatures implying the accumulation of mobile ions at the interfaces. If the pH of the PAH and the PAA dipping solutions is increased, a systematic decrease in the low frequency dielectric 'constant' at $110°C$ is observed. The max value of ε' decreases from 100 to 40 to 30 as the pH increases from 3.5 to 5.0 to 6.5 (samples A2, A7, and A8). This is attributed to fewer ions reaching the interface, and thereby causing an increase in the apparent dielectric 'constant', as the pH is increased. This can be caused by a number of effects which are related to the structure of the multilayer film. As the pH increases, the degree of ionization of the PAA during the sequential adsorption process also increases, and so the resultant film contains fewer free acid groups. So if protonic conduction is the predominant mechanism, a decrease in the concentration of free acid groups as the pH increases leads to a decrease in ε' by reducing the carrier density. However, decreasing the free acid concentration is not the only result of increasing the pH. The increase in the charge density of the PAA as the pH increases results in the formation of more polymer-polymer ion-pairs and so the film has a higher density of ionic cross-links that can act to make the film more rigid. This can then effectively decrease the mobility of any ions that are in the film. It is likely that both of these effects, decreasing the carrier density as well as the mobility, are playing a role.

The efforts at trying to increase the conductivity of PAH/PAA films by intentionally adding ions (samples A4, A5, and A6) proved to actually decrease the conductivity potentially due to the formation of a more rigid matrix with increasing salt concentration. However, plasticizing the film by equilibrating it with a humid

environment results in over a five order of magnitude increase in the conductivity as compared to the dry state, and an increase of ε' to about 325 (samples A1 and A3). Water, being a good solvent for the polyelectrolytes, can solvate the ions and act to increase both their mobility through the matrix as well as their density.

For the PAH/SPS films, both increasing the temperature as well as plasticizing them with water results in a large increase in their conductivity and low frequency dielectric 'constant'. This suggests that in the sequential adsorption of two fully charged macromolecules, some of the small ions do indeed remain in the film. Furthermore, the addition of salt to the dipping solutions tends to result in more ions being incorporated into the structure, either coming directly from the added salt, or possibly from the original counter-ions.

Recent XPS results, however, have indicated that during sequential adsorption, most of the small counter-ions are expelled from the film into the solution or rinse baths in favor of forming ion pairs between the two polymers[98, 100, 113]. This suggests that the concentration of ions responsible for the observed conductivity and dielectric characteristics is below the detection limit of XPS, which is typically on the order of 1%[114]. A rough idea of the actual concentration of ions that are present can be obtained by considering that the ionic conductivity is equal to the product of the concentration of ions (n), their mobility (μ), and the electronic charge (q). Relatively few studies on the actual mobility of ions in polyelectrolyte films have been made. However if a representative value of about 10^{-7} $cm^2/V \cdot s$ is used for the room temperature mobility in the dry state[115], then it is seen that for a conductivity of 10^{-12} S/cm, the concentration of ions is very low at about 10^{14} cm^{-3}. Given that the concentration of polymeric repeat units in these films is on the order of 10^{22} cm^{-3}, it is seen that very few ions indeed are incorporated into the film, consistent with recent XPS results.

It is interesting to speculate on the source of these small ions since it is frequently assumed that they are all eliminated from the film. One possible explanation could be due to the counter-ion condensation effect. As the charge density of the polymer chain increases, the average distance between charges decreases. Once the distance between charges reaches a certain critical length, the so called the Bjerrum length, no further

increase in the net charge density can occur. This length is just the distance between charges at which their electrostatic interaction energy just equals their thermal energy kT[116] and in water at 293K, it has a value of about 7Å. This distance is several times that which would be expected if every repeat unit were charged and so it is seen that enough counter-ions are condensed so as to maintain this minimum distance between charges. Recent theoretical and experimental results on polyelectrolyte complexes in solution have indicated that there is indeed a competition between polyelectrolyte complexation and counter-ion binding[117] and this could be a possible explanation of why some of the small ions remain in the film. Furthermore, Nordmeier[117] indicates that the addition of salt to the solutions destabilizes the formation of polyelectrolyte complexes, causing a lower degree of complexation and a consequent higher degree of counter-ion binding. This could explain the apparent larger concentration of ions seen here in PAH/SPS films made with additional salt in the dipping solutions.

The behavior of PAH/SPS films can be compared to that of PAH/PAA films when the latter is adsorbed at a pH of 6.5. Under these conditions the PAA is highly charged, like the SPS, and so the two systems should behave similarly. It is seen that at a temperature of 110°C, the PAH/PAA film (sample A8) reaches a conductivity of about 2×10^{-9} S/cm and ε' has increased to a value of about 30. On the other hand, the PAH/SPS films, both with and without salt, show no significant changes in their conductivity or dielectric characteristics from 25°C to 140°C (samples S1 and S4). Instead the films require much higher temperatures to achieve similar characteristics. By 260°C, the PAH/SPS film made without salt (sample S2) has the same conductivity and a similar value for ε' as the PAH/PAA film at 110°C (sample A8). This suggests that the ions are less mobile in the PAH/SPS system than in the PAH/PAA one. Since both the SPS and the PAA are fully charged in this regime, most of the conductivity likely comes from the residual counter-ions left in the film, however any residual free acid groups from the PAA might contribute to protonic conduction in the PAH/PAA films at low temperatures.

5. SUMMARY AND CONCLUSIONS

The subject of this thesis has basically been two fold. Initially, sequentially adsorbed layers of PPV precursor and PAA were examined both in terms of their adsorption characteristics and then in terms of their light emitting behavior. This then led to a more fundamental study of the impedance and dielectric characteristics of some non-electroactive model systems based on sequentially adsorbed layers of PAH/PAA and PAH/SPS.

The effects that the polyelectrolyte solution conditions have on the sequential adsorption of PPV precursor and PAA were initially examined. The resultant film thickness was shown to be independent of the PAA concentration down to 10^{-3} M, but it was highly dependent upon the PPV precursor concentration due to the fact that much more dilute PPV precursor solutions were required due to its high viscosity. This shows that the PPV precursor concentration should be closely monitored because subtle changes in the concentration can result in drastic changes in the film thickness. Furthermore, the pH of both of the solutions has been shown to influence the film thickness in a manner that depends upon the degree of ionization of the PAA. The PAA is a weak polyelectrolyte whose charge density varies with the pH such that a higher pH causes a larger degree of ionization. This results in the chain adopting a more extended chain conformation in solution, due to the electrostatic repulsion between like charges along the chain, and consequently thinner PAA layers are observed when the pH of the PAA solution increases. On the other hand, the degree of ionization of the PPV precursor does not change with pH. However, the pH of this solution affects the deposition process by controlling the charge density of the surface which is determined by the degree of ionization of the previously adsorbed PAA layer. A larger pH in the PPV precursor solution results in a higher charge density of the PAA on the surface and so a larger PPV precursor thickness contribution is observed. Finally, it is seen that the incremental layer thickness not only depends on the solution pH, but also on the thickness of the previously adsorbed layer. In general, a thicker underlying layer tends to cause an increase in the

thickness of the adsorbing layer, which is reflective of the fact that these layers are not discrete lamella, but rather highly interpenetrated networks.

The above argument for the pH dependence of the thickness holds for relatively low degrees of ionization of the PAA. As the PAA becomes more highly charged due to a continued increase in the solution pH, a point is eventually reached (at a pH of about 6.5) where the total film thickness is observed to drop to very low values. In this state, the system is behaving as two fully charged macromolecules both of which are in relatively extended chain conformations. They can form one-to-one contact ion-pairs with each other which result in the formation of very thin bilayers. This case can be likened to the sequential adsorption of two fully charged macromolecules like PAH and SPS where very thin bilayers are also observed. The transition between these regions is basically an interplay between enthalpy and entropy. At low charge densities, entropy dominates which results in relatively thick layers which maximize their configurational entropy. At high charge densities, enthalpy dominates thus causing a collapse of the film thickness to very small values.

These changes in bilayer thickness and composition with pH can significantly affect the performance of PPV/PAA light emitting devices. It was observed that increasing the PAA pH from 2.5 to 3.5, while holding the PPV precursor pH constant at 4.5, resulted in a 4 fold increase in the light output and a 1.5 order of magnitude increase in the external quantum efficiency for films of similar total thickness. The device made at PAA pH of 3.5 has a bilayer thickness that is almost half that for the pH 2.5 case, and its composition is made up of about 10% more PPV precursor. These two effects may combine to create a more interpenetrated bilayer structure with more efficient recombination of electrons and holes.

In addition, these LEDs have been shown to have many other interesting features that are not typically associated with pure spin coated films of PPV. A time dependent 'charging' process in which the light, current, and external quantum efficiency all increase with time has been interpreted in terms of an electrochemical mode of operation. Ions that are incorporated into the film, due to the counter polymer that is used for sequential adsorption, can move under the applied voltage and build up at the electrode

interfaces. These space charge layers can significantly decrease the barrier to charge injection and this manifests itself in a number of ways. It has been shown that as this 'charging' process proceeds, a systematic decrease in the turn-on voltage from about 8.5V to 3V is observed corresponding to the decrease in the injection barrier. Furthermore, the current density increases by about 8 fold upon charging, but the total light output and the external quantum efficiency increase by about 2 orders of magnitude or more. At a conversion temperature of 300°C, greater than 1000 cd/m^2 was observed. Given that the amount of light that is typical of a pure spin coated film of PPV with an aluminum electrode is on the order of 50-100 cd/m^2, this emphasizes the fact that a different mechanism must be responsible for the behavior. The reverse bias characteristics of these devices is also indicative of a light emitting electrochemical cell (LEC) type of behavior. It has been shown that significant light and current are detected when the device is tested in reverse bias. This behavior is usually a hallmark of electrochemical behavior since pure PPV films characteristically show rectification behavior where no current or light is generated in reverse bias.

One of the problems in dealing with this PPV precursor material, however, is in obtaining consistent results. Qualitatively, the device behavior that has been described above is virtually always observed, however the magnitudes of the light output, current density, efficiency, and turn-on voltages can vary over time. Attempts to improve the behavior by increasing the ionic conductivity through intentionally adding extra salt ions into the film failed. Whenever this was done, the device performance was much poorer than for the case when extra salt was not added to the film. It was shown that one of the effects of introducing these extra salt ions was to quench the photoluminescence and this may have been part of the reason for the decrease in device performance.

The desire to more fully understand and control the behavior of these devices led to the study of the impedance and dielectric characteristics of PAH/PAA and PAH/SPS sequentially adsorbed multilayers as model systems. In the PAH/PAA system, a temperature dependent DC conductivity and dielectric response was observed from 25°C to 110°C and was interpreted in terms of an activated ionic conduction process. The dielectric response showed a loss peak that shifted to higher frequencies with temperature

and a low frequency dielectric 'constant' of about 100 which was associated with the accumulation of ions at the electrode interfaces. The conductivities were quite low, consistent with that observed for other simple polyelectrolyte materials, and ranged from 1×10^{-12} S/cm at room temperature to about 4×10^{-9} S/cm at $110°C$. At higher temperatures, an irreversible change in the dielectric characteristics was observed in which the loss peak began shifting to lower frequencies as the temperature increased. This was interpreted in terms of an amidation reaction between the PAH and PAA to produce a dense, cross-linked film in which ionic motion became more hindered.

It was previously observed[115, 116] that the pH of the PAH and PAA solutions used during the sequential adsorption of these films drastically changes the resultant film structure in a manner similar to that just described for the PPV precursor/PAA system. Here, the impedance and dielectric characteristics were studied for PAH/PAA films adsorbed at a pH of 3.5, 5.0, and 6.5 in both solutions. All three cases showed a temperature dependent conductivity from $25°C$ to $110°C$ with an activation energy close to 1 eV. The conductivities observed for the pH 3.5 case were consistently about a factor of 2 higher that that observed for the other two cases. Furthermore, a continuous decrease in the low frequency dielectric 'constant' was observed as the pH was increased. As the pH of the dipping solutions is increased, the degree of ionization of the PAA increases and so fewer free carboxylic acid groups get incorporated into the film. So if protonic conduction is the dominant mechanism of ionic transport in these films, an increase in the pH corresponds to a decrease in the carrier density. Furthermore as the pH increases, more ionic cross-links are formed between the PAH and the PAA, due to an increasing PAA charge density, and so this could result in a decrease in the mobility of the ions. A combination of these two effects is likely responsible for the observed behavior.

Attempts at increasing the concentration of ions in the PAH/PAA layers, by dipping the completed film in a high pH salt solution, actually resulted in a decrease in the observed conductivity and a shifting of the dielectric loss peak to lower frequencies. It is believed that the increase in salt concentration results in a decrease in the mobility of the ions so as to cause an overall decrease in the conductivity. This effect is frequently observed in PEO:salt mixtures due an increase in the T_g as the salt concentration

increases. Plasticizing these films with water, however, resulted in a large increase in both the conductivity (up to 2×10^{-7} S/cm) as well as the low frequency dielectric 'constant' (up to 325). In the dry state, strong binding between the small ions and the macro-ions leads to low values of the conductivity. Water can act to solvate these ions thus increasing their mobility as well as the concentration of those that are free to move.

PAH/SPS layers behave slightly differently, however, in the sense that much higher temperatures are required to get any significant change in the impedance or dielectric response. For PAH/SPS layers made both with and without salt in the dipping solutions, no significant change in the conductivity or the dielectric characteristics was observed up to a temperature of 140°C, contrary to that seen for PAH/PAA layers. Below this temperature, a relatively constant value of ε' was observed and interpreted as a bulk value due to any local polarization of the medium and it was higher in the case with salt in the dipping solutions than without (5 as compared to 2). Above 140°C, the conductivity and the low frequency dielectric 'constant' do increase significantly with temperature for both cases suggesting that some of the small ions do indeed remain in the film after sequential adsorption. Furthermore, the value of the low frequency dielectric 'constant' at 350°C for PAH/SPS films made with salt in the dipping solutions is about 7 times higher than that for films made without salt. This, combined with the fact that the bulk value of ε' is greater in the case with salt, suggests that more ions are incorporated into the films for the case with salt into the dipping solutions than for the case without. These additional ions could either be coming directly from the added salt, or possibly from the original counter-ions due to the formation of fewer polymer-polymer ion-pairs. Testing these PAH/SPS layers in a humid environment at room temperature results in a low frequency dielectric 'constant' of 500 and 80 and a conductivity of 3×10^{-7} S/cm and 3×10^{-8} S/cm, for the case with and without salt in the dipping solutions, respectively. These relatively large values, compared to the dry state, again imply that some level of ion concentration does indeed remain in the film and that a higher concentration exists in the case with salt.

Finally, the properties of PAH/SPS layers has been compared to PAH/PAA layers adsorbed at a pH of 6.5 where the PAA can be considered to be highly charged, similar to

the SPS. It was shown that even though both systems result in the formation of very thin bilayers, significant differences in their conductivities and dielectric properties exist. The PAH/SPS film had to be heated to about 260°C in order for the film to exhibit similar characteristics to the PAH/PAA film at 110°C. This implies that the ions are significantly less mobile in the PAH/SPS structure than they are in the PAH/PAA. This could be due to a more rigid matrix of the PAH/SPS film, however any residual protonic conductivity that exists in the PAH/PAA film might also be responsible for the conductivity at relatively low temperatures.

In summary, then, it has been shown that the light emitting characteristics of sequentially adsorbed layers of PPV and PAA are related to the finite ionic conductivity that exists in these films. The ionic conductivity as well as the dielectric characteristics of PAH/PAA and PAH/SPS sequentially adsorbed multilayers were then studied using impedance spectroscopy to provide some insight into the nature of the sequential adsorption process. Further work on improving the ionic conductivity of these films may result in better control and an improvement in the device performance. This line of work has recently been started by trying to incorporate a PEO-like segment into the polyanion. A copolymer has been made from monomers containing a PEO-like pendant group and another containing a PAA-like pendant group in the hopes that the PEO-like group will facilitate ion motion in these film. On the whole, it seems that the sequential adsorption process provides a unique opportunity with which to control the architecture of these films on a molecular level, but more work is required to fully realize its potential.

BIBLIOGRAPHY

Chapter 1

1.   G. Decher, J.-D. Hong, *Makromol. Chem. Macromol. Symp.* **46** (1991).
2.   G. Decher, J. D. Hong, *Ber. Bunsenges. Phys. Chem.* **95**, 1430-1434 (1991).
3.   G. Decher, J. D. Hong, J. Schmitt, *Thin Solid Films* **210/211**, 831-835 (1992).
4.   G. Decher, J. Schmitt, *Progress in Colloid and Polymer Science* **89**, 160-164 (1992).
5.   J. Schmitt, T. Grunewald, G. Decher, P. S. Pershan, K. Kjaer, M. Losche, *Macromolecules* **26**, 7058-7063 (1993).
6.   G. Decher, Y. Lvov, J. Schmitt, *Thin Solid Films* (1993).
7.   G. B. Sukhorukov, J. Schmitt, G. Decher, *Ber. Bunsenges. Phys. Chem.* **100**, 948-953 (1996).
8.   J. J. Ramsden, Y. M. Lvov, G. Decher, *Thin Solid Films* **254**, 246-251 (1995).
9.   Y. Lvov, G. Decher, G. Sukhorukov, *Macromolecules* **26**, 5396-5399 (1993).
10.   Y. Lvov, G. Decher, H. Mohwald, *Langmuir* **9** (1993).
11.   M. Losche, J. Schmitt, G. Decher, W. G. Bouwman, K. Kjaer, *Macromolecules* **31**, 8893-8906 (1998).
12.   A. C. Fou, O. Onitsuka, M. Ferreira, M. F. Rubner, B. R. Hsieh, *Journal of Applied Physics* **79** (1996).
13.   A. C. Fou, Ph.D. Thesis, Massachusetts Institute of Technology (1995).
14.   O. Onitsuka, A. C. Fou, M. Ferreira, B. R. Hsieh, M. F. Rubner, *Journal of Applied Physics* **80** (1996).
15.   M. Ferreira, J. H. Cheung, M. F. Rubner, *Thin Solid Films* **244**, 806-809 (1994).
16.   M. Ferreira, O. Onitsuka, A. C. Fou, B. Hsieh, M. F. Rubner, Light emitting thin film devices based on self-assembled multilayer heterostructures of PPV, Materials Research Society, Boston, MA (1995).
17.   J. W. Baur, P. Besson, S. A. O'Connor, M. F. Rubner, *MRS Proceedings* (1995).
18.   J. W. Baur, Ph.D. Thesis, Massachusetts Institute of Technology (1997).
19.   D. Yoo, Ph.D. Thesis, Massachusetts Institute of Technology (1997).
20.   D. Yoo, S. S. Shiratori, M. F. Rubner, *Macromolecules* **31**, 4309-4318 (1998).
21.   S. Shiratori, M. F. Rubner, *To be published* .
22.   J. H. Cheung, W. B. Stockton, M. F. Rubner, *Macromolecules* **30**, 2712-2716 (1997).
23.   W. B. Stockton, M. F. Rubner, *Macromolecules* **30**, 2717-2725 (1997).
24.   F. Oosawa, *Polyelectrolytes* (Marcel Dekker, Inc., New York, 1971).
25.   H. Dautzenberg, W. Jaeger, J. Kotz, B. Philipp, C. Seidel, D. Stscherbina, *Polyelectrolytes: formation, characterization, and application* (Hanser Publishers, New York, 1994).
26.   J. M. Andre, J. Delhalle, J. L. Bredas, *Quantum Chemistry Aided Design of Organic Polymers* (World Scientific, 1991).
27.   S. Roth, *One-Dimensional Metals* (1995).

28.   M. J. Bowden, S. R. Turner, Eds., *Electronic and Photonic Applications of Polymers* (1986).

29.   A. J. Heeger, in *Conjugated Polymers and Related Materials: The Interconnection of Chemical and Electronic Structure* I. L. W.R. Salaneck, B. Ranby, Ed. (1993).

30.   J. H. Burroughes, D. D. C. Bradley, A. R. Brown, R. N. Marks, K. Mackay, R. H. Friend, P. L. Burns, A. B. Holmes, *Nature* **347** (1990).

31.   M. Fahlman, M. Logdlund, S. Stafstrom, W. R. Salaneck, R. H. Friend, P. L. Burns, A. B. Holmes, K. Kaeriyama, Y. Sonoda, O. Lhost, F. Meyers, J. L. Bredas, *Macromolecules* **28** (1995).

32.   I. D. Parker, *Journal of Applied Physics* **75** (1994).

33.   Y. Park, V. Choong, E. Ettedgui, Y. Gao, B. R. Hsieh, T. Wehrmeister, K. Mullen, *Applied Physics Letters* **69**, 1080-1082 (1996).

34.   B. R. Hsieh, E. Ettedgui, Y. Gao, *Synthetic Metals* **78**, 269-275 (1996).

35.   K. Konstadinidis, F. Papadimitrakopoulos, M. Galvin, R. L. Opila, *Journal of Applied Physics* **77** (1995).

36.   V. E. Choong, Y. Park, B. R. Hsieh, C. W. Tang, Y. Gao, *SPIE* **3148** (1996).

37.   J. Shinar, H. Tang, F. Li, *SPIE* **3148** (1996).

38.   D. R. Baigent, N. C. Greenham, J. Gruner, R. N. Marks, R. H. Friend, S. C. Moratti, A. B. Holmes, *Synthetic Metals* **67** (1994).

39.   A. R. Brown, D. D. C. Bradley, J. H. Burroughes, R. H. Friend, N. C. Greenham, P. L. Burn, A. B. Holmes, A. Kraft, *Applied Physics Letters* **61** (1992).

40.   F. Cacialli, R. N. Marks, R. H. Friend, R. Zamboni, C. Taliani, S. C. Moratti, A. B. Holmes, *Synthetic Metals* **76** (1996).

41.   D. J. Dick, A. J. Heeger, Y. Yang, Q. Pei, *Advanced Materials* **8** (1996).

42.   Y. Cao, G. Yu, A. J. Heeger, C. Y. Yu, *Applied Physics Letters* **68** (1996).

43.   Q. Pei, Y. Yang, G. Yu, C. Zhang, A. J. Heeger, *Journal of the American Chemical Society* **118**, 3922-3929 (1996).

44.   J. Gao, G. Yu, A. J. Heeger, *Applied Physics Letters* **71** (1997).

45.   G. Yu, Y. Cao, M. Anderson, J. Gao, A. J. Heeger, *Advanced Materials* **10** (1998).

46.   Y. Li, J. Gao, G. Yu, Y. Cao, A. J. Heeger, *Chemical Physics Letters* **287**, 83-88 (1998).

47.   J. C. deMello, N. Tessler, S. C. Graham, X. Li, A. B. Holmes, R. H. Friend, *Synthetic Metals* **85**, 1277-1278 (1997).

48.   J. C. deMello, N. Tessler, S. C. Graham, R. H. Friend, *Physical Review B* **57** (1998).

49.   D. Neher, J. Grüner, V. Cimrová, W. Schmidt, R. Rulkens, U. Lauter, *Polymers for Advanced Technologies* **9**, 461-475 (1998).

50.   D. L. Smith, *Journal of Applied Physics* **81** (1997).

51.   I. Riess, D. Cahan, *Journal of Applied Physics* **82**, 3147-3151 (1997).

52.   J. R. Macdonald, *Impedance Spectroscopy* (John Wiley & Sons, New York, 1987).

53.   A. R. Blythe, *Electrical Properties of Polymers* (Cambridge University Press, Cambridge, 1979).

54.   J. P. Runt, J. J. Fitzgerald, Eds., *Dielectric Spectroscopy of Polymeric Materials* (American Chemical Society, Washington, DC, 1997).

55.   P. G. Bruce, in *Polymer Electrolyte Reviews-1* C. A. V. J.R. MacCallum, Ed. (Elsevier Applied Science, New York, 1987).

56.   S. Matsuoka, in *Encyclopedia of Polymer Science & Engineering* . (1995), vol. 5,.

57.   K. N. Mathes, in *Encyclopedia of Polymer Science & Engineering* . (1995), vol. 5,.

58.   R. H. Cole, K. S. Cole, *Journal of Chemical Physics* **9**, 341 (1941).

59.   D. W. Davidson, R. H. Cole, *Journal of Chemical Physics* **18**, 1417 (1950).

60.   S. Havriliak-Jr., S. J. Negami, *Polymer Science C* **14**, 99 (1966).

61.   S. Havriliak-Jr., S. J. Negami, *Polymer* **161** (1967).

Chapter 2

62.   G. J. Fleer, M. A. C. Stuart, J. M. H. M. Scheutjens, T. Cosgrove, B. Vincent, *Polymers at Interfaces* (Chapman & Hall, London, 1993).

63.   J. W. Baur, Ph.D. Thesis, Massachusetts Institute of Technology (1997).

64.   G. Decher, J. Schmitt, *Progress in Colloid and Polymer Science* **89**, 160-164 (1992).

65.   G. B. Sukhorukov, J. Schmitt, G. Decher, *Ber. Bunsenges. Phys. Chem.* **100**, 948-953 (1996).

66.   J. B. Schlenoff, L. J. Wang, *Macromolecules* **24**, 6653-6659 (1991).

Chapter 3

67.   N. C. Greenham, R. H. Friend, D. D. C. Bradley, *Advanced Materials* **6**, 491-494 (1994).

68.   F. Cacialli, R. N. Marks, R. H. Friend, R. Zamboni, C. Taliani, S. C. Moratti, A. B. Holmes, *Synthetic Metals* **76** (1996).

69.   V. Cimrova, D. Neher, *Synthetic Metals* **76** (1996).

70.   F. Papadimitrakopoulos, K. Konstadinidis, T. M. Miller, R. Opila, E. A. Chandross, M. E. Galvin, *Chemistry of Materials* **6**, 1563-1568 (1994).

71.   M. Herold, J. Gmeiner, W. Riess, M. Schwoerer, *Synthetic Metals* **76**, 109-112 (1996).

72.   D. D. C. Bradley, *Synthetic Metals* **54**, 401-415 (1993).

73.   R. H. Friend, N. C. Greenham, , 479-487 (1995).

74.   Q. Pei, Y. Yang, G. Yu, C. Zhang, A. J. Heeger, *Journal of the American Chemical Society* **118**, 3922-3929 (1996).

75.   Y. Cao, G. Yu, A. J. Heeger, C. Y. Yu, *Applied Physics Letters* **68** (1996).

76.   D. J. Dick, A. J. Heeger, Y. Yang, Q. Pei, *Advanced Materials* **8** (1996).

77.   G. Yu, Y. Yang, Y. Cao, Q. Pei, C. Zhang, A. J. Heeger, *Chemical Physics Letters* **259**, 465-468 (1996).

78.   J. Gao, G. Yu, A. J. Heeger, *Applied Physics Letters* **71** (1997).

79.   Y. Yang, Q. Pei, *Journal of Applied Physics* **81** (1997).

80. G. Yu, Y. Cao, M. Anderson, J. Gao, A. J. Heeger, *Advanced Materials* **10** (1998).

81. J. C. deMello, N. Tessler, S. C. Graham, X. Li, A. B. Holmes, R. H. Friend, *Synthetic Metals* **85**, 1277-1278 (1997).

82. J. C. deMello, N. Tessler, S. C. Graham, R. H. Friend, *Physical Review B* **57** (1998).

83. D. L. Smith, *Journal of Applied Physics* **81** (1997).

84. D. Neher, J. Grüner, V. Cimrová, W. Schmidt, R. Rulkens, U. Lauter, *Polymers for Advanced Technologies* **9**, 461-475 (1998).

85. I. Riess, D. Cahan, *Journal of Applied Physics* **82**, 3147-3151 (1997).

86. J. B. Schlenoff, L. J. Wang, *Macromolecules* **24**, 6653-6659 (1991).

87. O. Onitsuka, A. C. Fou, M. Ferreira, B. R. Hsieh, M. F. Rubner, *Journal of Applied Physics* **80** (1996).

88. M. Ferreira, O. Onitsuka, A. C. Fou, B. Hsieh, M. F. Rubner, Light emitting thin film devices based on self-assembled multilayer heterostructures of PPV, Materials Research Society, Boston, MA (1995).

89. Y.-E. Kim, H. Park, J.-J. Kim, *Applied Physics Letters* **69**, 599-601 (1996).

Chapter 4

90. J. W. Baur, Ph.D. Thesis, Massachusetts Institute of Technology (1997).

91. D. Yoo, Ph.D. Thesis, Massachusetts Institute of Technology (1997).

92. D. Yoo, S. S. Shiratori, M. F. Rubner, *Macromolecules* **31**, 4309-4318 (1998).

93. S. Shiratori, M. F. Rubner, *To be published* .

94. G. Decher, J. D. Hong, J. Schmitt, *Thin Solid Films* **210/211**, 831-835 (1992).

95. G. Decher, J. Schmitt, *Progress in Colloid and Polymer Science* **89**, 160-164 (1992).

96. J. Schmitt, T. Grunewald, G. Decher, P. S. Pershan, K. Kjaer, M. Losche, *Macromolecules* **26**, 7058-7063 (1993).

97. G. Decher, Y. Lvov, J. Schmitt, *Thin Solid Films* (1993).

98. G. B. Sukhorukov, J. Schmitt, G. Decher, *Ber. Bunsenges. Phys. Chem.* **100**, 948-953 (1996).

99. J. J. Ramsden, Y. M. Lvov, G. Decher, *Thin Solid Films* **254**, 246-251 (1995).

100. M. Losche, J. Schmitt, G. Decher, W. G. Bouwman, K. Kjaer, *Macromolecules* **31**, 8893-8906 (1998).

101. F. M. Gray, *Polymer Electrolytes*. J. A. Connor, Ed., RSC Materials Monographs (The Royal Society of Chemistry, 1997).

102. P. G. Bruce, in *Polymer Electrolyte Reviews-1* C. A. V. J.R. MacCallum, Ed. (Elsevier Applied Science, New York, 1987).

103. M. A. Ratner, D. F. Shriver, *Chemical Reviews* **88**, 109-124 (1988).

104. L. C. Hardy, D. F. Shriver, *Macromolecules* **17** (1984).

105. L. C. Hardy, D. F. Shriver, *Journal of the American Chemical Society* **107**, 3823-3828 (1985).

106. E. Tsuchida, N. Kobayashi, H. Ohno, *Macromolecules* **21**, 96-100 (1988).

107. S. Toyota, T. Nogami, H. Mikawa, *Solid State Ionics* **13**, 243-247 (1984).

108. E. Tsuchida, H. Ohno, K. Tsunemi, N. Kobayashi, *Solid State Ionics* **11**, 227-233 (1983).

109. E. Tsuchida, .

110. M. F. Daniel, B. Desbat, J. C. Lassegues, *Solid State Ionicd* **28-30**, 632-636 (1988).

111. F. M. Gray, *Solid Polymer Electrolytes, Fundamentals and Technological Applications* (VCH Publishers, 1991).

112. J. J. Harris, P. M. DeRose, M. L. Bruening, *Journal of the American Chemical Society* **121**, 1978-1979 (1999).

113. G. Decher, , Conference of the American Chemical Society, Boston, MA (1998).

114. B. J. Hunt, M. I. James, *Polymer Characterization* (Blackie Academic & Professional, 1993).

115. J. L. Crowley, R. A. Wallace, R. H. Bube, *Journal of Polymer Science: Polymer Physics Edition* **14**, 1769-1787 (1976).

116. G. J. Fleer, M. A. C. Stuart, J. M. H. M. Scheutjens, T. Cosgrove, B. Vincent, *Polymers at Interfaces* (Chapman & Hall, London, 1993).

117. E. Nordmeier, P. Beyer, *Journal of Polymer Science: Part B: Polymer Physics* **37**, 335-348 (1999).

Chapter 5

115. D. Yoo, S. S. Shiratori, M. F. Rubner, *Macromolecules* **31**, 4309-4318 (1998).

116. S. Shiratori, M. F. Rubner, *To be published* .